Flexibility Provisions from Energy Hubs for Sustainable Energy Systems

by

Walied Alharbi

A thesis
presented to the University of Waterloo
in fulfillment of the
thesis requirement for the degree of
Doctor of Philosophy
in
Electrical and Computer Engineering

Waterloo, Ontario, Canada, 2018

Examining Committee Membership

The following served on the Examining Committee for this thesis. The decision of the Examining Committee is by majority vote.

External Examiner:	Bala Venkatesh Professor
Supervisor:	Kankar Bhattacharya Professor
Internal Member:	Mehrdad Kazerani Professor
Internal Member:	Sheshakamal Jayaram Professor
Internal-External Member:	Kaamran Raahemifar Professor

I hereby declare that I am the sole author of this thesis. This is a true copy of the thesis, including any required final revisions, as accepted by my examiners.

I understand that my thesis may be made electronically available to the public.

Abstract

Power systems have some inherent level of flexibility built into the system, to meet the continuous mismatches between the supply and demand. Variability and uncertainty are not new to power systems as loads change over time and generators can fail in unpredictable manners. Penetration of renewable resources and plug in electric vehicles (PEVs) can make this mismatch even more difficult to meet and new flexibility resources will be needed to supplement the flexibility capabilities of the existing system. There are many options to provide flexibility at the distribution system level, but their potential have not been fully utilized. This thesis addresses some of the pertinent issues relating to flexibility provisions from energy hubs.

In the first research problem, an electric vehicle charging facility (EVCF) is transformed to operate as a smart energy hub in order to build its flexibility provision. The EVCF demand mostly occurs during the evening, coinciding with the peak demand, and has no flexibility because of the short stay of PEVs at the charging facility. From the system planner's and operator's point of view, such transformation of the EVCF presents a new source of flexibility to the distribution system, which could alleviate network stress and defer upgrades, and the transformation to a smart energy hub will also reduce the EVCF's operating costs through improved energy management. A generic and novel framework is proposed to optimally design and plan an EVCF as a smart energy hub that controls the energy flow between the renewables-based generation units, the battery energy storage system (BESS), the external grid, and local consumption. The proposed framework is based on a bottom-up approach to design and planning of an EVCF, incorporating a detailed representation of vehicle mobility statistics to estimate the charging load profile, and then integrating all dimensions of planning, such as technical feasibility assessment, economics, and distribution system operations impact assessment.

The thesis further presents a new mathematical model to design an EVCF with distributed energy resources (DERs) to provide flexibility services in wind integrated power grids. Two different ownership structures of the EVCF and the wind generation facility

(WGF) are presented and analyzed for the first time. The DER options considered for the EVCF design are solar photovoltaic (PV) units and BESS. The effects of wind power uncertainty on power system operations are mitigated through the designed EVCF with DERs via the upward and downward flexibility provisions. Monte Carlo simulations are used to simulate the uncertainties in PV and wind generation, and market price.

In the third research problem, residential loads are transformed to residential energy hubs (REHs) to develop an inherent flexibility in their portfolios, and hence offer a wide range of benefits to the power grid, such as peak reduction, congestion relief and capacity deferral. A generic and novel framework is proposed, to simultaneously determine the optimal penetration of REHs in distribution systems and the optimal incentives to be remunerated by the local distribution company (LDC) to residential customers for flexibility provisions, considering economic benefits of both parties. The proposed framework models the relationship between the participation of residential customers in transforming their houses to REHs and the incentives to be offered by the LDC. A new concept of unloaded and loaded states of REHs is also introduced for quantifying the power availability of REHs, from which power flexibility can be provided considering the penetration of REHs in the system.

Acknowledgements

First and foremost, all praise to Allah almighty for His blessing in the successful completion of this thesis.

Then I would like to express my sincere gratitude and appreciation to my supervisor Professor Kankar Bhattacharya for his guidance, encouragement, and support throughout my PhD studies. It was my privilege to complete my graduate studies under his supervision.

I would like to thank my PhD Advisory Committee members: Professor Mehrdad Kazerani, Professor Sheshakamal Jayaram, and Professor Kaamran Raahemifar for their valuable comments and support. I am also very thankful to Professor Bala Venkatesh, from Ryerson University, for serving as the external thesis examiner and for his helpful comments and observations. I would like also to thank Professor Daniel Smilek for chairing my thesis examination committee.

I gratefully acknowledge the Saudi Arabian Ministry of Higher Education represented by Majmaah University, Majmaah, Saudi Arabia, for the financial support to pursue my graduate studies.

I would like to thank my parents, brothers and sisters for their continuous support, encouragement, and prayers.

I cannot find the right words to express my gratitude to my lovely wife, Sara, for her endless love, understanding, support and encouragement during my PhD journey. I am grateful to have a little girl, Dania, who has brought great beauty and joy into my life.

Finally, I would like to thank all my friends in Waterloo, who have enriched my life and made it enjoyable.

Dedication

TO MY DEAR PARENTS

Table of Contents

List of Tables

List of Figures

List of Abbreviations

AMI	Advanced Metering Infrastructure
BESS	Battery Energy Storage System
BSF	Battery-Swapping Facility
BEV	Battery Electric Vehicles
CAISO	California Independent System Operator
CAES	Compressed Air Energy Storage
CPM	Customer Profitability Model
DLC	Direct Load Control
DOD	Depth of Discharge
DR	Demand Response
DSO	Distribution System Operator
DER	Distributed Energy Resources
DSM	Demand Side Management
DLMP	Distribution Locational Marginal Prices
DG	Distributed Generator
EAM	Economic Assessment Model
ESS	Energy Storage System
EHMS	Energy Hub Management System
EVCF	Electric Vehicle Charging Facility
FIT	Feed-in-Tariff
GHG	Greenhouse Gas
HOEP	Hourly Ontario Electricity Price
HEV	Hybrid Electric Vehicles

IRR	Internal Rate of Return
ISO	Independent System Operator
IL	Interruptible Load
LDC	Local Distribution Company
LOLE	Loss of Load Expectation
MARR	Minimum Acceptable Rate of Return
MCS	Monte Carlo Simulations
MILP	Mixed Integer Linear Programming
MINLP	Mixed Integer Non-linear Programming
NHTS	National Household Travel Survey
NPV	Net Present Value
NLP	Non-Linear Programming
O&M	Operations and Maintenance
OPF	Optimal Power Flow
PCU	Power Conditioning Unit
PEV	Plug Electric Vehicles
PHEV	Plug in Hybrid Electric Vehicles
PV	Photovoltaic
QM	Queuing Model
REH	Residential Energy Hubs
RER	Renewable Energy Resources
SMES	Superconducting Magnetic Energy Storage System
SOC	State of Charge
TOU	Time-of-Use
VDT	Vehicle Decision Tree
WGF	Wind Generation Facility

Nomenclature

Indices

i, j	Index for buses, $i, j \ \varepsilon \ N$
k	Index for time, $k \ \varepsilon \ K$
l	Index for EVCF buses, $l \ \varepsilon \ N$
s	Index for season, $s \ \varepsilon \ S$
ss	Index for substation buses, $ss \ \varepsilon \ N$
y	Index for years, $y \ \varepsilon \ Y$
r	Index for REH locations, $r \ \varepsilon \ N$

Parameters

μ	Charging service rate
c	Number of fast chargers
C^{TH}	Transformer capacity for EVCF
C^{Inv}	Investment cost of a REH for a house [$]
C^{PK}	Peak load charge [$/$kW$]
C^{TOU}	Time-of-Use electricty price [$/$kWh$]
$\overline{EPR}$,$\underline{EPR}$	Maximum and minimum energy to power ratio
$E[Z]$	Expected number of occupied fast chargers
G	Real part of the admittance matrix element
IC^{E}	Variable installation cost associated with BESS energy size [$/kWh]
IC^{P}	Variable installation cost associated with BESS power size [$/kW]
IC^{PV}	PV generation installation cost [$/kW]
M^{C}	Fast charger maintenance cost [$/kVA]

M^{TH}	Transformer maintenance cost [$/kVA]
n	Number of discharged PEV at an EVCF
Nd	Number of days in a season
OM^f	Annual fixed O&M cost of BESS [$/kW]
OM^{PV}	O&M cost of PV generation [$/kW]
OM^V	Variable O&M cost of BESS [$/kWh]
OM^W	Fixed O&M cost of wind energy, [$/$kWh$]
P^{AW}	Actual wind power output [kW]
P^{FW}	Forecasted wind power output [kW]
P^{AVG}	Average power per fast charger [kW]
Pd, Qd	Active and reactive power demand [p.u]
$P^{DG^{Max}}$	Maximum penetration of connected DG [p.u]
PD^{PEV}	Expected demand of an EVCF [kW]
$S^{SS_{Cap}}$	Substation capacity [p.u]
$S^{F_{Cap}}$	Feeder capacity [p.u]
φ^{PV}	Available photovoltaic output power as a percentage of its rated capacity [$p.u$]
$\overline{P^{+s}}, \overline{P^{-S}}$	Maximum power in unloaded and loaded states of REH, [kW]
$\overline{\omega}$	Maximum rebate given to a residential customer, [%]
γ	Percentage of deferrable load, [%]
P^{HL}	House load, [%]
α	Discount rate [%]
η_c	Efficiency of a fast charger [%]
η^{in}, η^{out}	BESS charging/discharging efficiency [%]
η^{PV}	PV array inverter conversion efficiency [%]
λ	Probability of PEV arrival at an EVCF
$\theta_{i,j}$	Angle of bus admittance matrix element, rad
$Y_{i,j}$	Magnitude of admittance matrix element, p.u.
ρ	Contract price of energy exported to grid by EVCF [$/kWh]

ρ^{MG}	Main grid electricity price [$/kWh]
ρ^{PEV}	Price for charging PEV [$/kWh]
ρ^{Fdown}	Downward flexibility power price [$/$kWh$]
ρ^{dw}	Penalty for deficit wind generation [$/$kWh$]
ρ^{sw}	Penalty for surplus wind generation [$/$kWh$]
ρ^{Fup}	Upward flexibility power price [$/$kWh$]
ψ	Probability of occupied fast chargers

Variables

C^{OP}	Operation cost of a distribution grid, [$]
C^{Flex}	Flexibility cost for transforming houses to REHs, [$]
C^{E}	Cumulative BESS energy capacity [kWh]
C^{PV}	Cumulative solar PV capacity [kWh]
$Cost$	Annual cost of new EVCF design [$]
$Cost^{Inv}$	Investment cost of new EVCF design[$]
$Cost^{OM}$	O&M cost of EVCF [$]
X^{REH}	Penetration of REHs p.u
P^{PK}	Daily peak load imported by substation, $[p.u]$
P^{+S}, P^{-S}	Power in unloaded/loaded state of REH, $[kW]$
P^{-DR}, P^{+DR}	Downward/upward DR $[kW]$
P^{-ABESS}	Power discharge of aggregated BESSs $[p.u]$
P^{+ABESS}	Power charge of aggregated BESSs $[p.u]$
P^{-ADR}, P^{+ADR}	Aggregated downward/upward DR $[p.u]$
P^{F}, Q^{F}	Active and reactive power flow from i to j, $[p.u]$
ρ^{Inc}	Variable component associated with flexibility services [$/$kWh$]
ω	Rebate given to residential customers $[p.u]$
V	Voltage magnitude, $[p.u]$
δ	Voltage phase angle $[rad]$
E^{EX}	Energy exported to the main grid [kWh]

E^{SH}	PEV energy shedding at an EVCF [kWh]
NC^{E}	New BESS energy capacity [kWh]
NC^{P}	New BESS power rating [kW]
NC^{PV}	New PV power capacity [kW]
P, Q	Active and reactive power drawn by substation from the main grid [p.u]
P^{EX}	Power exported by the EVCF to the main grid [kW]
P^{IM}	Power imported by the EVCF from the main grid [kW]
P^{in}, P^{out}	BESS charging/discharging power [kW]
P^{SH}	PEV load shedding at an EVCF[kW]
$Psize^{BESS}$	Cumulative BESS power rating [kW]
P^{UN}	Unserved power in distribution system [p.u]
P^{Fdown}	Downward power flexibility provision $[kW]$
P^{Fup}	Upward power flexibility provision $[kW]$
P^{dw}	Deficit wind power $[kW]$
P^{sw}	Surplus wind power $[kW]$
S^{F}	Complex power flow from i to j [p.u]
SOC	BESS state of charge [kWh]
u^{Fdown}	Downward flexibility decision: 1 when downward flexibility power takes place and 0 otherwise
u^{dw}	Deficit wind power decision: 1 for deficit in wind power and 0 otherwise
u^{sw}	Surplus wind power decision: 1 for surplus wind power and 0 otherwise
u^{Fup}	Upward flexibility decision: 1 for providing upward flexibility power and 0 otherwise
u^{EX}, u^{IM}	Exporting/importing binary variable: 1 when power is exported/imported to/from the main grid by EVCF and 0 otherwise

Chapter 1

Introduction

1.1 Motivation

As two major consumers of fossil fuels, the electricity and transportation sectors are directly responsible for the depleting reserve of fossil fuels, and the release of tremendous amounts of harmful gases [1]. The former leads to competition amongst nations to secure sufficient natural resource reserves to ensure energy security. The latter is responsible for global warming and the deterioration of human health. For these reasons and to safeguard the future development of individual nations, alternative energy resources must be sought.

The adoption of renewable energy resources (RERs) and plug-in electric vehicles (PEVs) can alleviate dependency on fossil fuels, and also foster a greener and cleaner living environment. However, connecting a large fleet of PEVs to the grid and meeting their charging loads entirely from a coal-fired power plant will still result in significant greenhouse gas (GHG) emissions, which would only be shifted from the transportation sector to the electricity sector, rather than being reduced. RERs and PEVs must therefore be deployed together in a smart grid to ensure both environment and economic benefits.

A significant challenge associated with the reduction of GHG emissions is the fact that the world's electrical energy consumption is expected to grow at an annual rate of about

2.2% from 2010 to 2040, in contrast to an average growth of 1.4% for all other sources of delivered energy [2]. In addition, sales of PEVs are expected to reach over 50,000 vehicles in Ontario by 2020 [3]. Significant increase in charging demand will create a surge in the demand for electrical energy. In this context, there is a need to find intelligent and cost effective means to make better use of electricity resources, improve the system flexibility, and slow the growth in demand. Smart grid developments can help provide feasible solutions for this dilemma, through Demand Side Management (DSM), Distributed Energy Resources (DERs), and Advanced Metering Infrastructure (AMI). A smart grid is an intelligent power network that incorporates technologies and communication infrastructure, so that existing capability can be maximized, and the grid, particularly at the distribution system and load levels is modernized [4].

The Government of Ontario is investing $20 million to develop public infrastructure for Electric Vehicle Charging Facility (EVCF) across the province [3]. A network of EVCFs will be in place, in cities, along highways, at workplaces, and public places across Ontario. This program will create, by far, the largest public network of EVCFs in Canada. However, the fast charging power demand, which often coincides with the system peak demand, will significantly increase in the coming years. It is essential that PEV charging be controlled and shifted to time periods which are favorable to the local distribution company (LDC) with respect to grid availability, so as not to stress the system components while also improving system flexibility. As well, and most importantly, PEV charging must be coordinated with RERs as much as possible but with little or no effect on customer satisfaction.

Nevertheless, unlike home and parking lot charging, a fast EVCF has no flexibility and can neither be controlled or shifted. As fast charging demand most frequently occurs during the evening, often coinciding with peak demand, and cannot be controlled, there is a need to make this demand flexible by planning and operating an EVCF as a smart energy hub, incorporating, but not limited to, a smart meter, battery energy storage systems (BESS), and renewables-based distributed generation (DG), with the option of exchanging power with the external grid. Transformation of the EVCF to a smart energy hub can be seen

or realized as a new source of flexibility from the system planners' and operators' point of view in a smart grid.

The installed capacity of RERs will be 20,000 MW in 2025, representing about half of Ontario's installed capacity [5]. That would result in a notable increase in wind and solar generation installed capacity in 2025. Hence, variability and uncertainty will significantly increase in supply of electricity. Intermittency of supply is an issue particularly applicable to wind genration whose typical forecasting errors, with respect to the final output power, are in the range of 30%-50% [6, 7]. As EVCFs are typically located along a highway to support long trips for PEVs, they can coordinate with a wind generation facility (WGF) and help mitigate wind power imbalances, particularly when the EVCFs are equipped with DERs. However, the technical feasibility and economic viability of flexibility provisions from EVCF equipped with DERs, for wind integrated power grids have to be investigated.

The increasing penetration of RERs results in reduced share of controllable generation capacity, and consequently less generation reserves. To circumvent this issue, more flexibility provisions are necessary from the demand side. In a smart grid environment, residential loads are being transformed to residential energy hubs (REHs) with energy demand, generation, and storage capabilities [8]; such transformation of residential loads can increase the system flexibility. Offering appropriate incentives by the LDC can encourage residential customers to transform their houses to REHs, and thereby build a portfolio of flexibility at the demand-side. The willingness of residential customers to transform their houses to REHs will depend on the incentive being offered; higher the incentive, more houses would transform to REH. However, offering high incentives will result in increased financial burden to the LDC. Therefore, there is a need to determine the appropriate incentives that would induce an optimal penetration of REHs from the residential customers, while minimizing the LDC's cost and also considering the economic benefit to residential customers from transforming their houses to REHs.

1.2 Literature Review

1.2.1 Power System Flexibility

As electric power production and consumption occur concurrently, mismatches between them risk wide-scale power system outages. Certain controllable power plants have been traditionally responsible for balancing the supply and demand by adjusting their power output, so as to maintain the system frequency within a predefined acceptable band. Although such practice still continues today, the introduction of RERs and PEVs increases the need for flexibility in the power system [9, 10]. Integrating more variable resources in the power system increases the supply and demand uncertainty significantly. This requires the energy system to have the ability to react to a sudden change and accommodate new states within an acceptable time period and cost. Hence, the notion of flexibility has been receiving significant attention in the recent years.

Power system flexibility is defined as the ability of a system to deploy its resources in response to changes in the net demand [11], wherein a resource expectation index, similar to the Loss of Load Expectation (LOLE) for capacity adequacy, is proposed to assess the flexibility of a system. A comprehensive review of the research on flexibility metrics in both long- and short- terms is presented in [12]. A Monte Carlo simulation (MCS) is proposed in [13], to determine the additional reserve needed to provide flexibility in generating systems with large amounts of renewable energy sources, so that an adequate level of energy supply is ensured. Ramping services that quantifies the difference between the net load in short time intervals have been introduced by some Independent System Operators (ISOs) to procure flexibility services. For instance, a market ramping product, based on the expected scarcity of ramping resources, has been introduced by Mid Continental ISO [14]. A flexible ramp product has also been established by California ISO (CAISO) [15]. In estimating the technical flexibility of both individual generators and the generation mix, based on their ramping and generating capability, a flexibility index is proposed in [9]. Zhao et. al. [10] proposes a flexibility metric to evaluate the largest range of uncertainties that the system

can accommodate, while taking into account transmission network and system operation constraints. The proposed metric is calculated using a robust optimization technique.

The flexibility at the supply side is either from the provision of increased reserve, the construction of transmission, or operational procedures, as investigated in renewable generation integration studies [11, 12]. However, the increasing penetration of RES results in reduced share of controllable generation capacity, and consequently less generation reserves. To circumvent this issue, more flexibility provisions are necessary from the demand side, which has been investigated in the literature. A scheduling model is developed in [16] to exploit demand flexibility from residential devices in a micogrid with a large share of renewable generation. A method is presented in [17] to employ the flexibility service by swapping of electric vehicles charging and heat pumps consumption for congestion management in distribution systems. The congestion is mitigated by reducing consumption at the congested nodes while increasing the same amount of consumption at other nodes, so as to maintain the total power balance.

Energy and reserve provision from flexible buildings for mitigating congestion in distribution grids is studied in [18], using distribution locational marginal prices (DLMP) and iterative DLMP methodologies. The objective was to maximize the utility of the overall system, considering network and load constraints, and energy requirements of the building. However, only flexibility of the buldings' loads was considered. An optimization model is proposed in [19] to coordinate flexible loads of the building with BESS to provide energy arbitrage, frequency regulation and spinning reserve services for power grid, and energy cost and demand charge reduction for end user. Cost savings was achieved from such optimal coordination; and also consideration of demand charge was recommended in addition to time-of-use price to flatten the load profile when providing end user services. An integrated energy management approach is proposed in [20] for residential consumers to make decisions to manage their loads while minimizing their energy bills. A mixed-integer linear programming model is proposed in [21] to integrate the energy flexibility of water distribution system in power system operations, so as to minimize the energy cost of water distribution systems, and reduces the system peak demand and the operation cost of

power systems. A residential energy consumption scheduling algorithm is proposed in [22] to schedule and shift the operation of flexible loads from peak demand hours to hours with high power availability from the PV units, so as to reduce reverse power flow that causes voltage rise problem in the power system.

From the brief review of the literature, it is noted that only flexibility of demand has been considered while transforming loads, in particular commercial and residential loads, to energy hubs, while their associated capital costs and profits have not been investigated in flexibility provisions. Such transformation of loads to energy hubs empower customers to increase their responsiveness in the power system, so as to provide flexibility via interchange of power between the customer and the LDC system operator, when needed, at the distribution grid level.

1.2.2 Energy Hub

An energy hub can be recognized as a generalization or extension of a network node in an electric power system that exchanges power with the surrounding systems, primary energy sources, loads, and other components via multi-energy input and output ports [23, 24, 25]. It is not limited in size and can range from a single household energy system to an entire city energy system. The energy hub provides operational flexibility in such a way that different input energy carriers can be used to provide one output energy carrier. Another aspect of operational flexibility is the fact that the energy hub can simply operate as a classical load, if input and output prices result in unprofitable and infeasible exchanges.

The Energy Hub Management System (EHMS) is a novel concept in smart grids that manages energy hub activities such as production, consumption, storage, and conservation in real-time at lower and upper levels [26, 8, 27, 28]. At the lower level, referred to as hub, the activities of the EHMS are optimized with respect to the customer's preferences. At the upper level, referred to as macrohubs, the energy activities of several hubs are optimized considering the benefits of both the customers and utilities. Mathematical optimization frameworks of EHMSs for different customer sectors, e.g. residential, commercial

and agricultural, are proposed in [8, 27, 28], to optimize the energy activities of the EHMS, according to the customer's preferences and with the objective of minimizing its cost of energy consumption. Major household devices in a residential energy hub are modeled [8] and a mathematical optimization framework that can be solved in real-time to optimally control these energy devices, while taking into account the customer preferences and comfort level is proposed. The authors of [8] also propose a mathematical optimization model of greenhouses in [27], to incorporate it into EHMSs in the context of smart grids, and hence optimize the operation of their energy systems, with an objective of minimizing the total energy costs and demand charges.

An optimal industrial load management model is developed in [28], to incorporate it into EHMSs for industrial customers, in interaction with LDCs, to optimal schedule their processes, while minimizing their total energy costs and/or demand charges. An optimization-based framework for home energy management in the context of a renewable-based energy hub is proposed in [29], with the objective of minimizing the customer's energy cost. The energy hub model includes combined heat and power, a PEV, a heat storage unit, solar panels, and generic household appliances. The role of heat storage and roof top solar panels on customer payment and load profiles are investigated using different cases. However, only the operation of the energy hub from the perspective of a customer for minimizing its energy cost is considered.

Flexibility provisions accrued from transforming a residential load, *i.e.* a house, to operate as an REH were not considered. Inter-relationships between the penetration of REHs for flexibility provisions and the incentives offered by the LDC have not been investigated. There is a need to develop a generic mathematical framework to determine such inter-relationships between residential customers and the LDC, taking into account their respective operational perspectives, system flexibility, and economic benefits from penetrating REHs in distribution systems.

1.2.3 PEVs and Electric Vehicle Charging Facility

PEV penetration is expected to increase significantly in the near future, and given their uncertain charging demand, many technical problems pertaining to their impact on the power grid have been investigated. A full study that includes technical, policy, regulatory, consumer, and market aspects to assess the implication arising from adoption of PEVs in Ontario is reported in [30]. In the context of Ontario, specific measures and policy initiatives are presented and discussed.

To estimate the power and energy consumption of PEVs, an analytical methodology is proposed in [31], wherein the travel patterns of light-duty vehicles in the U.S. extracted from the 2009 National Household Travel Survey (NHTS) [32] is used. Two uncontrolled charging scenarios are considered and simulated for PEVs: One charging scenario is assumed to occur at any time the vehicle is parked at home, while the other takes place at any location such as home, shopping mall, work, etc. An MCS is utilized in[33] to generate virtual trip distances, and takes into account the variations in driving habits, different electric range vehicles, multiple charging events per day, and recharging time variation; hence an annual energy consumption model of light duty fleet of PEVs is presented. A spatial and temporal model based on a fluid dynamic traffic model and queuing theory is proposed in [34] to estimate the PEV charging demand for an EVCF located near a highway exit. In [35], a single plug-in hybrid electric vehicle (PHEV) charging demand model is established, and queuing theory is then employed to describe the behavior of multiple PHEVs. Four different types of PHEVs along with factors that affect their charging behavior are considered and discussed. The design, planning, and operational analysis of an EVCF in distribution systems have been discussed in [36]-[44]. To optimize the siting of EVCFs in a distribution system, a two-stage screening method that takes into account environmental factors and the EVCF service radius is proposed in [36]; then an optimal EVCF sizing model is developed for the short-term, *i.e.*, 3-year horizon. Zheng et al. [37] proposed a model and efficient optimal EVCF planning method with respect to a primarily battery-swapping facility (BSF) in a distribution system. The model includes BSF

locations, sizes, and charging strategies and is formulated as the maximization of the net present value (NPV) during the life cycle of the project. For the planning of an integrated power distribution system and EVCF, a multi-objective collaborative planning model is proposed in [38], with minimization of the overall annual investment costs and energy losses, and maximization of the annual captured traffic flow. Brenna et al. [39] propose an urban-scale integrated EVCF system to examine the potential and technical benefits of using photovoltaic (PV) systems as the energy supplier vis-a-vis the external grid, for charging PEVs. Machiels et al. [40] studied the technical design of an EVCF, including mobility needs. The findings indicated that 99.7% of the PEVs visiting the EVCF could begin charging within 10 min, with a configuration limit of five charging poles; otherwise, additional charging poles are required for the accommodation of PEV drivers who are unwilling to wait. The charging of PEV in an existing office building microgrid equipped with a PV system and a combined heat and power unit is discussed in [41]. Different charging strategies and charging power ratings for workplace charging are examined with regard to their impact on the grid and on the self-consumption of locally generated electricity.

A solar parking lot for efficiently operating a slow EVCF is reported in [42]. The facility presented is a grid-tied parking lot that charges PEVs via an overhead PV array, and then exports the excess power to the main grid. When power shortages occur, power is imported from the main grid. An EVCF equipped with a BESS is considered as a solution for low-voltage feeders with high PV penetration in [43]; a method based on mixed integer linear programming (MILP) is proposed to determine the BESS charging schedule for voltage regulation. Liu et al. [44] studied the function and effect of small-sized superconducting magnetic energy storage system (SMES) in an EVCF that included PV generation. An energy management strategy that focused on the voltage stability of the dc bus and the energy transfer among the resources is developed.

From the aforementioned literature review, it is noted that most of the work concentrated on the technical aspects of EVCF design without taking into account the economic viability of such an investment. Furthermore, there is a need to examine how the EVCF functionalities can be adopted to the smart grid environment considering BESS and other

renewables based DG options in this design, from the perspectives of the investor and the LDC. Also, none of the reported works examined how the charging load profile will impact the EVCF design and the distribution system capability considering realistic penetration of PEVs in the long term.

1.2.4 Intermittency of Wind Generation

Intermittency of supply is an issue particularly applicable to wind generation whose typical forecasting errors, with respect to the final output power, are in the range of 30%-50% [6, 7]. Penalties associated with wind power imbalances, imposed by the system or market operator, increases wind integration costs.

Fast response generators, such as gas turbines or hydro generators were reported in [45, 46] to provide reserve capacity in systems with high wind penetration; which however increased the operation and maintenance cost and emissions from gas turbines. A security constrained unit commitment model was proposed in [47] to study the impacts of Flexible AC Transmission Systems (FACTS) devices on a system with high wind penetration; it was noted that their deployment helped reduce wind energy curtailment. Sizing a battery energy storage system (BESS) to reduce the forecast uncertainty and accommodate high penetration of renewables was studied in [48, 49]. But relying on a BESS alone to compensate for the difference between the forecasted and actual wind generation, required a BESS of large rating and consequent high installation cost. A BESS was also employed in [50] to ensure that WGFs could provide frequency regulation services through a coordinated control strategy. In [51] an approach was proposed to deploy demand response (DR) such that the rebound effect coincided with high wind generation and low demand, and thereby reduced wind energy curtailment; scheduling of both BESS and DR resulted in a further reduction in curtailed wind energy. However, only operational aspects of BESS and DR were studied, and these were assumed to be owned by the system operator.

Ghofrani et al. [7] proposed a framework to mitigate the effects of wind power imbalances using the vehicle-to-grid capability of PEVs, as an alternative to BESS. A robust

scheduling model was proposed in [52] to match PEV charging loads with wind generation and hence reduce the impact of wind variations on the grid. Tavakoli et al.[53] proposed a bid/offer strategy for energy exchange between PEV charging loads and WGFs participating in day-ahead electricity markets to mitigate wind fluctuations and optimize PEV charging schedules. A bi-level, multi-time scale scheduling approach was proposed in [54] to match wind supply with PEV charging demand. A method was proposed in [55] for integrating battery-based energy storage transportation with power system scheduling, so as to optimize power system operations with a high penetration of wind energy.

It is noted from the brief review of literature, that none of the reported works have investigated the technical feasibility and economic viability of flexibility provisions from EVCFs equipped with DERs, for wind integrated power grids. To the best of the author' knowledge, there is no reported work in the literature that takes into account different ownership structures of WGF and EVCF and the resulting operational and financial differences, arising therefrom. Whereas, consideration of ownership aspects can present entirely different perspectives on power system operational objectives, and design of EVCF.

1.3 Research Objectives

The main objectives of the research presented in this thesis are summarized as follows:

- Develop a Vehicle Decision Tree (VDT) using realistic vehicle statistics extracted from the 2009 (US) National Highway Travel Survey (NHTS) data [32] to predict times PEVs need fast charging in rural and urban areas, and develop a Queuing Model (QM) to estimate the charging load for multiple PEVs served at an EVCF, considering medium and high PEV penetration levels in the long-term. Thereafter, examine the effects of PEV penetration levels on the PEV charging demand profile and hence arrive at an appropriate configuration of the EVCF, such as the required number of fast chargers, and the transformer capacity.

- Develop a generic framework for designing the EVCF as a smart energy hub and hence determine the optimal investment decisions and appropriate design options at a specific location in the distribution system, from both the investor's and the LDC's point of view. Furthermore, assess distribution system capability to accommodate multiple EVCFs in the long-term, with and without the new design of EVCFs.

- Create two different ownership structures to study the feasibility of an EVCF equipped with DERs for wind integrated grids, from the perspectives of the WGF and EVCF owners, respectively.

- Develop a generic framework and an associated mathematical optimization model to design the EVCF with DERs, that provides the upward and downward flexibility provisions for hedging wind power forecast uncertainty, in each ownership structure. MCS will be used to investigate the impact of variability and uncertainty of wind and PV generation, and market price, on the optimum design in both ownership structures. Furthermore, investigate the effects of low and high wind imbalance penalties, and different flexibility service prices on the feasibility and economic viability of the design of EVCF with DERs in different ownership structures.

- Develop a generic framework and associated mathematical models to determine the optimal incentives to be offered by the LDC, that will induce an optimal penetration of REHs for flexibility provisions in distribution grids, considering system operations and economic benefits of both the LDC and residential customers.

1.4 Outline of Thesis

The remainder of this thesis is organized as follows: Chapter 2 reviews the background of power system flexibility, DERs and DR, PEV characteristics and their charging level, and theory and analysis pertaining to the research carried out in this thesis. Chapter 3 presents PEV charging load modelling, the proposed framework for designing an EVCF as

a smart energy hub, and findings. Chapter 4 presents a new mathematical model to design an EVCF with DERs to provide flexibility services in wind integrated power grids, under two different ownership structures of the EVCF and WGF. Chapter 5 presents a generic and novel framework to simultaneously determine the optimal penetration of REHs in distribution systems and optimal incentives paid by the LDC to residential customers for flexibility provisions, considering economic benefits of both parties. In Chapter 6, summary and conclusions, main contributions, and directions for future research work are presented.

Chapter 2

Background

2.1 Power System Flexibility

Flexibility is the ability of a system to take an alternative course of action at a given state, within an acceptable cost threshold and time window, in order to respond to a range of uncertain future states [10], [12] and [56]. An overview of flexibility flow in a power system is presented in Figure 2.1. As noted from the figure, the traditional system is characterized by a unidirectional flow of flexibility, *i.e.* from generation to demand side, that comes mainly from controllable power plants. However, with the development of smart grid, a bi-directional flow of flexibility has been introduced in the power system (Figure 2.1). This bi-directional flexibility in modern grids comes from controllable power plants and renewables based DG units in the supply side, and particularly from various resources called DERs in the demand side.

Power system flexibility services include "up regulation" and "down regulation." The former refers to providing additional power as needed to maintain system balance, while the latter refers to reducing the available power supply in the system. System ramping capability is an example of how fast, flexible resources can change the demand or power supply. Ramping is defined as the power change between two consecutive time pe-

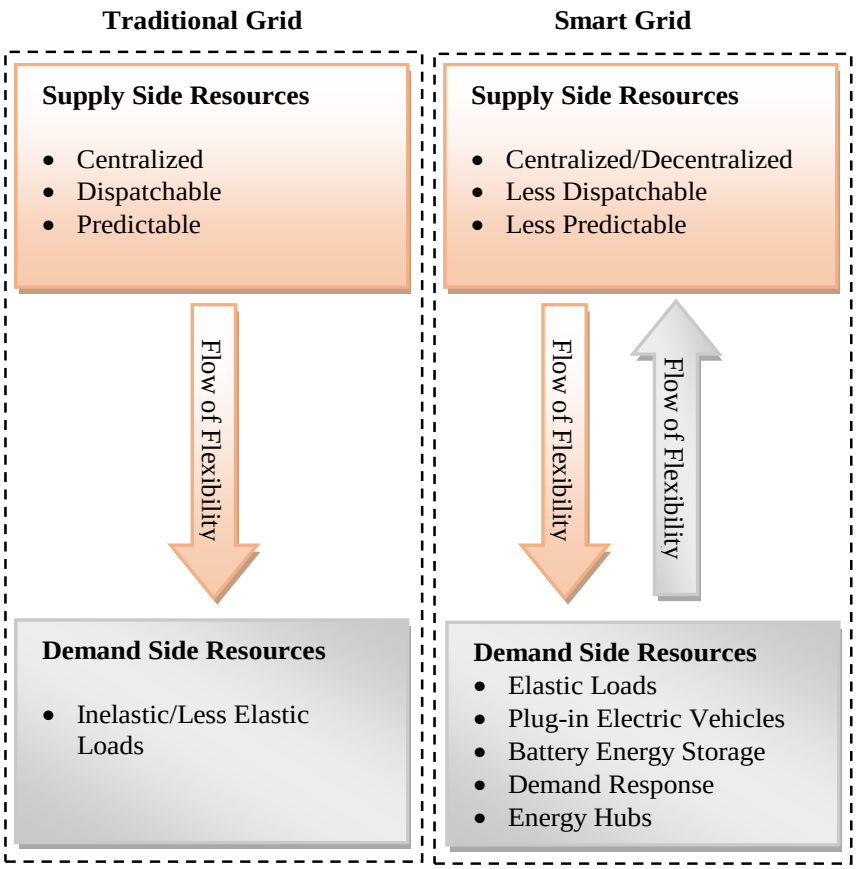

Figure 2.1: An overview of flexibility flow in a power grid.

riods, which could come from either generation or load. The adoption of flexible supply and demand-side technologies will contribute to increased system ramping capability and thereby increased system flexibility.

2.2 Energy Resources and Demand Response

2.2.1 Rooftop PV Generation

Gradual decline in prices of PV generation technologies, rising global warming concerns, and new incentive programs initiated by governments have led to the increased penetration of grid-connected PV systems. The main components of a grid connected PV system are the PV array, and power conditioning unit (PCU), as shown in Figure 2.2 [57]. The solar insolation is the instantaneous solar power received on a unit surface, and is measured in watts per square meter (W/m^2).

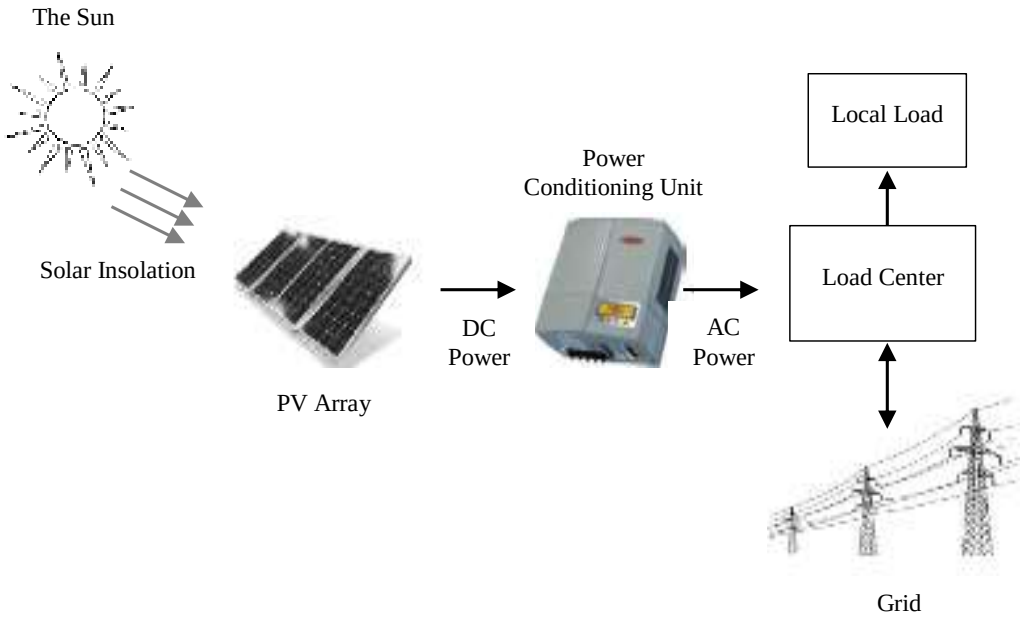

Figure 2.2: Main components of grid connected PV systems

To form a PV module, solar cells are usually connected in series, and then modules are connected in series to form a string. Strings are finally connected in parallel to form a PV array. Interfacing grid-connected PV systems with the utility is by means of PCUs, and hence two basic functions are usually performed using PCUs, controlling the output voltage or current of PV arrays, and converting the dc output of PV arrays into ac power. The former function extracts the maximum power available at a certain temperature and irradiance, whereas the latter function makes the output power of PV arrays suitable to be fed into the utility grid.

A commercial/residential load, when equipped with a rooftop PV system can provide flexibility to the grid; the rooftop PV generation can supply the local load and export the excess power when available. However, due to the high degree of variability associated with PV generation, and its peak output power that does not coincide with the system peak demand, equipping energy storage with the rooftop PV generation can further benefit from both parties in providing flexibility to the power system. These resources, PV generation and the energy storage in coordination, are the main elements of flexibility provision in the context of a smart energy hub.

2.2.2 Energy Storage System (ESS)

Energy storage technologies have the potential to support large-scale integration of renewables in power systems, and provide some level of system flexibility. There is a wide range of technologies for energy storage; each with its own characteristics. Generally, any ESS comprises energy storage reservoir and power conversion system that is either a dc-ac converter or a motor-generator set, depending on the ESS type. For instance, superconducting magnetic energy storage (SMES) and batteries have the dc-ac converter. On the other hand, pumped hydro, compressed air energy storage (CAES), and flywheels [58], have the motor-generator set. ESSs can be classified as static or dynamic devices, according to their physical construction. Static ESS include SMES, capacitors, and batteries, while examples of dynamic ESS are pumped hydro, CAES, and flywheels. As no moving parts are

associated with static devices, they have relatively low operation and maintenance (O&M) costs, in comparison to the dynamic ESS. Furthermore, the dynamic ESS have a lower efficiency than the static ESS because of mechanical and friction losses [59].

The applications of ESS in the power system can be divided into three categories: bridging power, energy management, and power quality [60]. The ESS can be used to bridge power when switching from one power source to another, *i.e.*, about seconds to minutes, and hence ensure the continuity of power supply. Energy management applications use the energy stored during off-peak periods at times of peak load. Finally, the ESS can be used to mitigate power quality problems such as voltage and frequency variations in time durations of seconds or less. The selection of a specific ESS technology is solely based on the application.

As the main focus of this thesis is on flexibility provisions on an hourly basis or energy management applications, batteries are chosen as the candidate ESS technologies. The mathematical equations of BESS operation are presented below [61]

BESS Balance Constraint: This constraint ensures that the BESS state of charge (SOC) at the next hour is equal to its SOC at the current hour plus/minus the charged/discharged energy from/to the BESS at that hour.

$$SOC_{k+1} = SOC_k + (P_k^{in}\eta^{in} - P_k^{out}/\eta^{out})\Delta T \qquad \forall k \tag{2.1}$$

$$0.2C^E \leq SOC_k \leq C^E \qquad \forall k \tag{2.2}$$

BESS Power Limits and Initial/Final Status of the SOC: The power drawn or discharged by/from the BESS is constrained by the limits, as follows:

$$P_k^{in} \leqslant Psize^{BESS} \qquad \forall k \tag{2.3}$$

$$P_k^{out} \leqslant Psize^{BESS} \qquad \forall k \tag{2.4}$$

The initial and final status of the SOC is assumed to be 50% of BESS energy capacity.

Hence,

$$SOC_k = 0.5C^E \qquad \forall k = 1 \quad \& \quad k = 24, \tag{2.5}$$

2.2.3 Demand Response (DR)

The concept of DR or DSM refers to modifying the load demand to increase customers satisfaction and simultaneously producing desired changes in the load shape of the electric utility [62]. Increased flexibility can also come from effective DR programs over short timeframes when an unpredictable change in the net load occurs. Two categories of DR programs can be distinguished [63]: direct, and indirect, also referred to as price-based DR. The classification of DR depends on whether the alteration of the demand is a utility decision or a choice of the customers. Direct DR programs reduce the need for investment in peaking generation capacity, and are used when system reliability is being jeopardized. Since direct DR impacts the customers' comfort, incentives are offered to encourage them to participate which thereby allow the utility to take control over a portion of their load. Examples of direct DR programs are the Direct Load Control (DLC) and Interruptible Load (IL) programs [64], and the Peaksaver Plus program in Ontario, Canada [65]. On the other hand, customers can also take decision through indirect DR programs to adjust their demand levels depending on price changes, which are referred to as price-based DR. Time-of-Use and Real Time Pricing schemes are examples of indirect DR program [66]-[67].

PEV charging demand, particularly slow charging at home or parking lot, can be assumed to be a flexible demand and hence can also be considered in DR programs. However, fast charging demand is assumed to be inflexible because of the short stay of PEVs at an EVCF.

2.3 Plug-in Electric Vehicles (PEVs)

Fossil fuel depletion and environmental concerns make PEVs a promising future direction for the transportation sector, as they have the potential to reduce the dependency of the sector on fossil fuels and thereby reduce emissions. Energy efficiency, low cost recharging capability, and overall reduced cost of operation, are factors leading to the popularity of PEVs.

2.3.1 PEV Types

PEVs are generally grouped into three classes: Battery Electric Vehicles (BEV), Hybrid Electric Vehicles (HEV), and PHEV [30]. A typical BEV has a battery to store energy that is transformed into mechanical power through an electric motor, without the need for internal combustion engines. A battery charger is used to energize the batteries from the grid. The BEV has a simple design and a low part count, but its driving range depends on the size of the battery and may take a few hours for recharging, depending on the battery SOC, type, and charging level [68]. HEVs help to reduce gasoline consumption by virtue of their ability to recover a substantial amount of kinetic energy in the battery storage system using regenerative braking. PHEVs are variants of HEVs, but include a battery to attain a large All Electric Range (AER) capability for the portion of driving trip, and a plug-in charger used to draw power from the grid; making them bi-fuel vehicles that are operated even when the battery is fully depleted. This allows PHEVs to operate on electric mode and reduce fuel consumption as much as possible. PHEVs are characterized based on their AER; for instance, a PHEV that can drive x miles solely on electricity is referred to as PHEV-x. Hence, PHEV20, PHEV30, or PHEV60 donates electric vehicles that can drive on electricity, up to 20, 30, or 60 miles, respectively [30].

2.3.2 PEV Charging Levels

Three levels of PEV charging are available and commonly used [69], and their specifications are listed in Table 2.1. The duration of charging is directly affected by the charging level; a higher charging level reduces the charging time.

Table 2.1: PEV Charger Ratings

Charging Level	Specifications
Level 1	• 110/120 V, AC, 15-20 amp • Does not require installation for residential charging • Takes 8-12 hours for typical charging times, which results in reduced battery life and performance
Level 2	• 208-240 V, AC, 15-30 amp • Requires special installation, *e.g.* an upgrade of a household electric outlet • Takes 3-8 hours for typical charging times • May also be found in public charging facility
Level 3	• Referred to as "DC fast charging" • 440 V, DC, 125 amp, 50 kW or higher • Requires specific installation, and several companies design these facilities and offering them to customers • Expected to attain 50% SOC in a few minutes

2.4 Queuing Theory

An inevitable component of modern life is queue or waiting line. Queuing phenomena exists in real-life situations where there are limited resources that cannot instantly render the amount or the kind of services requested by their users. Examples of these resources are machines at a factory, elevators, telephone lines, etc. Also, in modern communication

systems, messages or emails are transmitted from one computer to another by queuing them up inside the network in a complicated fashion, and hence queues are not just for humans [70]. A queuing system typically involves a stream of customers that arrives at a facility service, get served according to a given service discipline, and then depart the system within a time interval. A shorthand notation to characterize a range of queuing models is introduced by Kendall [71], which are a three-part code a/b/c. The inter-arrival time distribution and the service time distribution are specified, respectively, in the first and the second letter. For instance, letter G is used for a general distribution, M for the exponential distribution and stands for Memoryless, and for deterministic distribution, letter D is used. The number of servers is specified in the third or last letter. Some examples of queuing models are M/M/1, M/M/c, M/G/1, G/M/1, and M/D/1. Also, an extra letter can be added to the notation to cover other queuing models. This extra letter is used when having waiting room with limited N customers. An example of such queuing model is M/M/1/N or M/M/c/N. The facility service might consist of one or more servers, and finite or infinite capacity. Among others and generally, the following factors characterize a queuing model:

- Arrival process of customers: the inter-arrival times are usually assumed to be independent and have a common distribution. In many practical situations, customers arrive based on a Poisson stream, *i.e.* exponential inter-arrival times. Customers may arrive one at a time, or in batches such as plane passengers who have to be checked at the customs office at the airport.

- Service times: The service times are usually assumed to be identically distributed, and independent of inter-arrival times. The service times can be deterministic or exponentially distributed.

- Service discipline: There are many possibilities for the order in which customers enter service, such as first come first served, or priorities (*e.g.* rush orders first, shortest processing time first).

- Service capacity: There may be a single or a group of servers providing services to customers.
- Waiting space or room: There could be limitations with respect to the number of customers in the system. For instance, only a finite number of cells can be buffered in a switch in a data communication network.

The *M/M/c* queuing model is used to the research problems presented in this thesis, due its suitability. Based on the QM formulation [71], the system is stable if and only if the occupation rate of the fast chargers is less than unity, the occupation rate denotes the probability that a fast charger is occupied. The probability can be determined for each hour by dividing the probabilistic arrival rate of PEVs at the EVCF by the number of identical fast chargers at the EVCF and by the charging service rate, and can be expressed as follows:

$$\psi_k = \frac{\lambda_k}{c\mu_k} \leq 1 \tag{2.6}$$

Based on (2.6) and a sufficient condition for the stability of the QM, the minimum number of fast chargers that ensures a stable EVCF queuing system [70] should adhere to the following inequality:

$$c > \frac{\lambda_k}{\mu_k} \tag{2.7}$$

The determination of the expected number of occupied fast chargers is based on a limiting-state probability that n discharged PEVs are present at the EVCF [70]:

$$P_{n,k} = \begin{cases} \frac{1}{n!}(\frac{\lambda_k}{\mu_k})^n P_0 & if \;\; 0 \leq n \leq c-1 \\ \\ \frac{1}{c!c^{n-c}}(\frac{\lambda_k}{\mu_k})^n P_0 & if \;\; n \geq c \end{cases} \tag{2.8}$$

where P_0 is defined as follows:

$$P_0 = [\sum_{n=0}^{c-1} \frac{1}{n!}(\frac{\lambda_k}{\mu_k})^n + \frac{1}{c!}(\frac{\lambda_k}{\mu_k})^c(\frac{c\mu_k}{c\mu_k - \lambda_k})]^{-1} \tag{2.9}$$

If n discharged PEVs are present at the EVCF, the number of occupied fast chargers is given by $\min(n, c)$. The expected number of occupied fast chargers $E[Z]$ can hence be calculated as follows:

$$E[Z_k] = \sum_{n=0}^{\infty} P_{n,k} min(n, c) = \frac{\lambda_k}{\mu_k} \tag{2.10}$$

The last step is to estimate the power demand (PD^{PEV}) of the EVCF by multiplying the average power per fast charger by the expected number of occupied fast chargers, as follows:

$$PD_k^{PEV} = E[Z_k]P^{AVG} \tag{2.11}$$

2.5 Optimal Power Flow

The optimal power flow (OPF) problem is a static, non-linear programming (NLP) problem, that determines the state of the power system operation, according to a given criteria, for instance, minimum cost, while not violating the system or equipment operating limits. Based on the specific application domain, the control/decision variables are selected. As examples of control variables are the active power generated by the available generators (*i.e.* optimal power dispatch), or the optimal location of generator resources (*i.e.* planning studies). The inequality constraints include voltage limits, active and reactive power generation limits, and the maximum power flow on transmission lines. Furthermore, the control and dependent variables should satisfy the power flow equations which represent the equality constraints. The OPF objective functions could integrate both technical and economic criteria, such as the production costs minimization, the minimization of transmission line losses, or voltage deviations minimization. The OPF model can be mathematically written

as follows [72]:

Objective Functions: Minimize the system power losses, as follows:

$$Min\frac{1}{2}\sum_{i\varepsilon N}\sum_{j\varepsilon N}G_{ij}\left[V_i^2+V_j^2-2V_iV_{j,k}\cos(\delta_j-\delta_i)\right] \tag{2.12}$$

Power Flow Equations: The power injected at a bus is governed by traditional power flow equations, as follows:

$$Pg_i-Pd_i=\sum_{j=1}^{N}V_iV_jY_{i,j}\cos(\theta_{i,j}+\delta_j-\delta_i)\qquad \forall i\varepsilon N \tag{2.13}$$

$$Qg_i-Qd_i=-\sum_{j=1}^{N}V_iV_jY_{i,j}\sin(\theta_{i,j}+\delta_j-\delta_i)\qquad \forall i\varepsilon N \tag{2.14}$$

Feeder Capacity Limits: These constraints ensure that the power flow through any line complies with the capacity limit of the line:

$$P_{i,j}^F=-V_i^2Y_{i,j}cos\theta_{i,j}+V_iV_jY_{i,j}cos(\theta_{i,j}+\delta_j-\delta_i)\qquad \forall(i,j)\in N:\exists(i,j) \tag{2.15}$$

$$Q_{i,j}^F=V_i^2Y_{i,j}sin\theta_{i,j}+V_iV_jY_{i,j}sin(\theta_{i,j}+\delta_j-\delta_i)\qquad \forall(i,j)\in N:\exists(i,j) \tag{2.16}$$

$$S_{i,j}^F\leq S_{i,j}^{F_{Cap}}\qquad \forall(i,j)\in N:\exists(i,j) \tag{2.17}$$

Limits on Active and Reactive Power: These limits ensure that the total power/reactive is within their generator limits:

$$Pg_i^{Min}\leqslant Pg_i\leqslant Pg_i^{Max}\qquad i\forall N \tag{2.18}$$

$$Qg_i^{Min}\leqslant Qg_i\leqslant Qg_i^{Max}\qquad i\forall N \tag{2.19}$$

Voltage Limits: The bus voltage limits are given as follows:

$$V^{Min} \leqslant V_i \leqslant V^{Max} \qquad i \forall N \tag{2.20}$$

2.6 Summary

In this chapter, an attempt was made to present an overview of power system flexibility, followed by rooftop PV system and BESS as they are two of the essential features of smart energy hubs. A brief overview of DR; PEVs, its types and charging levels were also presented given their relevance to the present research. Thereafter, a brief background on queuing theory and OPF was presented.

Chapter 3

Electric Vehicle Charging Facility as a Smart Energy Hub [1]

3.1 Introduction

In light of the growing concerns of global warming and depletion of petroleum resources, PEVs have been receiving significant attention in recent years. It is recognized that comprehensively designed EVCFs are vital for facilitating PEV penetration and their public acceptance. Investigating the feasibility of future accommodation of multiple EVCFs in power grids is important. Because fast charging occurs most frequently during evening hours, often coinciding with the peak demand, a distribution system planner must know how much load is expected to be served, as penetration of PEVs are expected to increase over the coming years. EVCFs can also serve as sources of capacity support for the distribution system when they are equipped with BESS and/or PV generation. An EVCF can provide such capacity support through appropriate considerations at the design stage by

[1] This chapter has been published in: W. Alharbi and K. Bhattacharya, "Electric vehicle charging facility as a smart energy microhub," *IEEE Transactions on Sustainable Energy*, vol. 8, no. 2, pp. 616-628, April 2017.

proper sizing of BESS and PV units. However, a more efficient way would be to control the PEV charging demand and offer a capacity support service to the distribution system during critical conditions. Such a design of an EVCF renders it a smart energy hub, providing flexibility to the distribution system and deferring upgrades. Such design may also contribute to decreased EVCF operating costs because of PV generation and energy from BESS.

However, the following research questions often arise with respect to EVCF design: Would such design be economically viable for an investor while also being technically acceptable for the LDC? Furthermore, when multiple EVCF locations are under consideration, to what extent can the distribution system accommodate the EVCFs? What EVCF design is most appropriate at a specific location in order to provide mutual benefits to both the investor and the LDC? What power and energy size of a BESS and/or PV generation are needed at an EVCF location?

The primary focus of this chapter is to address these research questions. A simple architecture of the EVCF as a smart energy hub is presented in Figure 3.1. The smart energy manager, which is the central controller, is the main control interface between the grid and the EVCF energy resources. It has the responsibility of optimizing the operation of the smart energy hub.

The primary objectives of the work presented in this chapter are as follows:

- Model the fast charging demand profile by coupling a VDT and a QM, considering medium and high PEV penetration levels in the long-term. The proposed VDT uses realistic vehicle statistics extracted from [32] to predict the times when PEVs need fast charging in rural and urban areas. The QM is developed to estimate the charging load for multiple PEVs served at an EVCF.

- Examine the effects of PEV penetration levels on the PEV charging demand profile and hence arrive at an appropriate configuration of the rapid EVCF, such as the required number of fast chargers, and the transformer capacity.

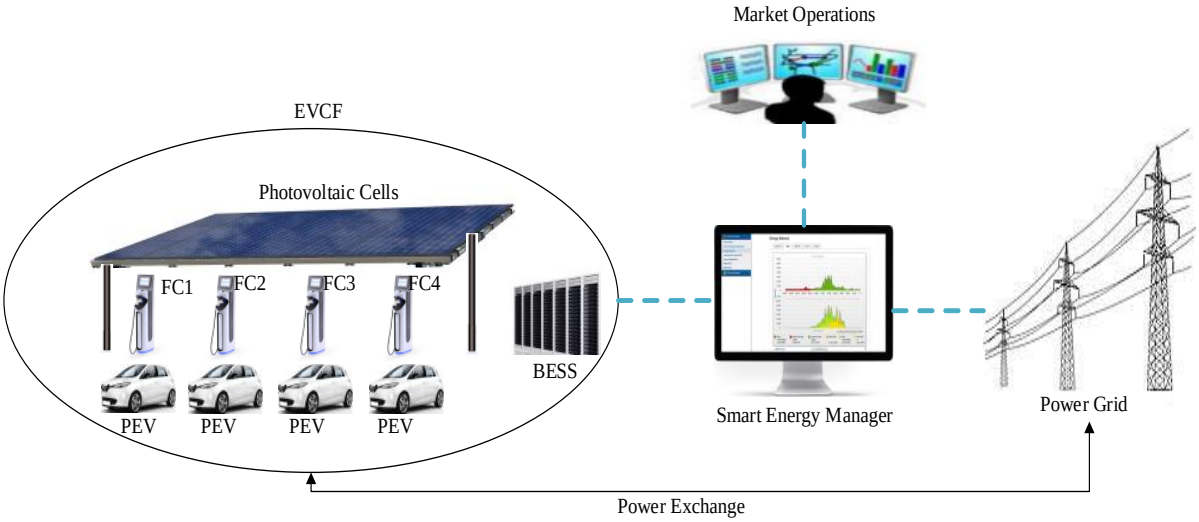

Figure 3.1: A simple architecture of the EVCF as a smart energy hub.

- Propose a novel framework for designing the EVCF as a smart energy hub and hence determine the optimal investment decisions and appropriate design options at a specific location in the distribution system, from both the investor's and the LDC's point of view.
- Assess distribution system capability to accommodate multiple EVCFs in the long-term, with and without the new design of EVCFs.

3.2 Proposed Framework

The proposed framework includes a Vehicle Decision Tree (VDT), QM, a Distribution Margin Assessment Model, a DG Penetration Assessment Model, an Economic Assessment Model (EAM), and a Distribution Operations Model. Figure 3.2 shows the architecture of the proposed framework, the linkages between the models, the input parameters, and the output decisions associated with them. The probability of PEV arrival per hour (λ) at an EVCF is modeled based on a VDT that uses realistic vehicle statistics extracted from [32].

The QM expresses the overall charging process for multiple PEVs served at the EVCF and estimates the expected PEV charging demand. The Distribution Margin and DG Penetration Assessment Models determine the maximum load serving capability and the maximum DG capacity that can be accommodated, respectively, at an EVCF bus over the planning period. The EAM facilitates a prospective investor to arrive at an optimal plan with respect to investment in new design of an EVCF. The Distribution Operations Model evaluates the effectiveness of the new EVCF design for distribution system operations and determines the desirable design options from the LDC's perspective. The five mathematical models are discussed in detail in the following subsections.

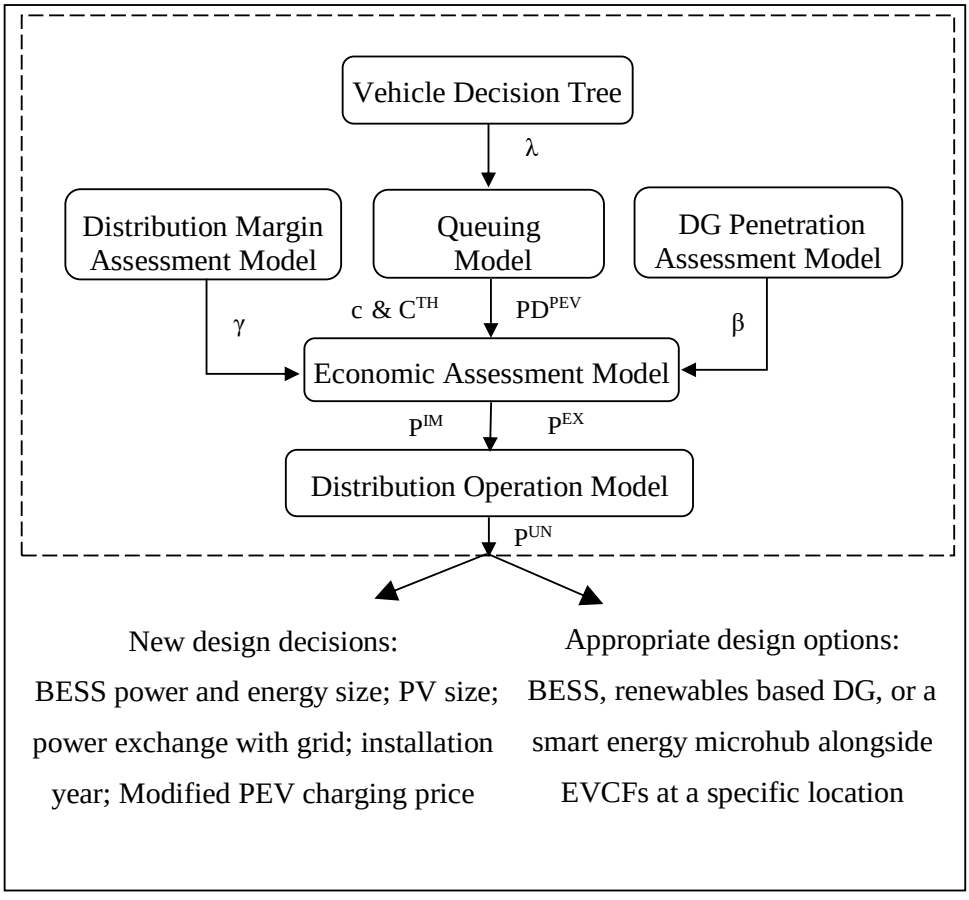

Figure 3.2: Architecture of the proposed framework for new design decisions of an EVCF

3.2.1 Vehicle Decision Tree (VDT)

To estimate the probabilistic arrival rate of PEVs per hour, detailed transportation data is needed. The distribution of trip distances, the time-of-day distribution of the trips, and the number of trips associated with each vehicle are extracted from [32] and are used for predicting the required times for PEV fast charging. Because of the lack of data pertaining to the travel patterns of PEVs, these are assumed to be similar to those of traditional vehicles, thus enabling the use of the same NHTS data set. The λ parameter is modeled using the proposed VDT, as presented in Figure 3.3.

For each trip, the battery SOC of a PEV is checked considering its distance-driven mileage, and when the PEV depletes the entire SOC window, either the start time or the end time of that trip is recorded. For example, if the PEV depletes its SOC before finishing the trip, the start time of that trip will be recorded for a fast charge. However, if the trip is completed prior to depletion, the finish time of that trip is recorded instead. This helps to avoid trip interruptions.

However, since no geospatial data was available for correlating the distance of the vehicles from a central charging facility, the outcome of the VDT is presented as the probability of a vehicle call for charging, rather than that of a vehicle arrival at the EVCF. To compensate for the missing distance correlation between the PEV and the EVCF, the following points have been taken into consideration:

- Point-a: The exact time between a PEV call for a fast charge and the arrival of that PEV at an EVCF is unknown and is dependent only on the distance from the point of the call to the EVCF. Therefore, the hour, rather than the minute, when the PEV calls for a fast charge is considered for estimating the probability of a PEV arrival at an EVCF each hour, based on the assumption that the PEV will definitely reach the local EVCF within that one-hour calling window.

- Point-b: US gasoline fueling facilities numbered nearly 160,000 in 2010 [73], or about one facility for every 1500 vehicles. Assuming a similar use of one or two fills per

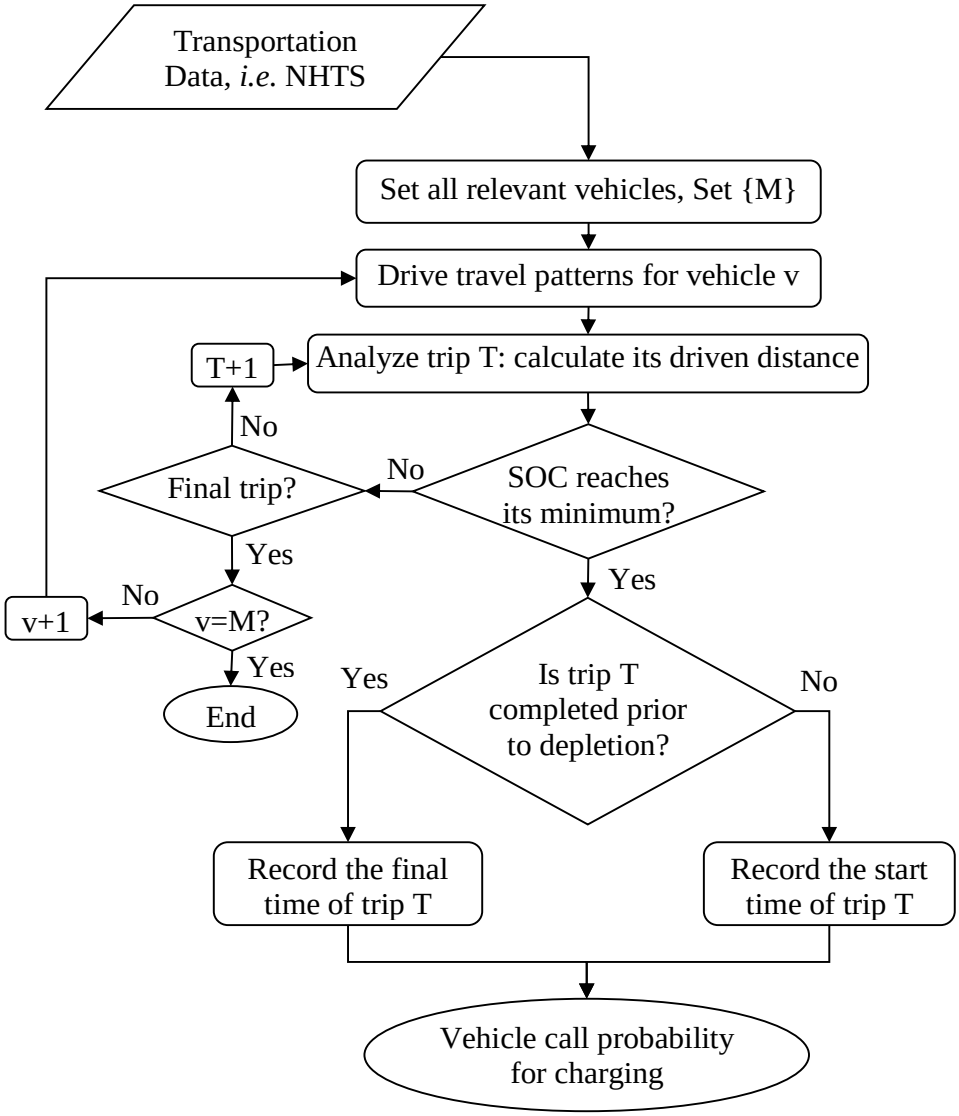

Figure 3.3: Flow chart of the proposed Vehicle Decision Tree (VDT)

week, one EVCF is chosen for addressing the needs of a few hundred PEVs. In this work, each EVCF is considered to be serving up to 20% of the total forecasted number of vehicles in the distribution system, which represents the transformation percentage for a few hundred PEVs, for each year of the planning period.

In such a design-planning problem, from the EVCF investor's perspective, in order to estimate the expected demand, two important pieces of information must be known: when the charging demand is expected to take place, and how much power is required. The VDT for the first consideration (Point-a) estimates when the charging demand will take place for each hour, while the VDT for the first and second considerations (Point-a and b) determines how many PEV arrivals will occur per hour. The results are then incorporated into the QM for use in the estimation of the PEV charging demand.

Essentially, the EVCF is considered to be similar to a gas station, where the PEV driver arrives to charge and then leaves, without the possibility of shifting its demand to time periods that are favorable to the LDC. As a result, DR is not considered as an option in this thesis in the transformation of an EVCF to a smart energy hub.

3.2.2 Queuing Model

Queuing theory is employed to describe the overall process of charging multiple PEVs served at a rapid EVCF. Using the VDT and M/M/c queuing theory, the expected PEV charging demand is estimated. PEVs at an EVCF can be considered queuing customers that may have to wait at the EVCF in order to charge their batteries. In line with reported research [35] and [36], the following conditions are assumed at the EVCF:

- PEV inter-arrival times are independent and exponentially distributed because the arrival of one PEV carries no information about the arrival of another, hence making it a Poisson process.

- For the same reason, the hourly service rates for charging PEVs at an EVCF are independent and exponentially distributed, and are also categorized as Poisson process.
- The EVCF has c identical fast chargers.
- A first-come-first-served rule is applied for charging PEVs, which form a single queue upon arrival.

These assumptions allow the charging service at an EVCF to be modelled as an M/M/c queuing model. The mathematical equations of the QM were presented in Chapter 2, Subsection 2.3.1, from equation (2.6) to equation (2.11).

3.2.3 Technical Assessment Models of a Distribution System

Two mathematical models are developed to determine the maximum load serving capability and DG capacity that can be accommodated at a fast charging facility bus, over the planning period, as follows:

Distribution Margin Assessment Model

Objective Function: This model seeks to maximize the load serving capability (γ) at a fast charging facility bus in the distribution system, as follows:

$$Max \sum_{l \in N} \sum_{k \in K} \sum_{s \in S} \sum_{y \in Y} \gamma_{l,k,s,y} \tag{3.1}$$

The following constraints apply:

Power Flow Equations: These constraints ensure that the power injected at the substation bus and net of the load is governed by traditional power flow equations.

$$P_{ss,k,s,y} - Pd_{i,k,s,y} - \gamma_{l,k,s,y} = \sum_{j=1}^{N} V_{i,k,s,y} V_{j,k,s,y} Y_{i,j} \cos(\theta_{i,j} + \delta_{j,k,s,y} - \delta_{i,k,s,y}) \qquad i\forall N, \forall k, \forall s, \forall y \tag{3.2}$$

$$Q_{ss,k,s,y} - Qd_{i,k,s,y} = -\sum_{j=1}^{N} V_{i,k,s,y} V_{j,k,s,y} Y_{i,j} \sin(\theta_{i,j} + \delta_{j,k,s,y} - \delta_{i,k,s,y}) \qquad i\forall N, \forall k, \forall s, \forall y \tag{3.3}$$

Feeder Capacity Limits: These constraints ensure that power flow through any distribution feeder complies with the feeder capacity limit.

$$P^{F}_{i,j,k,s,y} = -V^{2}_{i,k,s,y} Y_{i,j} cos\theta_{i,j} + V_{i,k,s,y} V_{j,k,s,y} Y_{i,j} cos(\theta_{i,j} + \delta_{j,k,s,y} - \delta_{i,k,s,y}) \\ \forall (i,j) \in N : \exists (i,j), \forall k, \forall s, \forall y \tag{3.4}$$

$$Q^{F}_{i,j,k,s,y} = V^{2}_{i,k,s,y} Y_{i,j} sin\theta_{i,j} + V_{i,k,s,y} V_{j,k,s,y} Y_{i,j} sin(\theta_{i,j} + \delta_{j,k,s,y} - \delta_{i,k,s,y}) \\ \forall (i,j) \in N : \exists (i,j), \forall k, \forall s, \forall y \tag{3.5}$$

$$S^{F}_{i,j,k,s,y} \leq S^{F_{Cap}}_{i,j} \qquad \forall (i,j) \in N : \exists (i,j), \forall k, \forall s, \forall y \tag{3.6}$$

Substation Capacity Limit: This ensures that the total power delivered by the substation transformer is within the capacity limit of the substation.

$$P^{2}_{ss,k,s,y} + Q^{2}_{ss,k,s,y} \leqslant (S^{SS_{Cap}}_{ss})^{2} \qquad \forall k, \forall s, \forall y \tag{3.7}$$

Voltage Limits: The bus voltage constraints are defined as follows:

$$V^{Min} \leqslant V_{i,k,s,y} \leqslant V^{Max} \qquad i\forall N, \forall k, \forall s, \forall y \tag{3.8}$$

The above model given by (3.1)-(3.8) is a NLP model which is coded in GAMS and solved using the MINOS solver.

DG Penetration Assessment Model

Objective Function: Maximize the DG capacity (β) which can be accommodated at an EVCF bus, over the planning period in the distribution system, as follows:

$$Max \sum_{l\in N}\sum_{k\in K}\sum_{s\in S}\sum_{y\in Y}\beta_{l,k,s,y} \tag{3.9}$$

Real Power Flow Equation:

$$P_{i,k,s,y} - Pd_{i,k,s,y} + \beta_{l,k,s,y} = \sum_{j=1}^{N} V_{i,k,s,y}V_{j,k,s,y}Y_{i,j}\cos(\theta_{i,j} + \delta_{j,k,s,y} - \delta_{i,k,s,y}) \qquad i\forall N, \forall k, \forall s, \forall y \tag{3.10}$$

Maximum Reverse Power Flow Constraint: This constraint limits the allowable DG penetration which causes the maximum reverse power flow for the minimum load condition. The minimum load condition occurs at the first year (y=1) in this work. The maximum reverse active power flow is limited to 60% of the main substation rating, as per technical specifications of Hydro One [74]. Hence,

$$\sum_{l\in N}\beta_{l,k,s,y} \leqslant \sum_{l\in N} Pd^{Min}_{i,k,s,1} + 0.6S^{Cap}_{ss} \tag{3.11}$$

Maximum Bus Connection Constraint: According to the voltage level and the technical constraints associated with the LDC, the maximum capacity of the DG connection at any bus is limited by:

$$\beta_{l,k,s,y} \leqslant P_l^{DG^{Max}} \qquad \forall l \tag{3.12}$$

In addition to the above, equations (3.3) to (3.8) are also included in this model.

3.2.4 Economic Assessment Model

Objective Function: Maximize the NPV of an investor's profit, over the useful life of the new design of the EVCF, as follows:

$$Max \sum_{y=1}^{Y} \frac{Revenue_y - Cost_y}{(1+\alpha)^y} \tag{3.13}$$

where $Revenue_y$ includes the revenue accured from charging PEVs and exporting power to the main grid, as given by:

$$Revenue_y = ([\sum_{k=1}^{24} \sum_{s=1}^{2} \rho_{k,s}^{PEV} \cdot PD_{k,s}^{PEV}] \cdot Nd_s)_y + \rho \cdot E_y^{EX} \tag{3.14}$$

In (3.13), $Cost_y$ represents the installation, maintenance and operation costs of the EVCF; hence:

$$Cost_y = Cost_y^{Inv} + Cost_y^{O\&M} \tag{3.15}$$

where

$$Cost_y^{Inv} = IC^E \cdot NC_y^E + IC^P \cdot NC_y^P + IC^{PV} \cdot NC_y^{PV} \tag{3.16}$$

$$\begin{aligned} Cost_y^{O\&M} = {} & OM^f \cdot Psize_y^{BESS} + M^{TH} + M^{FC} + OM^{PV} \cdot C_y^{PV} \\ & + ([\sum_{k=1}^{24} \sum_{s=1}^{2} \rho_{k,s}^{MG} . P_{k,s}^{IM} + OM^v \cdot \eta^{out} \cdot P_k^{out}] Nd_s)_y + (\rho + 0.5) E_y^{SH} \end{aligned} \tag{3.17}$$

The first and second terms of (3.16) denote the installation cost of the BESS, based on the power rating and energy capacity, while the third term represents the installation cost of PV generation. Charging facility operating and maintenance costs are denoted by

(3.17), which includes the fixed cost of the BESS, maintenance cost of the transformer and fast charger, the operating and maintenance costs of PV generation, operation cost of the BESS, and the cost of importing power from the main grid, and the cost of shedding PEV charging loads which may occur when the PV generation (Design-2) is only considered. The cost of PEV energy shedding is considered to be higher than the energy export price, in order to limit this action for solution feasibility only. The energy shedding is defined as:

$$E_y^{SH} = \sum_{k=1}^{24} \sum_{s=1}^{2} P_{k,s,y}^{SH} \tag{3.18}$$

The following constraints apply

Demand Supply Balance: Total generation meets the demand at period k, on winter and summer days in year y.

$$P_{k,s,y}^{PV} + P_{k,s,y}^{out} + P_{k,s,y}^{IM} + P_{k,s,y}^{SH} = PD_{k,y}^{PEV} + P_{k,y}^{in} + P_{k,y}^{EX} \qquad \forall k, \forall y \tag{3.19}$$

where $P_{k,s,y}^{PV} = \varphi_{k,s}^{PV} C_y^{PV}$

Distribution Grid Interaction Limits: Two mathematical models, the Margin and DG Penetration Assessment models, are developed and first executed, for an accurate representation of the grid interaction limits with an EVCF at a given bus, over the planning period, so as to avoid oversizing or undersizing the power rating and energy capacity of BESS, and the capacity of PV generation for the EVCF. These constraints are given by:

$$0 \leq P_{k,s,y}^{IM} \leq \gamma_{k,s,y} \cdot u_{k,s,y}^{IM} \qquad \forall k, \forall s, \forall y \tag{3.20}$$

$$0 \leq P_{k,s,y}^{EX} \leq \beta_{k,s,y} \cdot u_{k,s,y}^{EX} \qquad \forall k, \forall s, \forall y \tag{3.21}$$

$$u_{k,s,y}^{IM} + u_{k,s,y}^{EX} \leq 1 \qquad \forall k, \forall s, \forall y \tag{3.22}$$

Energy Export Limits: These limits ensure that the energy exported is only from the solar PV generation and does not include the BESS energy. Since there is no incentive price yet for installing a BESS in Ontario, these constraints ensure that the contract price of Ontario PV generation cannot be used for exporting power to the main grid from the BESS. Moreover, it would be unprofitable to use the Hourly Ontario Electricity Price (HOEP) for exporting power to the main grid from the BESS, as compared to its high installation costs. Thus, the BESS is solely used for managing the EVCF energy consumption and not for selling energy to the main grid.

$$E_y^{EX} \leq \eta^{PV}[\sum_{k=1}^{24}\sum_{S=1}^{2} P_{k,s,y}^{PV}] \qquad \forall y \tag{3.23}$$

$$E_y^{EX} = \eta^{PV}[\sum_{k=1}^{24}\sum_{s=1}^{2} P_{k,s,y}^{EX}] \qquad \forall y \tag{3.24}$$

BESS Balance Constraint: This constraint is formulated using a simplified book-keeping model for the SOC of the BESS as follows [61]:

$$SOC_{k+1,s,y} = SOC_{k,s,y} + (P_{k,s,y}^{in}\eta^{in} - P_{k,s,y}^{out}/\eta^{out})\Delta T \qquad \forall k, , \forall s, \forall y \tag{3.25}$$

$$0.2C^E \leq SOC_{k+1,s,y} \leq C^E \qquad \forall k, \forall s, \forall y \tag{3.26}$$

where is $\triangle T$ considered to be one hour for this study.

BESS Power Limits and Initial/Final Status of SOC: The power drawn or discharged by the BESS is constrained by the limits, as:

$$P_{k,s,y}^{in} \leqslant Psize_y^{BESS} \;\; ; \;\; P_{k,s,y}^{out} \leqslant Psize_y^{BESS} \qquad \forall k, \forall s, \forall y \tag{3.27}$$

Initial and the final status of SOC is assumed to be 50% of BESS energy size. Hence,

$$SOC_{k+1,s,y} = 0.5C_y^E \qquad \forall k = 1 \;\; \& \;\; k = 24, \forall s, \forall y \tag{3.28}$$

Energy to Power Ratio of BESS and Maximum Discharge Time: Each battery technology has a specific range of energy-to-power ratios and maximum discharge times. The range of the energy size for a specific power size is thus constrained as follows:

$$\underline{EPR} \cdot Psize_y^{BESS} \leqslant C_y^E \leqslant \overline{EPR} \cdot Psize_y^{BESS} \tag{3.29}$$

This constraint also determines the maximum discharge time at the rated power.

Dynamic Constraint on BESS Capacity Additions: These limits ensure that the solar PV capacity, and the power and energy capacity of the BESS for the next year are the cumulative sum of the new capacity installed plus the existing capacity.

$$C_{y+1}^{PV} = C_y^{PV} + NC_{y+1}^{PV} \qquad \forall y = 1, 2, ..., (T-1) \tag{3.30}$$

$$C_y^{PV} = NC_y^{PV} \qquad \forall y = 1 \tag{3.31}$$

$$C_{y+1}^{E} = C_y^{E} + NC_{y+1}^{E} \qquad \forall y = 1, 2, ..., (T-1) \tag{3.32}$$

$$C_y^{E} = NC_y^{E} \qquad \forall y = 1 \tag{3.33}$$

$$Psize_{y+1}^{BESS} = Psize_y^{BESS} + NC_{y+1}^{P} \qquad \forall y = 1, 2, ..., (T-1) \tag{3.34}$$

$$Psize_y^{BESS} = NC_y^{P} \qquad \forall y = 1 \tag{3.35}$$

Constraint on Terminal Year Investment: The solar PV capacity and the BESS power and energy capacity remain unchanged beyond the planning period, implying that no new investment takes place beyond year T; thus,

$$C_{y+1}^{PV} = C_y^{PV} \qquad \forall y = T \tag{3.36}$$

$$C_{y+1}^{E} = C_E^{P} \qquad \forall y = T \tag{3.37}$$

$$Psize_{y+1}^{BESS} = Psize_y^{BESS} \qquad \forall y = T \tag{3.38}$$

3.2.5 Distribution Operations Model

Once the EVCF design is acceptable from an investor's perspective, this model is used to evaluate the investment decisions and determine the most desirable design for that specific site from the LDC's point of view.

Objective Function: Minimize the load shedding in the distribution system, as follows:

$$Min \sum_{l\in N}\sum_{k\in K}\sum_{s\in S}\sum_{y\in Y} P^{UN}_{i,k,s,y} \tag{3.39}$$

Real Power Flow Equation:

$$P_{ss,k,s,y} - Pd_{i,k,s,y} - P^{IM}_{l,k,s,y} + P^{EX}_{l,k,s,y} + P^{UN}_{i,k,s,y} = \sum_{j=1}^{N} V_{i,k,s,y} V_{j,k,s,y} Y_{i,j} \cos(\theta_{i,j} + \delta_{j,k,s,y} - \delta_{i,k,s,y})$$
$$i\forall N, \forall k, \forall s, \forall y \tag{3.40}$$

The power imported and exported by the EVCF in (3.40) are determined from the EAM. In addition to the above, this model also includes equations (3.3-3.8). In the above proposed framework, the models- Distribution Marian Assessment Model, DG Penetration Assessment Model, and Distribution Operations Model are nonlinear programming (NLP) problems, solved using the MINOS solver in General Algebraic Modeling System environment, while the EAM is a mixed integer nonlinear programming (MINLP) problem solved using the DICOPT solver [75].

3.3 Test System and Assumptions

The 33-bus radial distribution system described in [76], shown in Figure 3.4, is employed in this study. The system peak demand is 3.8 MW in year-0, with a base voltage of 12.66 kV. The network parameters and the load data are given in the Appendix. All

loads are assumed to be residential and grow 3% annually. Profiles of the system loads are from the IEEE Reliability Test System [77]. Winter and summer seasons are both considered, each season is represented by 24 weekday hours. It should be mentioned that the location of the EVCF is determined from a detailed planning analysis that includes technical, environmental, and economic studies, the results of which are assumed as input and are beyond the scope of this work. Otherwise spatial components of PEV trips cannot be ignored. Four arbitrary locations are selected for EVCFs, at buses 15, 22, 25, and 31. The maximum penetration of connected DG at each bus is 10 MW [74]. The maintenance cost of transformers and fast chargers are 11.96 $\$/kVA-year$ and 8.92 $\$/kVA-year$, respectively [35]. The charging price is assumed to be 0.06 $\$/kWh$.

Three years of historical data from May 2012 to May 2015 [78] are used to generate the average HOEP for typical winter and summer days, as depicted in Figure 3.5. Each EVCF is assumed to serve up to 20% of the total forecasted number of PEVs in the distribution system, on a typical day. Four EVCFs thus serve 80% of the total number of PEVs forecasted to be in the system, and the remaining 20% are assumed to be charged somewhere else, for example, by Level-2 charging at workplace/commercial buildings. This assumption is viewed as reasonable, given the fact that fast charging is still not dominant, and it would thus be unrealistic to assume that such charging would supply the needs of all PEVs in the distribution system. Medium and high PEV penetration levels over the period 2020 to 2030 are considered [79], as shown in Figure 3.6. Based on an average monthly residential electricity consumption of 1500 kWh, the average hourly residential load is calculated to be 2.08 kW. The total number of houses in the distribution system in year-0 is calculated to be 1486, and is assumed to grow at 1.08% annually [80]. According to the NHTS data, the average number of vehicles per household is estimated to be 1.9. Based on the knowledge of PEV penetration level, number of houses, and average number of vehicles per household, the number of PEVs in the system can be determined for each year of the planning period.

Historical hourly temperature and insolation data from Solar Radiation Research Laboratory for the period from May 2012 to May 2015 is used along with the empirical model

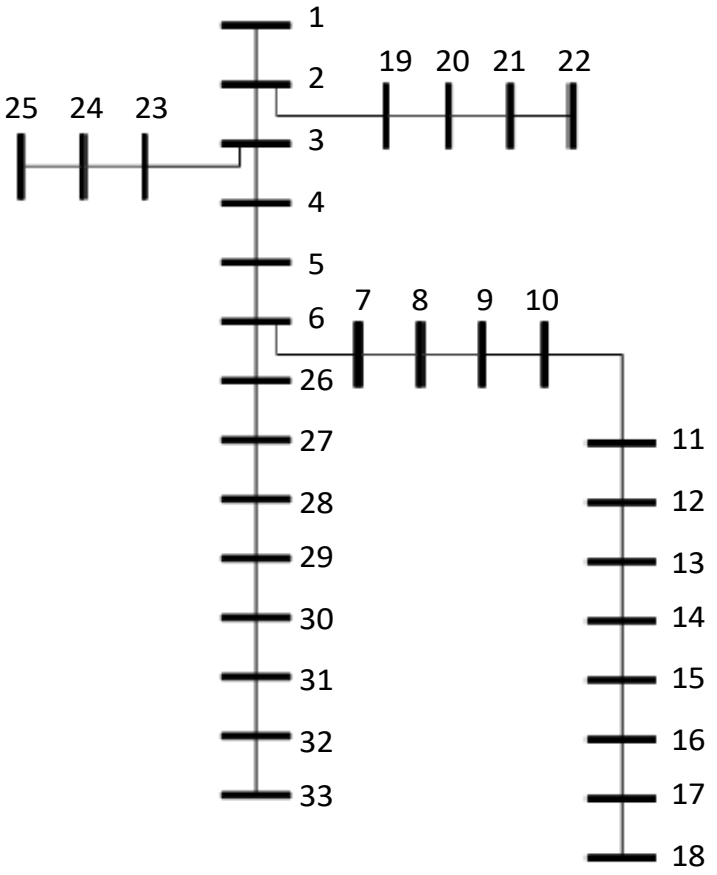

Figure 3.4: 33-bus distribution system

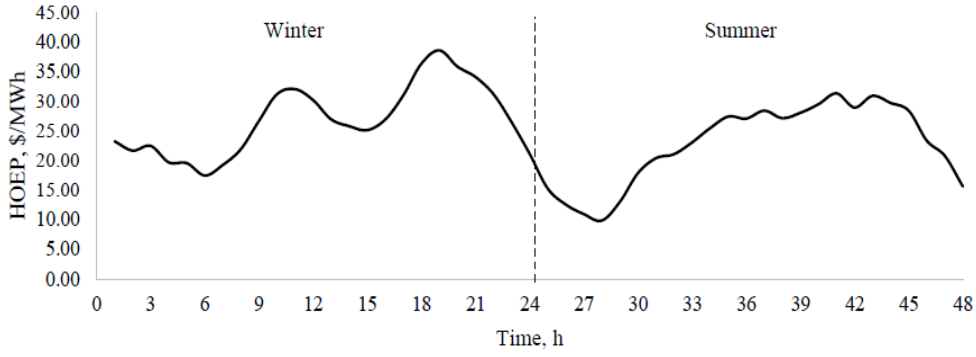

Figure 3.5: Hourly Ontario electricity price for winter and summer days

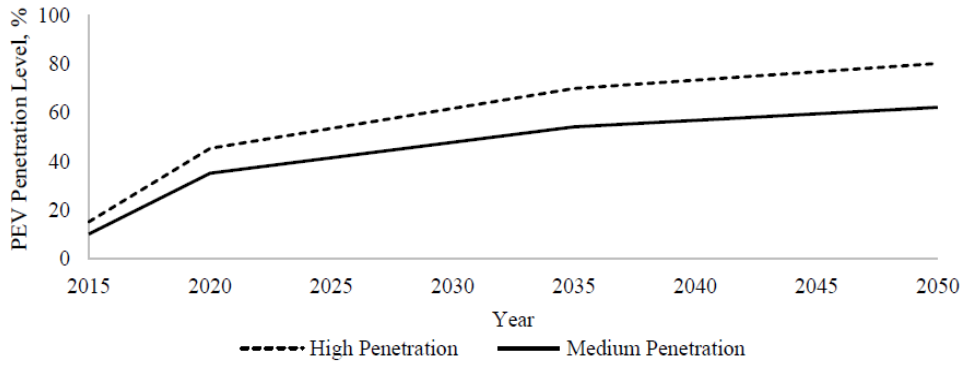

Figure 3.6: Medium and high PEV penetration levels from year 2015 to 2050

described in [81] to estimate PV array dc output power for typical winter and summer days. The PV output power, as a percentage of its rated capacity, is determined by dividing the PV array dc output power by its rated power. The average forecast installed costs of PV generation, within planning periods is given in [84]. The fixed O&M cost of PV generation is 19 $\$/kW-year$. The 2012 revised contract price of 0.549 $\$/kWh$ applicable in Ontario for PV generation facilities is considered [82]. The inverter conversion efficiency of the PV array is assumed to be 95

Due to its low self-charge level, low energy-specific price, and high degree of maturity, a lead-acid BESS is chosen for this study. The performance and cost parameters of the BESS are obtained from [83]. The charging and discharging efficiencies of the BESS are both 95%. The variable installation costs associated with the power and energy capacities are 1,407 $\$/kW$ and 275 $\$/kWh$, respectively. The fixed O&M cost is 26.8 $\$/kW-year$, and the variable O&M cost is 0.0011 $\$/kWh$ discharged. The BESS power size is considered to be a multiple of 30 kW, and the energy/power ratio varies between 1 and 5.

The estimation of λ is based on the following assumptions:

- The PEVs operate with an SOC window of 70% (between 20% and 90%).
- The vehicles are assumed to be fully charged at home before leaving on a trip so that

fast charging is considered to be complementing the home charge. There will not be any charge prior to the trips except the one occurred over the night at home.

- The data collected for NHTS reportedly represents 1,000,000 trips and 300,000 vehicles, but after consideration of four types of vehicles (automobiles, sports vehicles, vans, and pickup trucks) and excluding missing data, 850,000 trips and 150,000 vehicles have been taken into account for this study.

- The detailed study presented in this chapter considers a fully charged PEV20, *i.e.*, a compact sedan, with a battery capacity of 6.51 kWh, which can drive up to 20 miles on electricity. However, a variety of PEV battery types, i.e., PEV40 and PEV60, have been taken into consideration to demonstrate their impact on charging demand and EVCF design. The PEV40 and PEV60 vehicles are compact sedans, with battery capacities of 10.4 kWh and 15.6 kWh, which can drive up to 40 and 60 miles on electricity, respectively.

- To reduce the computational time, any vehicle whose cumulative mileage for daily trips is less than 20 miles is initially excluded, since such vehicle will not need fast charging.

3.4 Results and Discussion

3.4.1 PEV Charging Loads & Impact on EVCF Configuration

To estimate the expected PEV charging demand, the arrival rate of PEVs at an EVCF must first be determined. Figure shows the probability of PEV20 arrival at an EVCF, determined using the proposed VDT. The arrival rate of PEVs at an EVCF is obtained by multiplying the total estimated number of PEVs to be served at the EVCF, on a typical day, by the PEV arrival probability. Using the arrival rate of PEVs and the QM, the expected PEV charging demand can then be estimated, as illustrated in Figure 3.7.

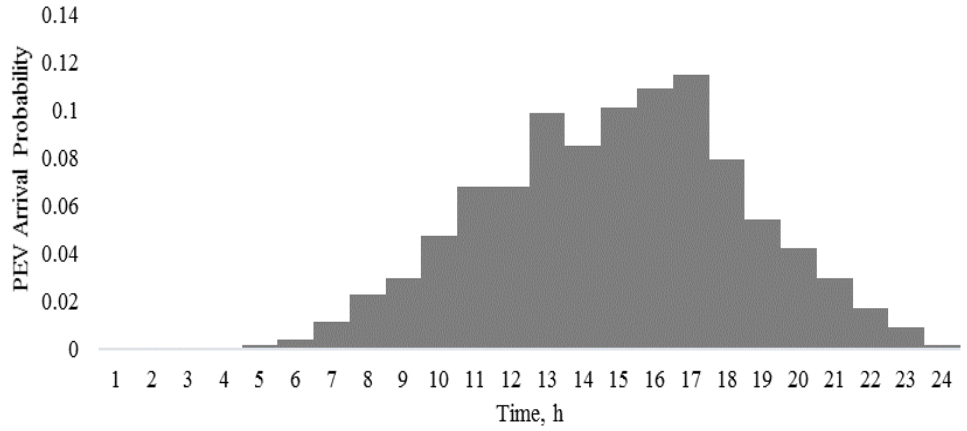

Figure 3.7: Probability of PEV20 arrival at an EVCF in the distribution system

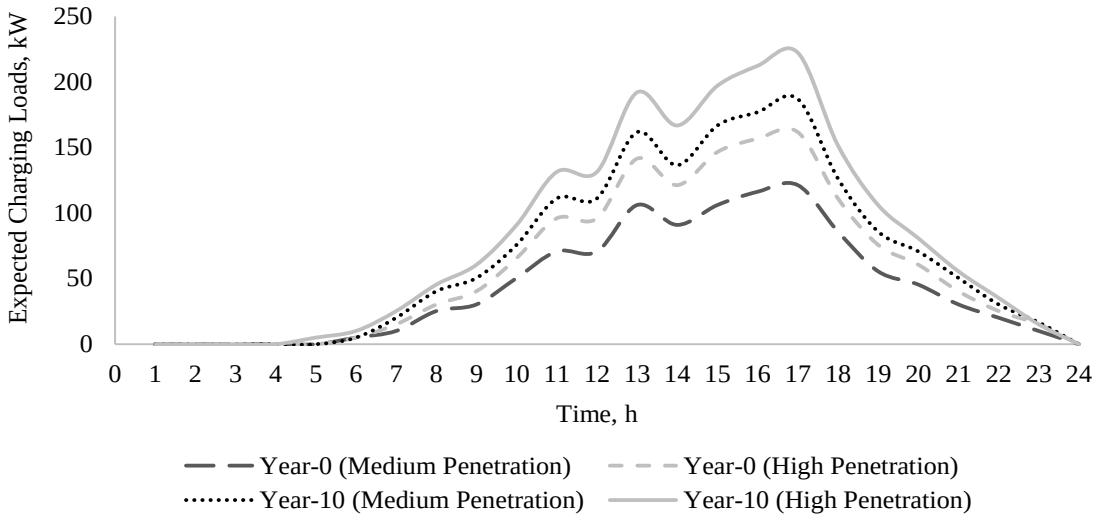

Figure 3.8: Expected charging demand with PEV20 at an EVCF, for different penetration levels

In order to maintain the queuing system stability, it is found that four fast chargers are sufficient for a medium PEV penetration level, while five fast chargers are required for high PEV penetration. The power of each fast charger is assumed to be 50 kW, and assuming a 25% margin, the four- and five-port facilities require a 250 kW and a 350 kW transformer on site, respectively. According to the QM, the EVCF is fully occupied from hour 12 to hour 18; the average waiting time in the queue is 1.13 min in year-0 and 20 min at the peak hour in year-10 for medium PEV penetration. For the waiting time to be acceptable in year-10, an additional port must be installed after year-9, but probably there is no necessity for it to be installed prior to year-9 because the average wait is 10 min during that year. The determination of the optimal number of fast chargers, however, is outside the scope of this work since prior existence of the EVCF is assumed. In case of high PEV penetration, the average waiting times in the queue are 1.02 min in year-0 and 8.14 min in year-10, which would be acceptable. A reasonable conclusion is that a 5-port facility is a suitable choice because it can ensure queuing system stability for high penetration and reduce the waiting time for medium penetration.

3.4.2 Investment Decisions and Appropriate Design Options

The load serving capability and the maximum DG penetration at the four chosen EVCF buses, determined using the proposed Distribution Margin Assessment and DG Penetration Assessment models, are shown for year-7 of the planning period in Figures 3.9 and 3.10, respectively. These provide an accurate representation of the limits of the distribution grid at a specific EVCF location.

The optimal investment decisions for an EVCF at the four chosen locations are determined using the proposed EMA, one of which is provided in Table 3.1. It is realized that at buses 22, 25 and 31, the BESS investment decisions are in the latter part of the planning horizon, which is governed by the load serving capability at these buses and the relatively high cost of BESS as compared to the main grid price. On the other hand, at Bus-15, designing EVCF with BESS (Design-1) is required from year-3 itself since the load serving

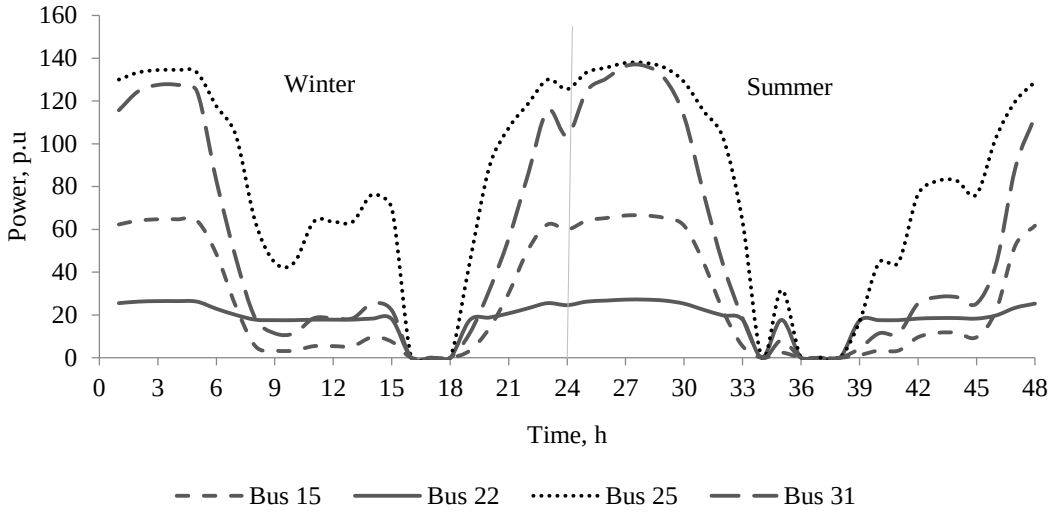

Figure 3.9: Load serving capability at EVCF buses in year-7

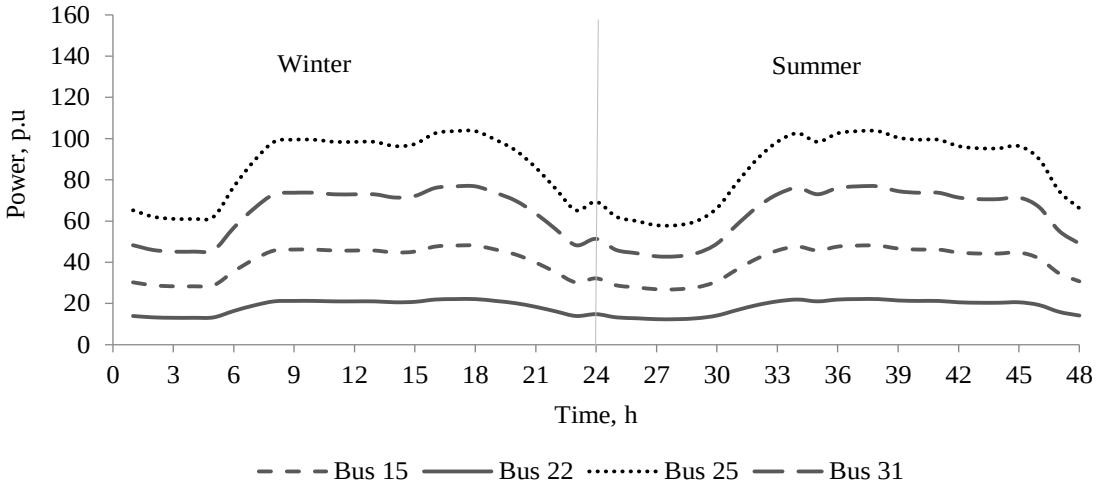

Figure 3.10: Maximum DG penetration at EVCF buses in year-7

capability at that bus is lower than the other chosen EVCF locations. It is observed that there is a clear trade-off between the load serving capability and the BESS capacity; the BESS capacity increases as load serving capability decreases. In case of Design-1, the net present value becomes negative at 0.06 $\$/kWh$ charging price, and in order to make it profitable for an EVCF and achieve a targeted internal rate of return (IRR) of 14%, PEV charging prices are optimally determined for each location, as shown in Figure 3.11. The EVCF located at Bus-25 attains an IRR of 14% with the lowest charging price, while the one at Bus-15 requires the highest charging price.

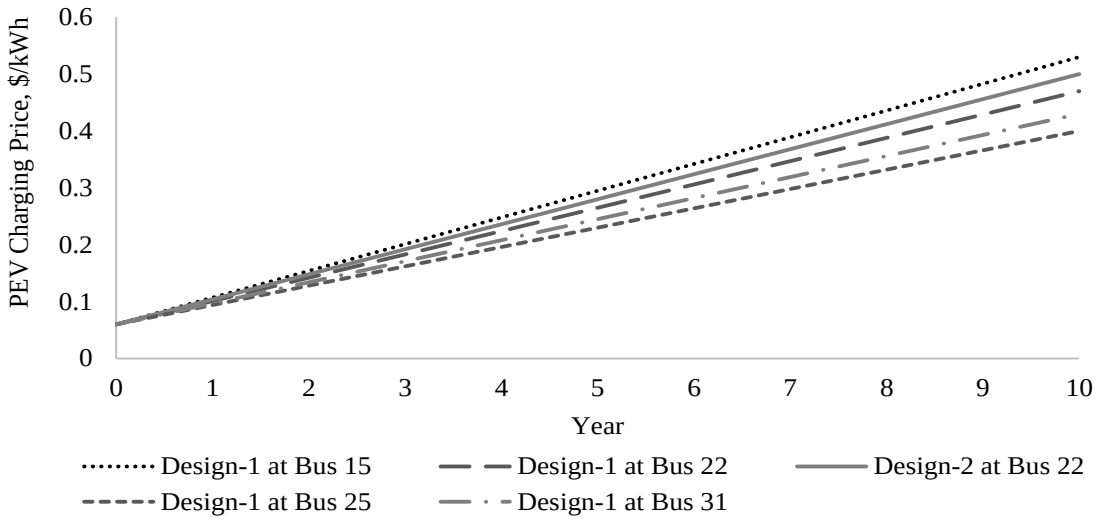

Figure 3.11: Charging price for 14% targeted IRR at EVCF buses considering PEV20

The PV generation capacity is governed by the maximum DG capacity that can be accommodated at each site, and hence it varies from one location to another. Consideration of Design-2 results in PEV load shedding or unserved PEVs, as shown in Figure 3.12, due to the limited availability of the load serving capability within the planning period as well as the high degree of variability associated with PV generation. Design-3 is desirable from an investor's perspective, as it results in the highest IRR since a BESS helps to manage the EVCF power consumption, while installing PV generation on a rooftop helps to earn additional revenue.

Table 3.1: New Design Decisions of an EVCF at Bus 31

Design Options	Inst. Year	Power Size of BESS (kW)	Energy Size of BESS (kWh)	PV Capacity Size (kW)	IRR%
Design-1: EVCF with BESS	5	150	750		14
	6	30	150		
	7	150	750		
	8	60	300		
	9	60	120		
Design-2: EVCF with Renewables based DG	1			1000	24
	2			220	
	3			60	
	4			40	
	5			20	
Design-3: EVCF as a Smart Energy Microhub	1	-	-	1000	31
	2	60	300	250	
	3	30	150	40	
	4	-	-	30	
	5	-	-	50	
	6	-	-	20	

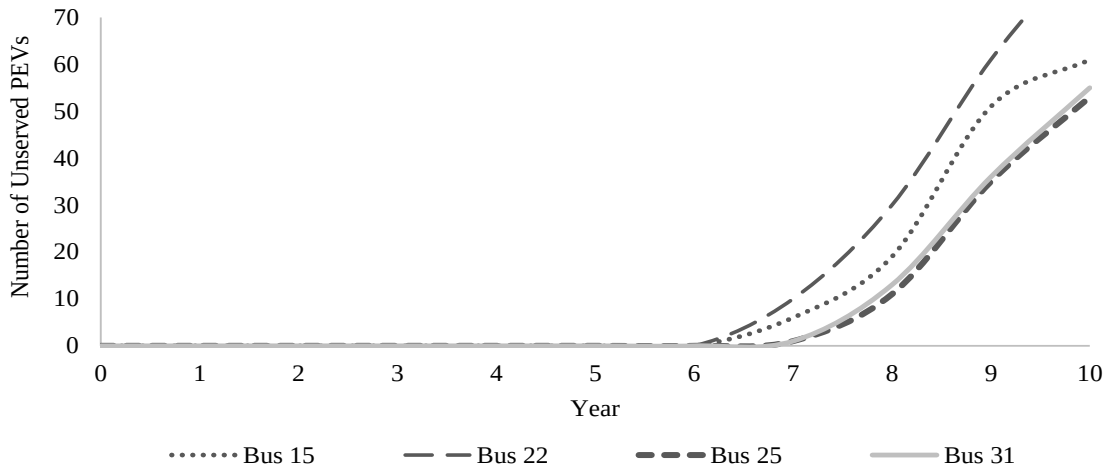

Figure 3.12: Number of unserved PEV20 determined from the EAM in Design-2 only, within the planning period

3.4.3 Assessment of Distribution System Capability

To assess distribution system capability in accommodating multiple EVCFs, with and without the new design of EVCF, the Distribution Operation Model is developed. Multiple EVCFs, simultaneously, with and without the proposed EVCF design for the three years (year-0, year-5, year-10) are presented in Table 3.2, considering medium PEV penetration. The base case with no EVCFs, is also presented. It is worth noting that the unserved energy in year-10 of the base case, can be mitigated by appropriate distribution planning, which is however beyond the scope of this research.

In case of multiple EVCFs without new design, there are several buses where loads are unserved and the LDC has to resort to load curtailment. Thus, there is a need and justification for a new EVCF design that can serve as an energy source and reduce the impact on the distribution system. Year-0 is not considered for EVCFs with the new design as the investment planning starts from year-1. With Desgin-1, a significant reduction in unserved energy is observed, but the LDC still has to resort to load curtailment. There are unserved PEVs in the outcomes of the proposed EAM in case of Design-2, as discussed

Table 3.2: Impact of Multiple EVCFs With/Without New Design

Case	Year	Unserved Energy at EVCF Buses (MWh/ 2 days)	Unserved Energy at Other Buses (MWh/ 2 days)
Base case (No EVCFs)	Year-0	-	-
	Year-5	-	-
	Year-10	-	0.120 at Bus 17 2.310 at Bus 18 0.358 at Bus 32 1.132 at Bus 33
Multiple EVCFs, without new design	Year-0	0.037 at Bus 22	-
	Year-5	0.577 at Bus 22	0.736 at Bus 18
	Year-10	1.359 at Bus 15 1.160 at Bus 22	1.188 at Bus 16 1.435 at Bus 17 2.990 at Bus 18 2.621 at Bus 32 1.815 at Bus 33
Multiple EVCFs with Design-1	Year-5	0.546 at Bus 22	0.026 at Bus 18
	Year-10	1.712 at Bus 22	0.036 at Bus 16 0.354 at Bus 17 2.815 at Bus 18 0.242 at Bus 32 1.298 at Bus 33
Multiple EVCFs with Design-2	Year-5	-	-
	Year-10	-	0.369 at Bus 18
Multiple EVCFs with Design-3	Year-5	-	-
	Year-10	-	0.336 at Bus 18

in the previous section. Therefore, Design-3 achieves the lowest unserved energy, and is valuable from the LDC's perspective, with respect to other EVCF design options.

3.4.4 Mix of PEV Battery Types and Impact on Probability of PEV Arrival

The studies presented thus far have considered only PEV20 vehicles, but since the electric range of PEV batteries can shape travel patterns, PEV40 and PEV60 vehicles have also been taken into account in order to demonstrate their impact on the probability of PEV arrivals at an EVCF. Figure 3.13 presents a comparison of the probabilities of PEV arrival at an EVCF for different PEV types. It is noted that, during the early hours of the day, an inverse relationship exists between PEV arrival probability and battery capacity, i.e., PEV arrival probability is higher for PEVs with smaller battery capacities. On the other hand, during the later hours of the day, the relation between PEV arrival probability and battery capacity is proportional, i.e., the PEVs with smaller battery capacity have lower probability of arrival at an EVCF.

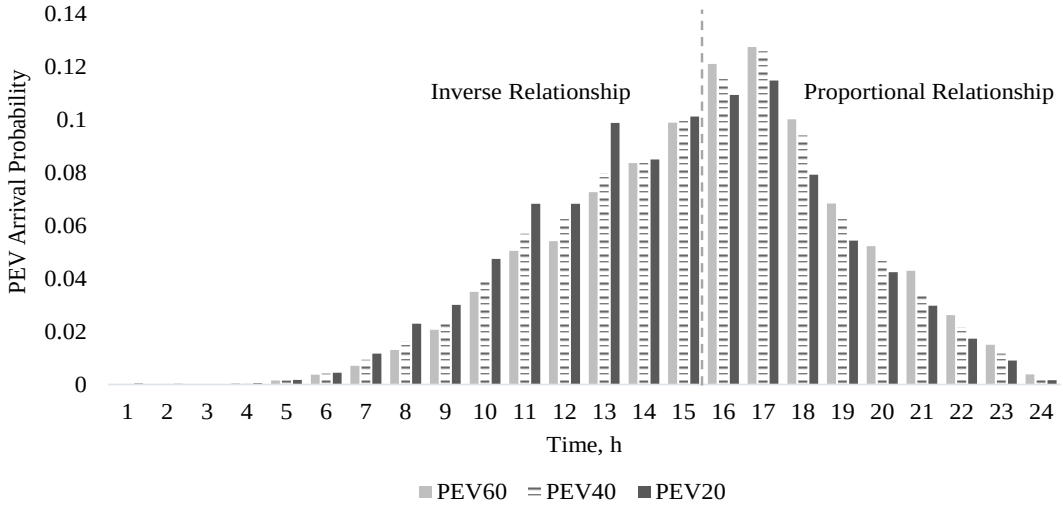

Figure 3.13: Probability of PEV arrival at an EVCF

3.4.5 Mix of PEV Battery Types and Impact on EVCF Demand

The earlier findings were based on a charging demand for only PEV20 vehicles at an EVCF. This subsection therefore presents the expected EVCF demand associated with a variety of PEV battery capacities, as shown in Figure 3.14. In the absence of historical data on arrival percentages of PEV types at an EVCF, the PEV arrival rates are assumed based on the different PEV battery capacities. The PEV arrivals is assumed to comprise a mix of 30% PEV20 vehicles, 40% PEV40 vehicles, and 30% PEV60 vehicles; the expected EVCF charging demand is estimated based on these percentages. Understandably, the shape and magnitude of the charging demand profile would differ from the profile with a unique PEV battery type (Figure 3.7). Such changes in the magnitude and shape of the EVCF demand profile will have a significant impact on the design of an EVCF as a smart energy hub, and the effect is examined in the following subsection.

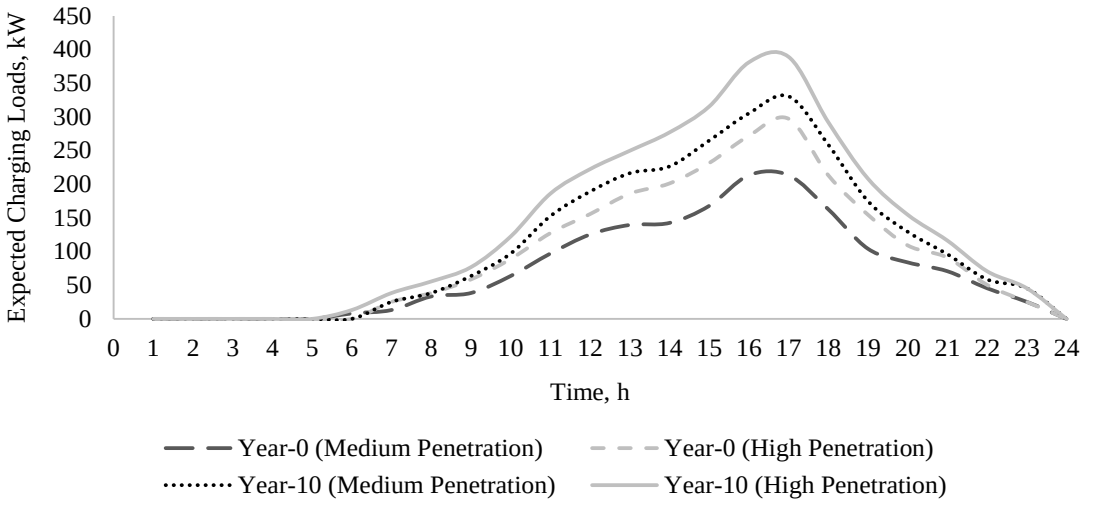

Figure 3.14: Expected charging demand at an EVCF with a mix of PEV types, for different penetration levels

3.4.6 Charging Demand and Impact on Design of EVCF as a Smart Energy Hub

When a mix of PEV battery types are considered, and the corresponding demand profile (Figure 3.14) is taken into account, the design of EVCF as a smart energy hub is expected to be different from the earlier reported design (Table 3.1). Table 3.3 presents the new design and it is noted that the power and energy sizing of the BESS increase, and similarly the PV capacity also increases, and the BESS installation years change. Because of the increased capital costs, the IRR of the new EVCF design is 27%, which is lower than the IRR with PEV20 only, which was 31%. Since the proposed framework is generic and applicable to any distribution system configuration, the results presented thus far, were not related to a specific geography. However, to demonstrate the relevance of specific geography on the outcomes of the proposed framework, studies are presented in the following subsections considering rural and urban areas.

Table 3.3: Design of EVCF as a Smart Energy Hub Considering Mix of PEV Types

Inst. Year	Power Size of BESS (kW)	Energy Size of BESS (kWh)	PV Capacity (kW)	IRR%
1	-	-	1000	
2	90	450	350	
3	-	-	50	
4	-	-	40	
5	-	-	50	27
6	30	150	30	
7	30	150	-	

3.4.7 Effect of Specific Geography on PEV Arrival Probability

The data collected by NHTS included both rural and urban areas, but these were not distinguished in the earlier studies presented here. Further data analysis has been carried out to extract the data for rural and urban areas separately, and applied to the VDT, to examine the PEV travel patterns in such areas and their time requirements for fast charging. A comparison of the effects of PEV travel patterns with respect to the probability of PEV arrival at an EVCF in rural and urban areas for PEV20, PEV40, and PEV60 vehicles is presented in Figures 3.15, 3.16 and 3.17, respectively. It can be seen that PEV charging behavior in rural and urban areas do not differ significantly. However, in rural areas, the probability of PEVs needing fast charging is higher, early in the day. The opposite is true for urban areas, where PEVs are more likely to need fast charging during the night than the day. The results of this comparison are reasonable and valid and are supported by the fact that more real-world activities and movement occur at night in urban than in rural areas.

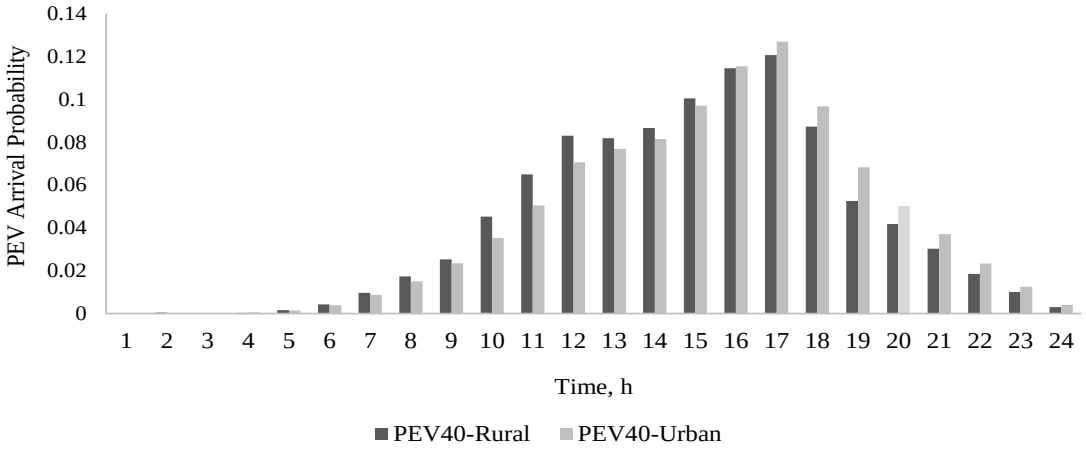

Figure 3.15: Probability of PEV20 arrival at an EVCF in rural and urban areas

Since the 33-bus system considered in the present study is a radial distribution system of the type more commonly used in rural than in urban areas, the design of an EVCF

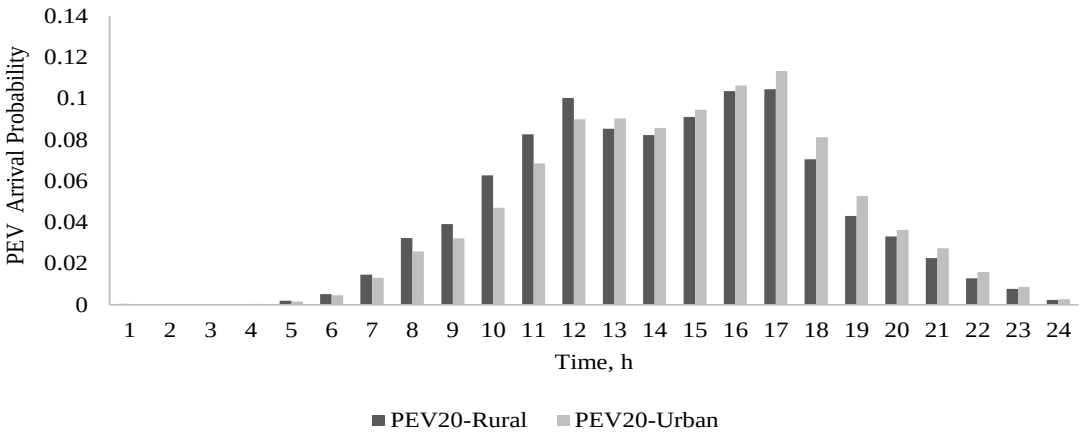

Figure 3.16: Probability of PEV40 arrival at an EVCF in rural and urban areas

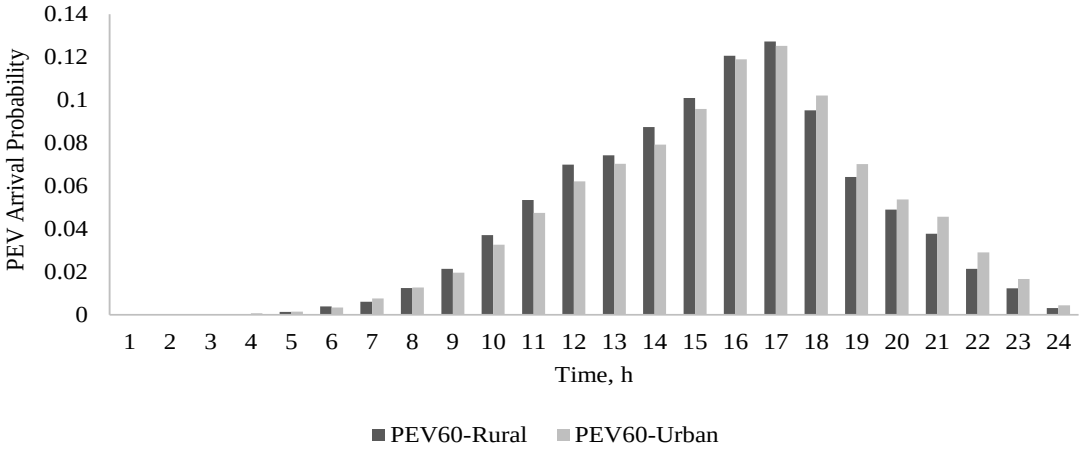

Figure 3.17: Probability of PEV60 arrival at an EVCF in rural and urban areas

as a smart energy hub is presented in the following case study for a rural area only. It should be noted that, for an urban area to be considered, the outcomes of the Distribution Margin and DG Penetration Assessment Models, that are indicated in Figures 3.9 and 3.10, respectively, for a radial configuration, would change to correspond with a different system configuration. The effects of a rural geography on EVCF demand and design are discussed in the following subsection.

3.4.8 Effect of Rural Geography on EVCF Demand

Considering a mix of PEVs, the charging demand at an EVCF in a rural area is estimated, as shown in Figure 3.18. The rural charging demand profile differs somewhat from the one obtained for the generic case with no specific geography (Figure 3.14). The former has only one peak period, *i.e.*, hour 17, while the latter has two peak periods: hours 12 and 17. The following case reveals the significance of such differences with respect to the design of an EVCF as a smart energy hub.

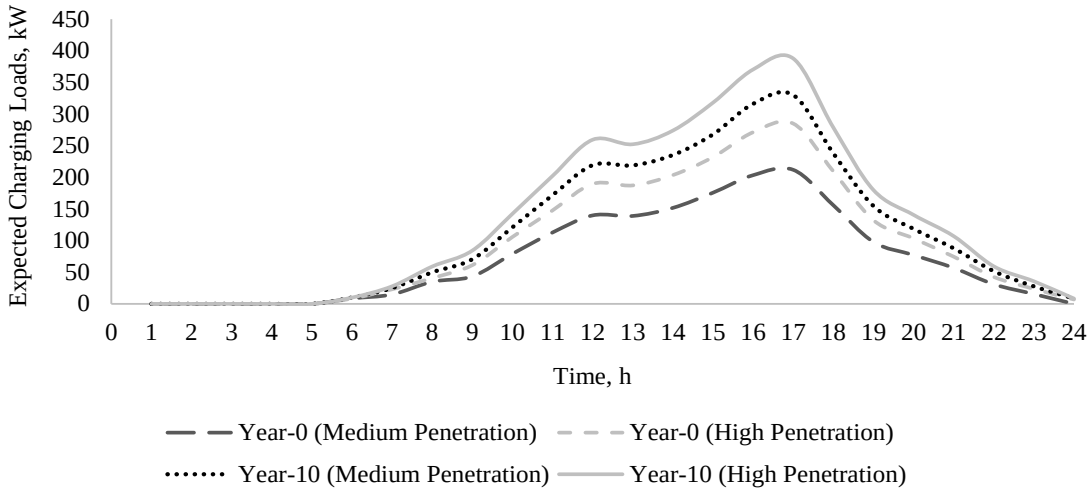

Figure 3.18: Expected mixed PEV charging demand at an EVCF in a rural area

3.4.9 Effect of Rural Geography on Design of EVCF as a Smart Energy Hub

A plan for design of an EVCF as a smart energy hub in a rural area is presented in Table 3.4. A notable change is evident pertaining to the use of PV capacity rather than BESS, which is installed only at the first year with a high power and energy capacity, while there is an increase in PV capacity, and one more installation year is added.

Table 3.4: Design of an EVCF as a Smart Energy Hub in a Rural Geography

Inst. Year	Power Size of BESS (kW)	Energy Size of BESS (kWh)	PV Capacity (kW)	IRR%
1	120	600	1000	27
2	-	-	370	
3	-	-	60	
4	-	-	40	
5	-	-	40	
6	-	-	50	
7	-	-	50	

The cumulative power and energy capacities of the BESS in the rural EVCF are 120 kW and 600 kWh, respectively, in contrast to 150 kW and 750 kWh, respectively, in the generic case in which no geography is specified. On the other hand, the total PV capacity in the rural EVCF is 1,610 kW, while it is 1,520 kW in the generic case. In a rural area, a lower power and energy capacity of BESS is chosen, but more PV units are installed. These findings correlate with the fact that in rural areas, more PEVs need fast charging during the day (Figures 3.15, 3.16 and 3.17), and justifies the increased PV capacity. Based on the times PEVs need fast charging in rural and urban areas (Figures 3.15 to 3.17), and considering the results obtained from the general and rural cases (Table 3.1 and Table 3.4), a reasonable conclusion is that more PV units would be required for EVCF design in

a rural area, while more BESS units would be recommended for an urban arean EVCF, adjustments that would help match the times PEVs need fast charging during the evening. With respect to the assessment of distribution system capability, it should be mentioned that, in cases involving mix of PEV types, and/or rural geography, the load-shedding is higher without an EVCF design and lower with the new EVCF design, as would certainly be expected. This impact has not been presented here because it would be similar to the results presented in Table 3.2, with only a difference in the load-shedding amount.

3.5 Summary

This chapter proposed a novel framework for optimal planning and integrating multiple EVCFs in distribution systems. Based on a specific location in the distribution system, and from the perspectives of both the investor and the LDC, the proposed framework determined new design decisions for three investment options for EVCFs commissioned in distribution systems. The effects of different PEV battery types and specific geographies, *i.e.*, rural and urban, on the probability of PEV arrivals at an EVCF were investigated. The proposed EVCF design was examined considering mix of PEV battery types, and a rural geography. The simulation results demonstrated that Design-3 was the most desirable option from the perspectives of both the investor and the LDC, which transformed the EVCF to a smart energy hub. However, this may not always be true when the distribution system included DGs.

Chapter 4

Flexibility Provisions from an EVCF Equipped with DERs for Wind Integrated Grids [1]

4.1 Introduction

EVCFs equipped with DERs, such as a solar PV generation and energy storage, can offer a wide range of benefits to the power system such as load leveling, hedge against forecast uncertainty, and ancillary services. As EVCFs are typically located along a highway to support long trips for PEVs, they can coordinate with a WGF and help mitigate wind power imbalances, particularly when the EVCFs are equipped with DERs.

Intermittency of supply is an issue particularly applicable to WGFs whose typical forecasting errors, with respect to the final output power, are in the range of 30%-50% [6, 7]. Penalties associated with wind power imbalances, imposed by the system or market oper-

[1] This chapter has been accepted for publication in: W. Alharbi and K. Bhattacharya. "Flexibility Provisions from a Fast Charging Facility Equipped with DERs for Wind Integrated Grids." *IEEE Transactions on Sustainable Energy.* (Accepted, available in IEEE Xplore Early Access).

ator, increases wind integration costs.

The work in Chapter 3 is extended here to investigate the technical feasibility and viability of flexibility provisions from the EVCF equipped with DERs in wind integrated power grids. Upward flexibility provisions are needed when the actual wind output is less than the forecasted output, to compensate the deficit in wind generation. This is provided by the proposed EVCF equipped with DERs, from PV generation, and/or discharging the BESS. On the other hand, downward flexibility is provided when actual wind output is greater than forecasted output, and surplus wind generation is absorbed by PEV and BESS charging loads. The WGF is considered to participate, both, via a market, and through a bilateral contract with the grid, considering different ownership structures. Furthermore, the variability and uncertainty arising from high penetration of renewables, in particular wind generation, is addressed in this chapter.

The main objectives of this chapter are as follows:

- Introduce an inherent flexibility in EVCF portfolio by equipping it with DERs to mitigate the impact of fast charging loads on the power grid while facilitating wind power integration in power systems.
- Propose two different ownership structures to study the feasibility of an EVCF designed with DERs for wind integrated grids, from the perspectives of the WGF and EVCF owners, respectively.
- Propose a new framework and an associated mathematical optimization model to design the EVCF with DERs, that provides the upward and downward flexibility provisions for hedging wind power forecast uncertainty, in each ownership structure.
- By application of MCS, investigate the impact of variability and uncertainty of wind and PV generation, and market price, on the optimum design in both ownership structures.

- Investigate the effects of low and high wind imbalance penalties, and different flexibility service prices on the feasibility and economic viability of the design of EVCF with DERs in different ownership structures.

4.2 Ownership Structures of WGF and EVCF with DERs

Two different ownership structures of WGFs and EVCF equipped with DERs are proposed, as shown in Figs.4.1 and 4.2, and are discussed below:

- *Structure 1: Same Ownership of WGF and EVCF Equipped with DERs, WGF Participates in Electricity Market*

  The WGF participates in the electricity market and receives dispatch schedules. If there are deviations in actual wind generation from the scheduled, the WGF owner would incur penalties. In order to alliviate the penalties, the EVCF seeks to equip with DERs to meet the WGF's generation mismatches. As shown in Figure 4.1, the EVCF equipped with DERs interacts with the WGF to provide flexibility services in real-time to balance the wind generation deviations from the schedules. The question that arises is, should the WGF pay the penalties for deficit/ surplus wind generation or invest in the design of the EVCF with DERs to avoid penalties.

- *Structure 2: WGF and EVCF Equipped with DERs have Different Ownerships, WGF Contract with Grid* In this structure, the WGF does not participate in the electricity market and hence is not dispatched by the market operator. Wind generation, as available, is injected into the grid by the WGF, for which it receives a fixed tariff rate (Figure 4.2). This arrangement is similar to that practised in Ontario, Canada, where WGFs receive a feed-in-tariff (FIT) rate [82]. Thus, there is no energy imbalance penalty if wind generation deviates from the forecasted values. On the other hand,

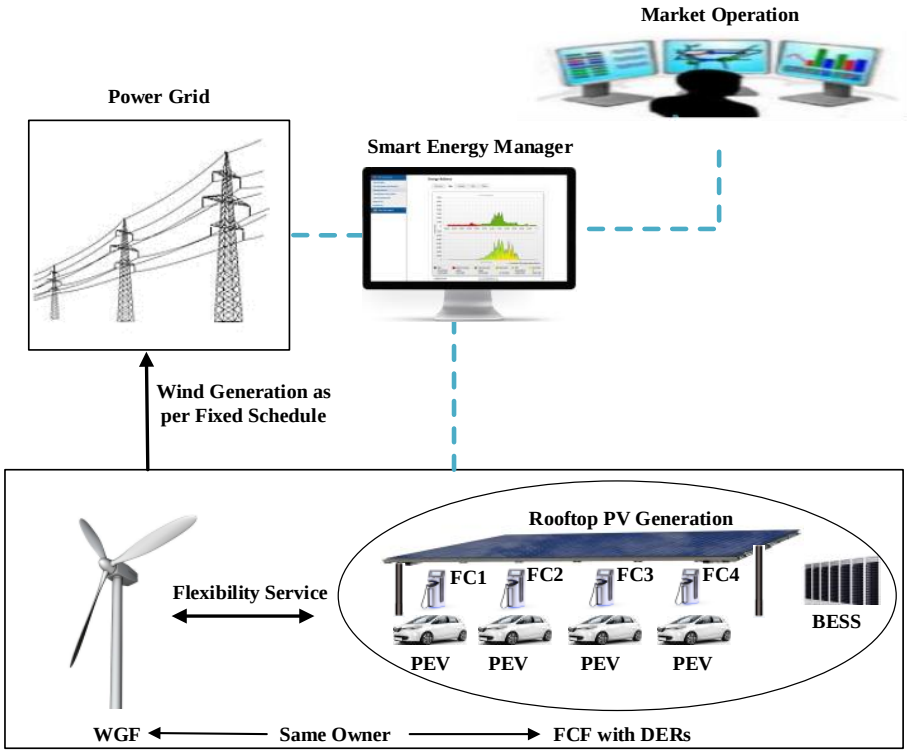

Figure 4.1: Structure 1: Same ownership of WGF and EVCF equipped with DERs.

the system operator has the responsibility of meeting the unbalances arising from uncertainties in wind generation. In this environment, the EVCF owner seeks to equip its facility with DERs so as to provide a flexibility service to the grid, under a rate contract with the system operator. It is hence necessary to examine if an investment in DERs is financially viable for the EVCF owner, and if so, at what rate contracts.

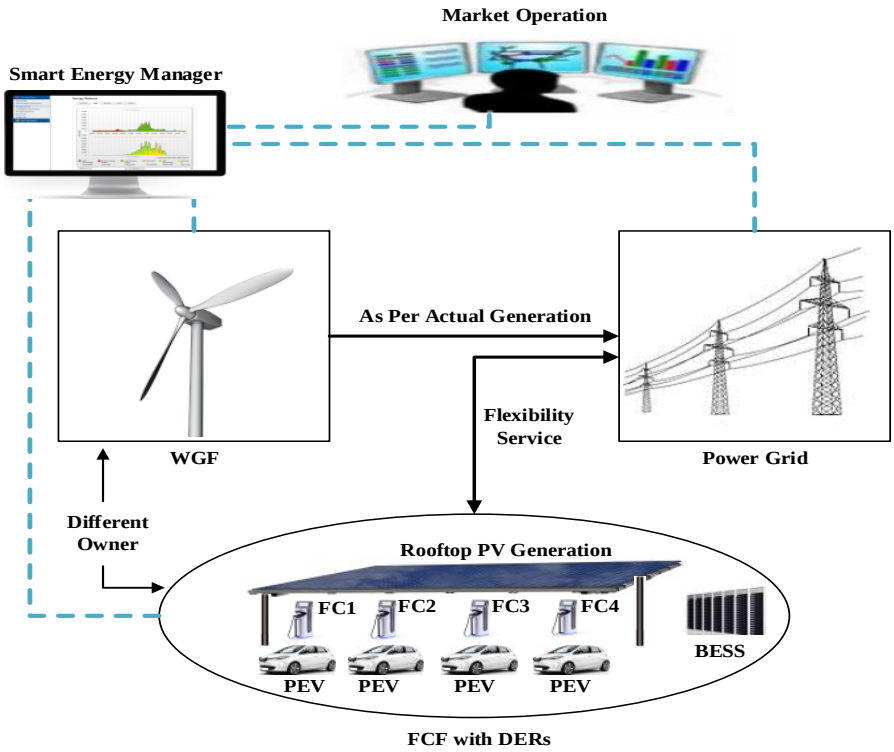

Figure 4.2: Structure 2: Different ownership of WGF and EVCF equipped with DERs.

4.3 Design of EVCF with DERs for Wind Power Integration

This section describes the mathematical model for the design of an EVCF with DERs to provide a flexibility service in wind integrated grids. The inputs include models of PEV charging loads at the EVCF, and wind and PV generation profiles, which are discussed next.

4.3.1 Modeling of PEV Charging Loads and Energy Resources

PEV Charging Load

The PEVs are assumed to adopt uncontrolled charging because of their short stay at the EVCF; essentially, the EVCF is similar to a gas station where PEVs arrive to charge and then leave, without any scope for shifting the charging demand to another time period. Consequently, smart charging is not considered in the EVCF. However, PEV charging loads may be able to match the wind generation at some periods during the day, and could be used to mitigate wind power imbalances. To develop the PEV charging load model, the NHTS 2009 data [32] is used. The probability distributions of the trip distances and how the trips are spread over the day, for each vehicle, are extracted and used in the VDT developed in Chapter 3 to estimate the expected arrival rate of PEVs at the EVCF for each hour. A set of rules are used in the VDT model, but briefly, the PEV battery SOC is checked considering its distance-driven mileage, and when the entire SOC is depleted, either the start or finish time of that trip is recorded to avoid trip interruptions. The PEV charging load depends on the required SOC and the PEV battery type. A queuing model is used to represent the overall charging process of PEVs at the EVCF. The reader may refer to Chapter 3 or [85] for further discussions of the VDT and queuing models.

Resources Associated with Charging Facility

The EVCF, when equipped with a rooftop PV system, can provide flexibility to the grid; the rooftop PV generation can supply the local load and export the excess power when available. However, because of the high variability in PV generation, and its peak power not coinciding with system peak, equipping it with a BESS can benefit both parties in providing flexibility to the grid. The empirical model described in [81] to estimate the output power from a PV array for a typical day is used in this work. The PV output power, as a fraction of its rated capacity, is determined by dividing the PV array dc output power by its rated power.

Wind Generation

The daily wind generation profiles are obtained by using the 24-hour wind speed data in the power curve of the wind generator [86], for multiple days. For deterministic studies, these profiles are averaged on an hourly basis to obtain a 24-hour average wind generation profile. This is multiplied by a normally distributed random forecasting error, varying at each hour of the day and each year of the plan period, to arrive at the forecasted average wind generation profile. For probabilistic studies, the actual wind generation profiles are randomly picked, and scaled by a random forecast error to create numerous simulation scenarios of MCS.

4.3.2 Proposed Mathematical Model

Objective Function: Maximize the NPV of investor's profit over the useful life of the EVCF equipped with DERs for providing flexibility services in wind integrated grids.

$$Max \sum_{y=1}^{Y} \frac{Revenue_y - Cost_y}{(1+\alpha)^y} \tag{4.1}$$

Where $Revenue_y$ denotes the revenue earned by the EVCF equipped with DERs, in year y, while $Cost_y$ denotes the total cost of new investments and O&M cost components of the EVCF equipped with DERs,in year y.

Note that in Structure-1, $Revenue_y$ includes revenue accrued from charging PEVs and selling scheduled wind generation (actual wind generation plus/minus upward/downward flexibility power) to the grid, given as follows:

$$R_y = ([\sum_{k=1}^{24} \rho_k^{PEV} PD_k^{PEV} + \rho_k(P_k^{AW} + P_k^{Fup} - P_k^{Fdown})]N_d)_y \tag{4.2}$$

In Structure-2, $Revenue_y$ is the revenue accrued from charging PEVs, and providing flexibility service to the grid, given as:

$$R_y = ([\sum_{k=1}^{24} \rho_k^{PEV} PD_k^{PEV} + \rho_k^{Fup} P_k^{Fup} + \rho_k^{Fdown} P_k^{Fdown}]N_d)_y \tag{4.3}$$

In (4.1), $Cost_y$ is given as follows:

$$Cost_y = Cost_y^{Inv} + Cost_y^{O\&M} \tag{4.4}$$

where

$$Cost_y^{Inv} = IC^E NC_y^E + IC^P NC_y^P + IC^{PV} NC_y^{PV} \tag{4.5}$$

The first and second terms of (4.5) are associated with BESS installation cost, the third term is installation cost of PV unit. The O&M cost, $Cost_y^{O\&M}$ of Structure-1 is given by:

$$\begin{aligned} Cost_y^{O\&M} = OM^f Psize_y^{BESS} + OM^W + M^{TH} + M^{FC} + OM^{PV} C_y^{PV} \\ + ([\sum_{k=1}^{24} OM^v \eta^{out} P_k^{out} + \rho_k^{dw} P_k^{dw} + \rho_k^{sw} P_k^{sw}]N_d)_y \end{aligned} \tag{4.6}$$

The O&M cost in (4.6) includes that of the BESS, the transformer and fast charger, the wind and PV units, and the penalty for deficit/surplus wind generation.

In Structure-2, the O&M cost of WGF and the penalty for deficit / surplus wind generation are excluded from $Cost_y^{O\&M}$ in (4.7), and is given as follows:

$$Cost_y^{O\&M} = OM^f Psize_y^{BESS} + M^{TH} + M^{FC} + OM^{PV} C_y^{PV} + ([\sum_{k=1}^{24} OM^v \eta^{out} P_k^{out}] N_d)_y \tag{4.7}$$

The objective function (4.1) is maximized subject to the constraints discussed next.

Demand Supply Balance: Total generation should meet the demand at period k on a typical day in year y.

$$P_{k,y}^{PV} + P_{k,y}^{out} + P_{k,y}^{Fdown} = PD_{k,y}^{PEV} + P_{k,y}^{in} + P_{k,y}^{Fup} \qquad \forall k \ \forall y \tag{4.8}$$

where $P_{k,y}^{PV} = \varphi^{PV} C_y^{PV}$

Upward and Downward Flexibility Limits: Flexibility provisions from the EVCF with DERs should not exceed the mismatch between wind power forecast and actual output.

$$P_{k,y}^{Fup} \leq u_{k,y}^{Fup} (P_{k,y}^{FW} - P_{k,y}^{AW}) \qquad \forall k \ \forall y \tag{4.9}$$

$$P_{k,y}^{Fdown} \leq u_{k,y}^{Fdown} (P_{k,y}^{AW} - P_{k,y}^{FW}) \qquad \forall k \ \forall y \tag{4.10}$$

In order to avoid the simultaneous provision of upward and downward flexibility, the following constraints are included:

$$u_{k,y}^{Fup} + u_{k,y}^{Fdown} \leq 1 \qquad \forall k \ \forall y \tag{4.11}$$

Balance of Wind Power Deviations: This constraint ensures that the mismatch between

forecasted and actual wind generation is balanced by upward/downward flexibility and the deficit/surplus wind generation, as follows:

$$P_{k,y}^{Fup} + P_{k,y}^{dw} = P_{k,y}^{FW} - P_{k,y}^{AW} \qquad \forall k \ \forall y \tag{4.12}$$

$$P_{k,y}^{Fdown} + P_{k,y}^{sw} = P_{k,y}^{AW} - P_{k,y}^{FW} \qquad \forall k \ \forall y \tag{4.13}$$

Deficit Wind Generation Flag: This flag is activated by setting $u_{k,y}^{dw} = 1$, when upward flexibility from the EVCF with DERs is unavailable and/or not enough to compensate all the deficit wind generation.

$$u_{k,y}^{dw} = \begin{cases} 1 & \text{if } (P_{k,y}^{FW} - P_{k,y}^{AW}) - (P_{k,y}^{PV} + P_{k,y}^{out} - PD_{k,y}^{PEV}) > 0 \\ 0 & \text{otherwise} \end{cases} \tag{4.14}$$

The constraint (4.14) is nonlinear, but for computational ease, it is linearized as follows:

$$-(P_{k,y}^{FW} - P_{k,y}^{AW}) + (P_{k,y}^{PV} + P_{k,y}^{out} - PD_{k,y}^{PEV}) \leqslant M(1 - u_{k,y}^{dw}) \tag{4.15}$$

$$(P_{k,y}^{FW} - P_{k,y}^{AW}) - (P_{k,y}^{PV} + P_{k,y}^{out} - PD_{k,y}^{PEV}) \leqslant M \cdot u_{k,y}^{dw} \tag{4.16}$$

$$P_{k,y}^{dw} \leqslant M \cdot u_{k,y}^{dw} \tag{4.17}$$

Surplus Wind Generation Flag: This flag is activated by setting $u_{k,y}^{sw} = 1$ when surplus wind generation cannot be absorbed or accommodated by downward flexibility from the EVCF with DERs.

$$u_{k,y}^{sw} = \begin{cases} 1 & \text{if } (P_{k,y}^{AW} - P_{k,y}^{FW}) - (PD_{k,y}^{PEV} + P_{k,y}^{in} - P_{k,y}^{PV}) > 0 \\ 0 & \text{otherwise} \end{cases} \tag{4.18}$$

Constraint (4.18) is linearized in a similar way as (4.14):

$$-(P_{k,y}^{AW} - P_{k,y}^{FW}) + (PD_{k,y}^{PEV} + P_{k,y}^{in} - P_{k,y}^{PV}) \leqslant M(1 - u_{k,y}^{sw}) \tag{4.19}$$

$$(P^{AW}_{k,y} - P^{FW}_{k,y}) - (PD^{PEV}_{k,y} + P^{in}_{k,y} - P^{PV}_{k,y}) \leqslant M \cdot u^{sw}_{k,y} \tag{4.20}$$

$$P^{sw}_{k,y} \leqslant M \cdot u^{sw}_{k,y} \tag{4.21}$$

Power Conversion Limits: These constraints ensure that the power from rooftop PV, converted from dc to ac, is within the inverter limit. Similarly, the power of the BESS converted from dc to ac and *vice versa*, should be within the inverter limits.

$$P^{PV}_{k,y} \leq P^{Inverter} \qquad \forall k \ \forall y \tag{4.22}$$

$$P^{out}_{k,y} \leq P^{Inverter} \qquad \forall k \ \forall y \tag{4.23}$$

$$P^{in}_{k,y} \leq P^{Inverter} \qquad \forall k \ \forall y \tag{4.24}$$

Balance Constraint of a BESS: This constraint ensures that the SOC of the BESS is within the limits, as follows.

$$SOC_{k+1,y} = SOC_{k,y} + (P^{in}_{k,y}\eta^{in} - P^{out}_{k,t}/\eta^{out}) \cdot dt \qquad \forall k \ \forall y \tag{4.25}$$

Power Limits of BESS and Initial/Final Status of its SOC: Power charging and discharging of a BESS is limited by the following:

$$P^{in}_{k,y} \leqslant Psize^{BESS}_{y} \qquad \forall k, \forall y \tag{4.26}$$

$$P^{out}_{k,y} \leqslant Psize^{BESS}_{y} \qquad \forall k, \forall y \tag{4.27}$$

Initial and final status of SOC is assumed 50% of BESS energy capacity; thereby,

$$SOC_{k,y} = 0.5C^{E}_{y} \qquad \forall k = 1 \ \ \& \ \ k = 24, \forall y \tag{4.28}$$

BESS Energy to Power Ratio: The range of the energy capacity of the BESS for a specific

power rating is limited by:

$$\underline{EPR} \cdot Psize_y^{BESS} \leqslant Cap_y^E \leqslant \overline{EPR} \cdot Psize_y^{BESS} \tag{4.29}$$

Capacity Additions Limits of EVCF Resources: The capacity of EVCF resources for the next year should be the cumulative sum of the new capacity installed and the capacity of the previous year; thus,

$$C_{y+1}^{PV} = C_y^{PV} + NC_{y+1}^{PV} \qquad \forall y = 1, 2, ..., (T-1) \tag{4.30}$$

$$C_{y+1}^{E} = C_y^{E} + NC_{y+1}^{E} \qquad \forall y = 1, 2, ..., (T-1) \tag{4.31}$$

$$Psize_{y+1}^{BESS} = Psize_y^{BESS} + NC_{y+1}^{P} \qquad \forall y = 1, 2, ..., (T-1) \tag{4.32}$$

$$C_y^{PV} = NC_y^{PV} \qquad \forall y = 1 \tag{4.33}$$

$$C_y^{E} = NC_y^{E} \qquad \forall y = 1 \tag{4.34}$$

$$Psize_y^{BESS} = NC_y^{P} \qquad \forall y = 1 \tag{4.35}$$

Terminal Year Investment Limit: This constraint ensures that since there are no new investments beyond the plan period, the capacity of EVCF resources do not change beyond year T.

$$C_{y+1}^{PV} = C_y^{PV} \qquad \forall y = T \tag{4.36}$$

$$C_{y+1}^{E} = C_E^{P} \qquad \forall y = T \tag{4.37}$$

$$Psize_{y+1}^{BESS} = Psize_y^{BESS} \qquad \forall y = T \tag{4.38}$$

The proposed mathematical model is a mixed integer linear programming (MILP) model and solved using the CPLEX solver in GAMS [75].

4.4 Results And Discussions

4.4.1 Model Data and Assumptions

An 18 MW WGF is considered for this study, and hourly data of wind speed for the period from Jan. 2014 to Dec. 2016 is obtained from [87]. The wind forecast error is assumed to follow a normal probability distribution with a standard deviation of 15%. Real-time electricity market price data for the period from Jan. 2016 to Dec. 2016 is used from [88]. The penalties for deficit/surplus wind generation, ρ_k^{dw} and ρ_k^{sw}, are assumed to be $1.1\rho_k$ and $0.1\rho_k$, respectively [7]. For high wind imbalance penalties, these prices are scaled up by 3. Because of the lack of data pertaining to flexibility service prices, the upward flexibility price (ρ^{Fup}) is assumed same as the FIT in Ontario in 2017, of 0.207 $\$/kWh$ for PV facilities. The downward flexibility price is 50% of the upward flexibility price (ρ^{Fdown} = 0.104 $\$/kWh$) since compensating for the deficit wind through upward flexibility services is more critical for the power grid than accommodating surplus. When considering high flexibility service prices, the above prices are scaled by 2. A minimum acceptable rate of return (MARR) of 14% is assumed for a viable investment in EVCF with DERs.

The data and assumptions pertaining to PEVs can be found in [85]; the PEV charging load is estimated considering a mix of 30% PEV20, 40% PEV40, and 30% PEV60 vehicles at the charging facility, at any given hour, with battery capacities of 6.51 kWh, 10.4 kWh and 15.6 kWh, and can drive up to 20, 40 and 60 miles on electricity, respectively. Each PEV is assumed to arrive at the charging facility with 20% SOC and depart after charging, with 90% SOC.

As mentioned earlier, the empirical model in [81] is used to estimate the PV output for a typical day, considering three years of historical hourly temperature and insolation data from Solar Radiation Research Laboratory, for the period May 2012 to May 2015. The fixed O&M cost of PV units is 19 $\$/kW\text{-}year$, the installation cost varies over the plan period and is obtained from [84]. A lead-acid BESS is chosen for this study because of its low energy-specific price and high degree of maturity. The performance and cost parameters of

the BESS are obtained from [83], and its charging and discharging efficiencies are assumed to be 95%. The BESS fixed and variable O&M costs are 26.8 $\$/kW\text{-}year$ and 0.0011 $\$/kWh$, respectively. The power rating of the BESS is a multiple of 30 kW, and the energy/power ratio varies between 1 and 5. The prior existence of the EVCF, including a 500 kW inverter is assumed, and hence its cost is not considered in the proposed framework. This inverter is also used for converting power from the PV unit and the BESS.

4.4.2 PEV Charging Demand

Prior to the design of an EVCF with DERs for mitigating wind power deviations, the PEV charging demand need be determined. Using the developed VDT and queuing model, and NHTS data 2009, the expected charging demand comprising a mix of 30% PEV20, 40% PEV40 and 30% PEV60 vehicles, at the first and terminal years of the plan period (year 10), are determined (Figure 4.3).

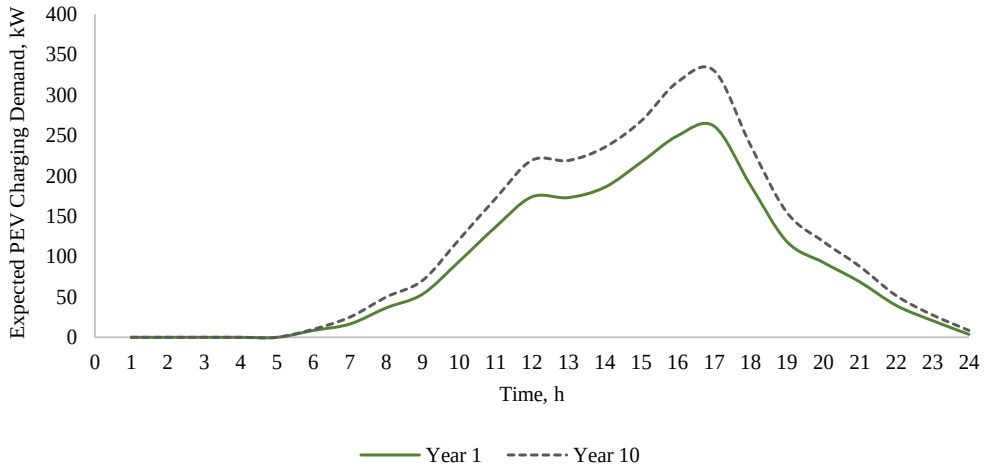

Figure 4.3: Expected PEV charging demand at the charging facility.

4.4.3 Economic Viability and Optimum Design of EVCF with DERs in Different Ownership Structures

In this work, 1,095 representative days of wind and PV generation outputs have been considered to determine their respective average daily profiles; and 365 representative daily market price profiles are used to develop an average daily price profile.

In Structure 1, the net cash flow diagram of the WGF and EVCF with DERs is compared with that of the WGF alone, to arrive at the incremental cash flow diagram, from which the incremental IRR is determined. It is noted that the incremental IRRs are 13% and 17% for low and high wind imbalance penalties, respectively. For a MARR=14%, it is therefore evident that the proposed investment in EVCF with DERs is viable with high wind imbalance penalties only. The NPVs of avoided penalties are \$78,106 and \$278,549 for low and high wind imbalance penalties, respectively.

It is also noted that wind imbalance penalties affects the optimal installation years of PV and BESS units. The optimal design of EVCF for Structure 1, considering low and high wind imbalance penalties, are presented in Table 4.1. When the penalties are low, the EVCF with DERs has a lower priority to mitigate wind power imbalances and hence low rating PV units are selected in the first year of the plan period, compared to the case with high wind imbalance penalties. Furthermore, the BESS is used more for supplying the PEV loads in the case of low wind penalties, which justifies the need for BESS installations in the latter years of the planning horizon. On the other hand, when high wind imbalance penalties are considered, the BESS is used for both, PEV loads and mitigating wind power imbalances, and therefore it is installed earlier in the planning horizon.

For Structure 2, the incremental cash flow diagram for the EVCF is obtained by comparing the net cash flow of the EVCF without and with DERs. It is observed that the incremental IRRs are 6% and 23% for low and high flexibility service prices, respectively, and hence, for MARR= 14%, the EVCF with DERs is viable only with high flexibility service prices. Table 4.2 presents the optimal design of the EVCF with DERs; it is noted

Table 4.1: Optimum Design of the EVCF with DERs in Structure 1

Wind Imbalance Penalty	Inst. Year	BESS		PV Units (kW)	Avoided Penalties ($)	Incremental IRR (%)
		Power (kW)	Energy (kWh)			
Low	1	180	840	220	78,106	13
	3	30	150	-		
	4	-	-	40		
	6	30	120	-		
	7	30	60	-		
High	1	150	690	270	278,549	17
	2	60	240	-		
	5	60	240	-		

that with low flexibility service prices, the PV units are installed at years 1 and 4, and are of low capacity, while when flexibility service price is high, they are installed in the first year, and of a higher capacity. The BESS units are installed in years 1-3 with low flexibility service prices, with a higher power rating and energy capacity at year 1, but lower power rating and energy capacity at years 2 and 3. With high flexibility service prices, the BESS units are installed in years 1 and 2 only, and are of higher power rating and energy capacity.

High fluctuations in PV power output are forcing the system operators to impose ramp rate limits. However, in this study, the penetration of PV generation is very low, less than 350 kW in both structures, and hence the fluctuations in PV power are not significant; and therefore, the ramp-rate limit is ignored. The control aspect of the proposed structures is out scope of the present work, but will be investigated as a separate study in the future, where ramp rate limits of the BESS and PV will be considered, and an appropriate control strategy will be chosen.

Table 4.2: Optimum Design of the EVCF with DERs in Structure 2

Flexibility Service Price	Inst. Year	BESS		PV Units (kW)	Incremental IRR (%)
		Power (kW)	Energy (kWh)		
Low	1	210	990	190	6
	2	30	90	-	
	3	30	150	-	
	4	-	-	60	
High	1	210	960	330	23
	2	150	750	-	

4.4.4 Flexibility Provisions from EVCF Equipped with DERs for Mitigating Wind Power Imbalances

Flexibility provisions from the EVCF with DERs, for mitigating wind power imbalances at year 10 in the two ownership structures, are shown in Figure 4.4. As wind forecasting errors are same in both structures and considering high wind imbalance penalties and high flexibility service prices, flexibility provisions from the EVCF with DERs would be similar in both structures. However, in Structure 1, it is observed that the EVCF with DERs compensates the deficit wind power fully at most of the hours, and partially at hour 14 when the power from PV units is not enough to supply all the PEV loads. It is also noted that the deficit wind power is not compensated at hours 3, 4 and 16 since there is no available power from PV units and the market price is not high enough to discharge the BESS at hour 3 and 4, while at hour 16, the BESS supplies the high demand of PEVs. In contrast, all deficit wind power is fully compensated in Structure 2. Furthermore, it is observed that surplus wind power is fully accommodated at all the hours, except, partially at hour 12, due to the fact that BESS charging reaches its maximum power

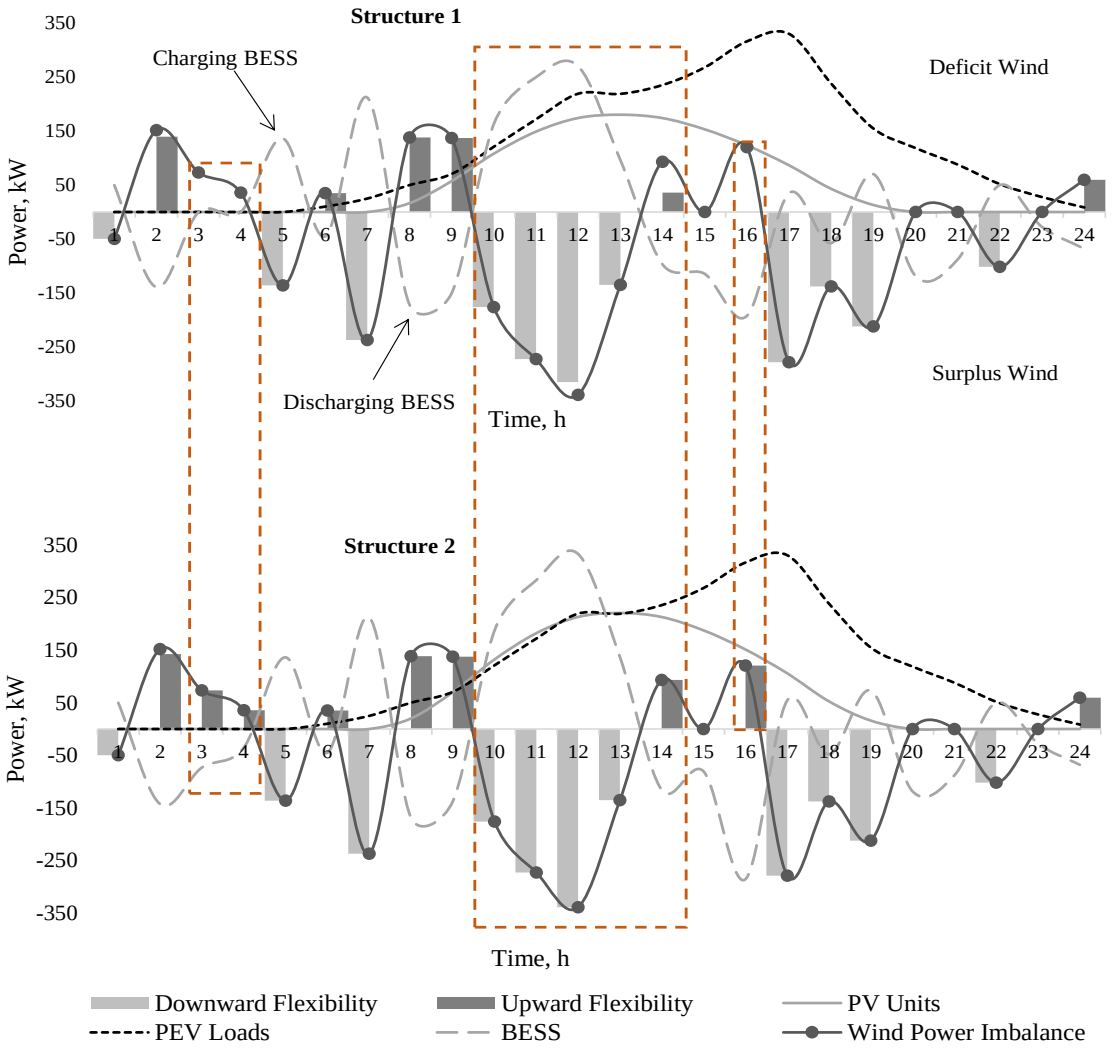

Figure 4.4: Flexibility provisions from the EVCF with DERs for mitigating wind power imbalances at year 10.

rating, *i.e.* 270 kW. Although this surplus power at hour 12 matches the PEV loads, there is power availability from PV units, and hence it mainly relies on charging the BESS to accommodate such surplus. In contrast, all surplus wind power is accommodated in Structure 2. As highlighted in Figure 5.5, in Structure 1, the output power of PV units is lower than PEV loads, while it matches PEV loads in Structure 2, due to the fact that the

total installed capacity of PV units is higher in Structure 2 with respect to Structure 1.

It should be noted that when there are too many charging and discharging cycles of the BESS, its degradation cost cannot be ignored. In this work, the depth of discharge (DOD) calculation approach [89], similar to the rainflow counting algorithm [90], is used to count the number of BESS cycles per day. Using the energy profile of BESS operation (Figure 4.5), the average number of charging and discharging cycles is calculated to be 2 cycles/day, in both structures. The number of BESS cycles is low because the proposed mitigation strategy does not depend only on the BESS, but also uses the compatibility of PV units and PEV charging loads to mitigate wind power imbalances, and hence the BESS degradation cost is not considered.

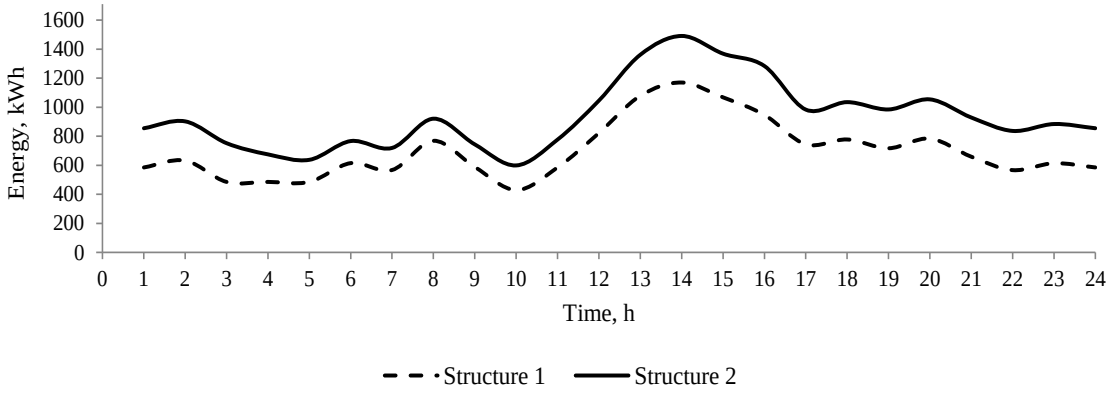

Figure 4.5: BESS energy profile during operation in year 10.

4.4.5 Impact of Variability of Wind and PV Generation, and Market Price on EVCF with DERs

MCS is a well established technique to estimate the probability density functions using historical data, and hence it is used to simulate the uncertainties of PV and wind generation, and market price. To capture the variability of wind and PV generation, and market

price, and illustrate their effects on design of EVCF with DERs, the proposed optimization model is executed over 200 MCS scenarios. The plot of expected incremental NPV is presented in Figure 4.6, considering high wind imbalance penalties in Structure 1, and high flexibility service prices in Structure 2. The expected incremental NPV of the EVCF with DERs for Structure 1 is 1.5 M$, while it is 0.8 M$ in Structure 2. In Structure 1, where the same ownership of WGF and EVCF with DERs is assumed, the revenue from WGF is taken into account, and that justifies the higher incremental NPV for Structure 1 with respect to Structure 2.

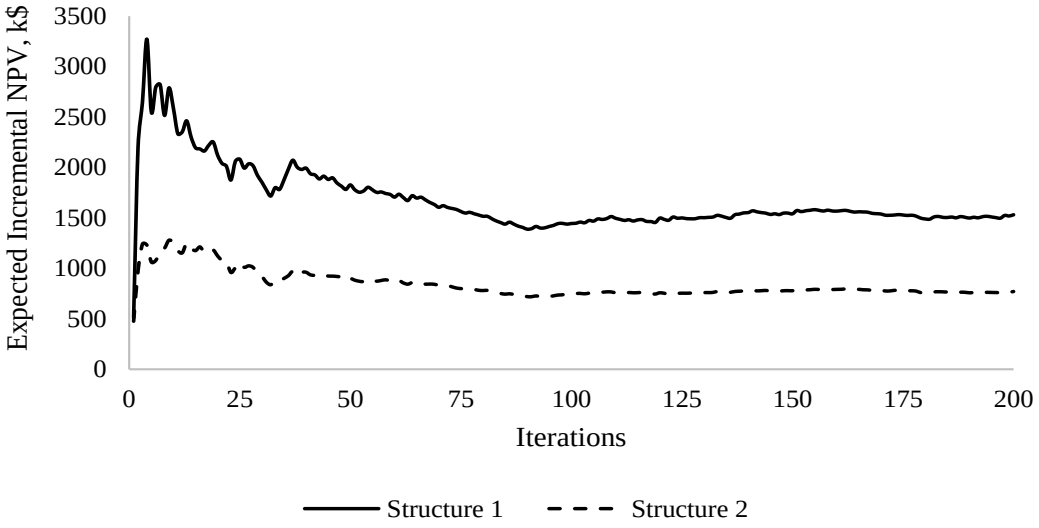

Figure 4.6: Expected incremental NPV of the EVCF with DERs in both structures.

Probability distributions of the power rating and energy capacity of the DERs integrated with EVCF are presented in Figures 4.7, 4.8, and 4.9 at year 10, considering high wind imbalance penalties for Structure 1 and high flexibility service prices for Structure 2. It is observed that, 600 kW of PV capacity has the highest probability in both structures, while the power and energy rating of the BESS with highest probability is 600 kW and 1800 kWh, respectively, in both structures.

The probability distributions of gross daily original deficit and surplus wind generation,

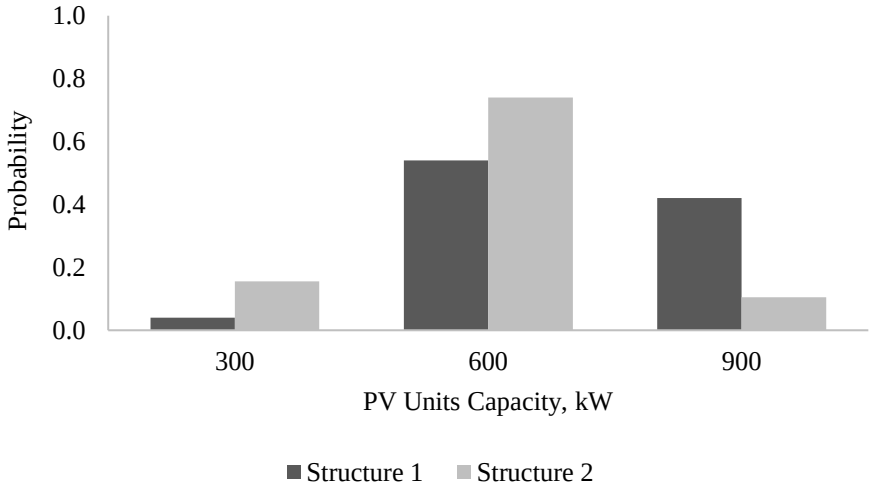

Figure 4.7: Probability distributions of the power unit capacity integrated with the EVCF at year-10.

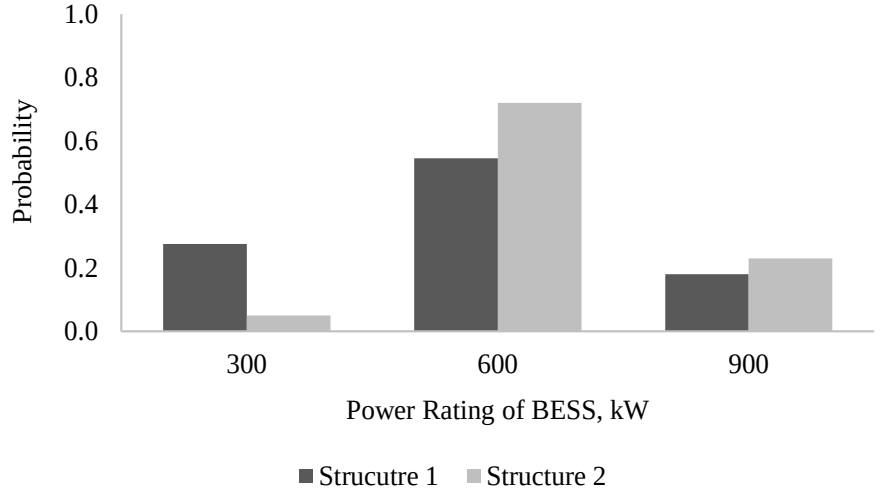

Figure 4.8: Probability distributions of the power rating of the BESS integrated with the EVCF at year-10.

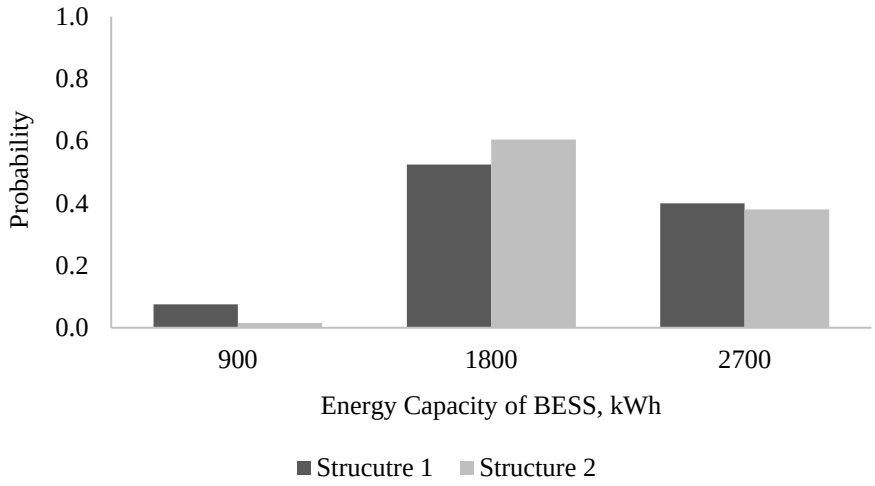

Figure 4.9: Probability distributions of the energy capacity of the BESS integrated with the EVCF at year-10.

and with flexibility provisions from the EVCF with DERs in both structures at year-10 are presented in Figurs 4.10 and 4.11, respectively. It is clear that the EVCF designed with DERs helps reduce the deficit and surplus wind energy. In both ownership structures, the compensation amount of deficit wind energy is same because the deficit wind penalty, *i.e.* $3.3\rho_k$ and upward flexibility price, *i.e.* 0.414 $\$/kWh$, are both high. On the other hand, the surplus wind penalty, *i.e.* $0.3\rho_k$ is not high in Structure 1, compared to the downward flexibility price, *i.e.* 0.207 $\$/kWh$, which justifies the higher accommodation of surplus wind energy in Structure 2 with respect to Structure 1.

4.5 Summary

This chapter proposed two different ownership structures to examine the effectiveness of using an EVCF with DERs for wind integrated grids, from the perspectives of WGF and EVCF owners. A new framework and an associated mathematical model were proposed to optimally design the EVCF with DERs that provided upward and downward flexibility

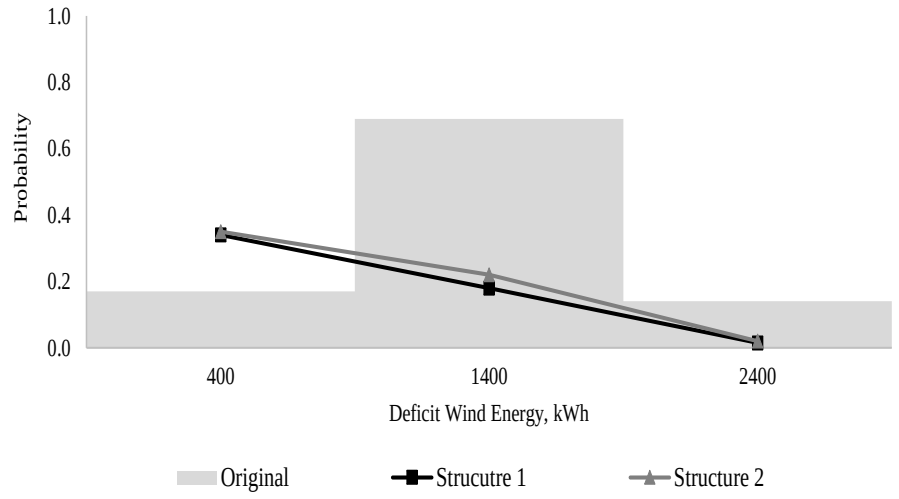

Figure 4.10: Probability distribution of original deficit wind energy and with flexibility provisions from the EVCF at year-10.

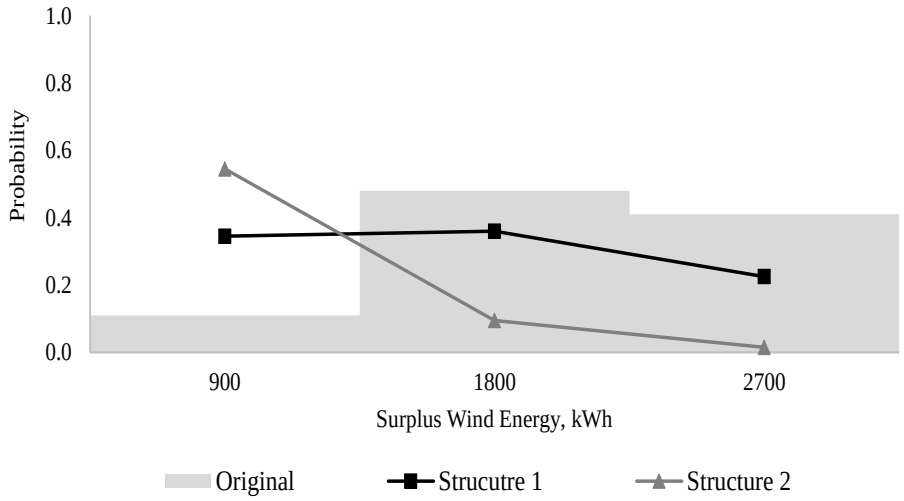

Figure 4.11: Probability distribution of original surplus wind energy and with flexibility provisions from the EVCF at year-10.

for mitigating wind power imbalances. The proposed framework also included an energy management system, which determined the optimal power supplied by DERs, and the power exchanged with the WGF in Structure 1 or with the grid in Structure 2. Simulation findings demonstrated that, from the perspective of a WGF, when wind imbalance penalties were high, it was economical to invest in the design of an EVCF with DERs and avoid such penalties. On the other hand, it required high flexibility service prices to encourage an EVCF owner to design its facility with DERs to provide flexibility service to the gird to mitigate wind power imbalances.

The proposed design of an EVCF with DERs is a superior solution for wind integrated smart grid as it can exploit the compatibility of PV units and PEV charging loads with WGF, and thus not only relying on the BESS for mitigating wind power imbalances. The installation cost of energy resources is expected to reduce in the future, and this will enhance the return on investments in EVCFs with DERs.

Chapter 5

Incentive Design for Flexibility Provisions From Residential Energy Hubs in Smart Grids [1]

5.1 Introduction

Flexibility in power systems has traditionally been provided by conventional generation units through adjustments to their power output to balance the supply and demand, and maintain the system frequency within an acceptable band. Although such practice still continues, the increasing penetration of RERs results in reduced share of controllable generation capacity, and consequently less generation reserves. To circumvent this issue, more flexibility provisions are necessary from the demand side.

In a smart grid environment, residential loads are being transformed to residential energy hubs (REHs) with energy demand, generation, and storage capabilities [8]; such

[1] This chapter has been submitted for publication in: W. Alharbi and K. Bhattacharya. "Incentive Design for Flexibility Provisions From Residential Energy Hubs in Smart Grids." *IEEE Transactions on Smart Grid*. (in revision).

REHs can increase the system flexibility and accrue benefits through deferment of system reinforcements and capacity investments. Consequently, it is reasonable to assume that the LDC establishes a rate structure that incentivizes the transformation of residential loads to REHs to provide flexibility, that can benefit both parties.

The main objectives of this chapter are as follows:

- Propose a novel and generic framework to determine the optimal incentives to be offered by the LDC, that will induce an optimal penetration of REHs for flexibility provisions in distribution grids, considering system operations and economic benefits of both the LDC and residential customers.
- Present a novel concept of unloaded and loaded states of REHs to mathematically quantify the flexibility provisions from an REH.
- Propose a Customer Profitability Model (CPM) along with a MCS based approach to determine the mathematical relationship between customer profitability of adoption of REHs and the incentives offered by the LDC.
- Develop a new mathematical model to simultaneously determine the optimal incentives to be paid by the LDC, and the optimal penetration of REHs for flexibility provisions in distribution systems, taking into account the operational aspects of both REHs and distribution systems.

5.2 Proposed Framework

5.2.1 Unloaded and Loaded States of REH

A novel concept of unloaded and loaded states of the REH is introduced in Figure 5.1. An *unloaded state* is when the REH supports the distribution system by reducing its load partially or fully, or providing energy to other loads at the same node. In this state,

the REH load that can be interrupted or the energy that the REH provides should not affect the customer's comfort requirements. A *loaded state* is when the REH adds extra load (more than its original load) on the distribution system. The REH also supports the system in a loaded state when the added load occurs at times of excessive generation from renewable energy resources. An idle state of an REH is when there is no change in the load from its baseline load, which may occur at certain times of the day as shown in Figure 5.1. Since the REH does not take any action in the idle state, this state is not considered in the present work. The daily output profile of the REH will be divided into unloaded and loaded states only.

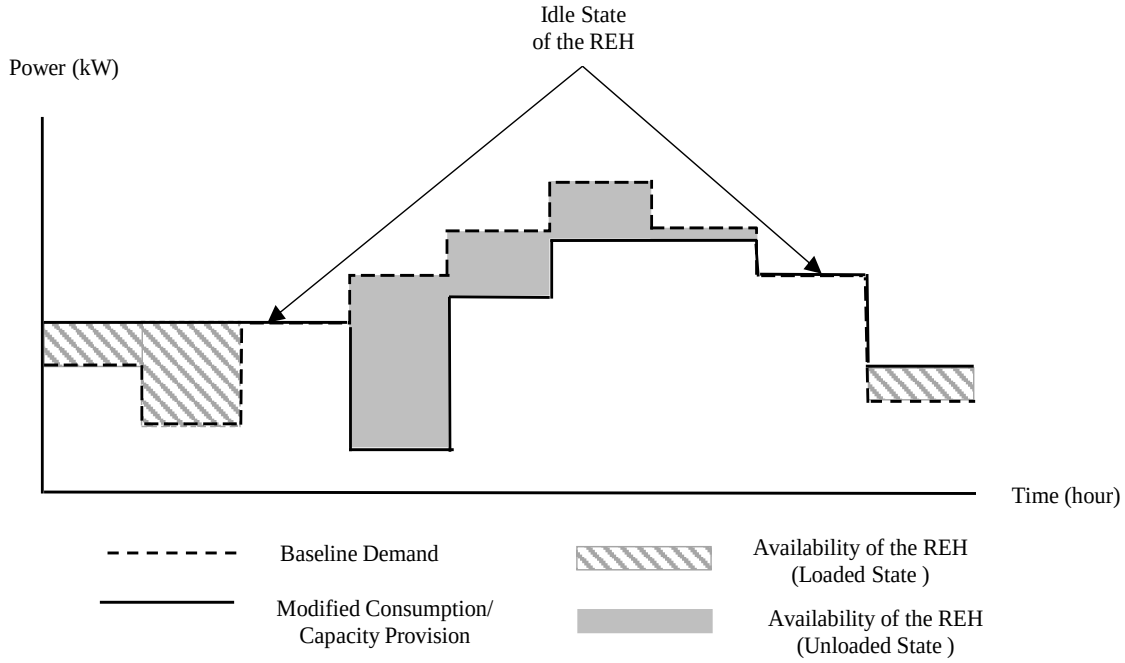

Figure 5.1: Unloaded and loaded states of the REH

The operation of REH switches from an unloaded state to a loaded state and *vice versa*, depending on the system conditions. In providing flexibility, the action taken by the REH in an unloaded state is a result of its action in a loaded state, at another period. Hence, to avoid double counting the incentive, the REH is paid for a single operational state only,

the unloaded states, over an operating horizon (1 day). On the other hand, to encourage the occurrence of the loaded states during off-peak periods, the loaded states are charged at Time-of-Use (TOU) prices.

5.2.2 Residential Load Willingness to Transform to REHs

In this section, a three-step approach, as depicted in Figure 5.2 is presented to model the customers' willingness to transform their houses to REHs. The main steps involved are: 1) Execute the Customer Profitability Model (CPM), 2) Regression Model and Cross Validations, and 3) Correlate Customer Profitability with Participation.

Customer Profitability Model (CPM)

Customer profitability is measured by the Internal Rate of Return (IRR) on investment to transform the house to an REH. In order to encourage customers to make such an investment, the LDC offers incentives that comprises two-parts, the first is a fixed rebate that represents a portion of the capital cost of transformation to an REH (ω), and the second is a variable component (ρ^{Inc}) associated with the flexibility service provided by the REH. To this end, the IRR need be modeled as a function of the incentives offered by the LDC. An MCS is used to generate numerous scenarios of ω and IRR using the proposed CPM, from which ρ^{Inc} is optimally determined for each scenario; hence a large date set of ω, ρ^{Inc}, and IRR is created, which is used to develop a mathematical relationship among these variables.

Objective Function: Minimize the variable component of the incentive (ρ^{Inc}), for a randomly selected value of IRR and ω, while considering energy management system of the REH.

$$Min \ \rho^{Inc} \tag{5.1}$$

The following constraints apply:

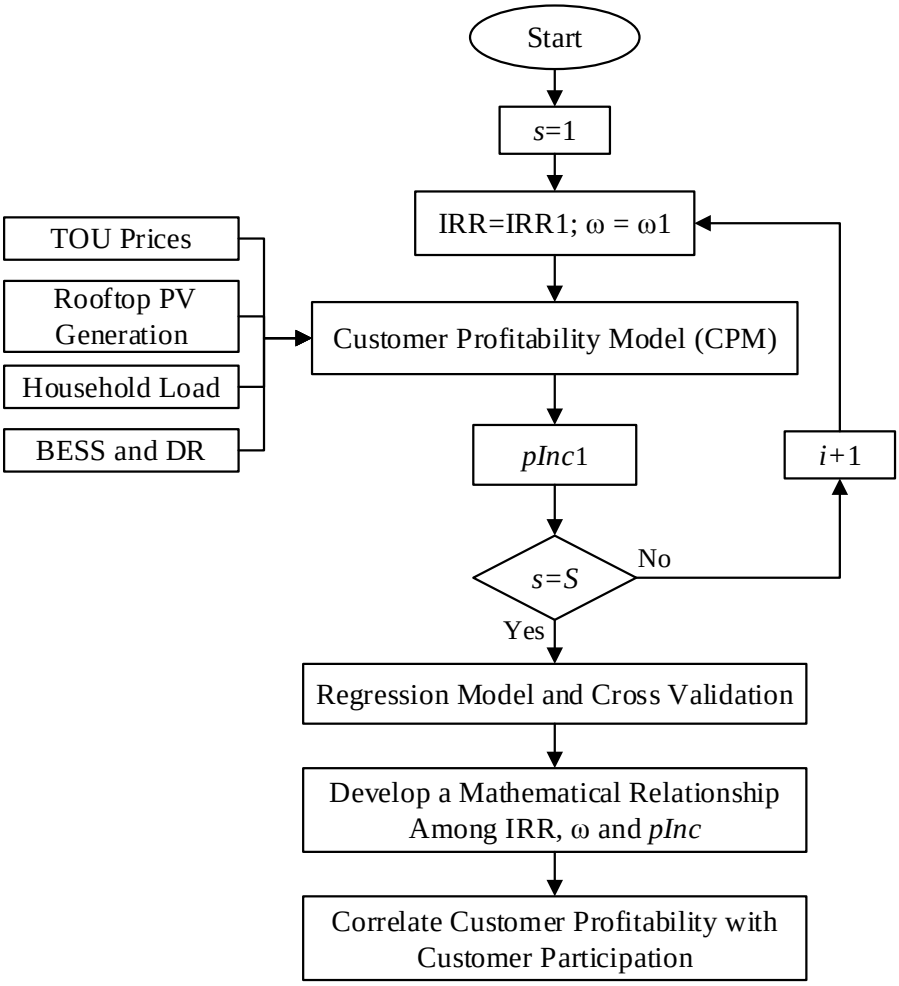

Figure 5.2: Modeling customers willingness to transform to REH.

Profitability Condition: This condition allows the selection of an appropriate IRR in the proposed CPM, which is the rate at which the net present value (NPV) of transforming a residential load to an REH, is equal to zero. It also relates the three variables, IRR, ω, and ρ^{Inc} together.

$$[\sum_{y=0}^{Y} \frac{Revenue_y - Cost_y^{O\&M}}{(1+IRR)^y}] - (1-\omega)C^{Inv} = 0 \tag{5.2}$$

where $Revenue_y$ denotes the revenue earned by the REH from providing flexibility service to the distribution grid, given by:

$$Revenue_y = \rho^{Inc} \sum_{k=1}^{24} P_{k,y}^{+S} \tag{5.3}$$

In (5.2), $Cost_t^{O\&M}$ denotes the operation and maintenance (O&M) cost of the REH, as follows:

$$Cost_y^{O\&M} = (OM^f Psize^{BESS} + OM^{PV} C^{PV})_y + [\sum_{k=1}^{24} OM^v \eta^{out} P_{k,y}^{out} + C_k^{TOU} P_{k,y}^{-S}] n_d \tag{5.4}$$

The first and third terms of (5.4) denote the fixed and variable O&M cost of the BESS, respectively. The O&M cost of PV generation is denoted by the second term, while the cost of adding load on the main grid in loaded states of the REH is denoted by the fourth term.

Demand-Supply Balance of REH: Total generation within the REH should meet the total demand at period k, taking into account flexibility provisions.

$$P_{k,y}^{PV} + P_{k,y}^{out} + P_{k,y}^{-DR} + P_{k,y}^{-S} = P_{k,y}^{HL} + P_{k,y}^{in} + P_{k,y}^{+DR} + P_{k,y}^{+S} \qquad \forall k \ \forall y \tag{5.5}$$

BESS Related Constraints: The dynamic variation of the BESS SOC depends on the

charging and discharging operations, and their respective efficiencies, as given below:

$$SOC_{k+1,y} = SOC_{k,y} + (P^{in}_{k,y}\eta^{in} - P^{out}_{k,t}/\eta^{out})\Delta T \qquad \forall k \ \forall y \tag{5.6}$$

The limits on BESS charging and discharging power, drawn or injected by the REH, from the grid, are limited by constraints given below; also the SOC of the BESS is bounded by specified limits.

$$P^{in}_{k,y} \leq Psize^{BESS} \qquad \forall k \ \forall y \tag{5.7}$$

$$P^{out}_{k,y} \leq Psize^{BESS} \qquad \forall k \ \forall y \tag{5.8}$$

$$0.2C^E \leq SOC_{k,y} \leq C^E \qquad \forall k \ \forall y \tag{5.9}$$

The initial and final status of the SOC is assumed 50% of BESS energy capacity; thus,

$$SOC_{k,y} = 0.5C^E \qquad \forall k = 1 \ \ \& \ \ k = 24, \forall y \tag{5.10}$$

The BESS should not be charged and discharged at the same time, which is ensured as follows:

$$P^{in}_{k,y}P^{out}_{k,y} = 0 \qquad \forall k \ \forall y \tag{5.11}$$

Demand Response Constraints: These constraints ensure that the DR is within capacity limits.

$$P^{+DR}_{k,y} \leq \gamma Pd_{k,y} \qquad \forall k \ \forall y \tag{5.12}$$

$$P^{-DR}_{k,y} \leq \gamma Pd_{k,y} \qquad \forall k \ \forall y \tag{5.13}$$

Moreover, demand variations must be balanced within the 24 hour horizon, so as not to shift the customers' activities to the next day. The following constraint is used:

$$\sum_{k}^{24} P^{+DR}_{k,y} = \sum_{k}^{24} P^{-DR}_{k,y} \qquad \forall k \ \forall y \tag{5.14}$$

Upward and Downward DR Coordination Constraint: To avoid simultaneous upward and downward DR selections, the following constraint is included:

$$P_{k,y}^{+DR} P_{k,y}^{-DR} = 0 \qquad \forall k \ \forall y \tag{5.15}$$

Power Conversion Limits: These constraints ensure that the power from rooftop PV, converted from dc to ac, is within the PV inverter limit. Similarly, the power of the BESS converted from dc to ac and *vice versa*, should be within the BESS inverter limits.

$$P_{k,y}^{PV} \leq P^{Inverter^{PV}} \qquad \forall k \ \forall y \tag{5.16}$$

$$P_{k,y}^{in} \leq P^{Inverter^{BESS}} \qquad \forall k \ \forall y \tag{5.17}$$

$$P_{k,y}^{out} \leq P_{k,y}^{Inverter^{BESS}} \qquad \forall k \ \forall y \tag{5.18}$$

Coordination of Unloaded and Loaded States of REH: These constraints ensure that the REH is not in an unloaded and loaded state simultaneously, as follows:

$$P_{k,y}^{+S} P_{k,y}^{-S} = 0 \qquad \forall k \ \forall y \tag{5.19}$$

The proposed mathematical model is a nonlinear programing model which is solved using the MINOS solver in GAMS environment.

Regression Model and Cross Validation

A multiple linear regression model [91] is used to capture the relationship among ω, ρ^{Inc}, and IRR: To this effect, MCS is carried out on the CPM considering a range of variations in ω and IRR to generate a large data set of corresponding values of ρ^{Inc}. This data set (ω, ρ^{Inc}, and IRR) is input to a multiple linear regression model to obtain a mathematical relation as follows:

$$IRR = A\rho^{Inc} + B\omega + C \tag{5.20}$$

Cross-validation [92] is a statistical method to evaluate the performance of the regression model by dividing the data into two segments: one to train the model and the other to validate it. The basic and known form of cross-validation, k-fold cross-validation, is used here, in which the data is partitioned into k-sized segments or folds to perform k iterations of training and validation. With each iteration, a different fold of the data is held out for validation while the remaining $k-1$ folds are used for training. The error in each iteration is calculated as follows:

$$Error = \sqrt{\frac{\sum_{i=1}^{N}(IRR_{tested} - IRR_{predicted})^2}{N}} \tag{5.21}$$

where N represents the total number of data points in each k iteration.

The average of k recorded errors is the cross-validation error that will be the performance metric for the regression model.

Correlating Customer Profitability with Participation

The residential customers will be encouraged to transform their houses to REHs when the IRR of such an investment is high; no investment is made if the IRR is lower than the minimum acceptable rate of return (MARR). Customer participation can be correlated with profitability, for two values of IRR: IRR^{NP} at which none of the households transform to REHs; while IRR^{FP} where all households tend to transform their houses to REHs. Thus, a positive linear correlation between customer participation and IRR is assumed as follows:

$$X^{REH} = \alpha IRR + \beta \tag{5.22}$$

where

$$\alpha = \frac{1}{IRR^{FP} - IRR^{NP}} \tag{5.23}$$

By substituting $X^{REH} = 0$ and $IRR = IRR^{NP}$, b is obtained as:

$$\beta = -\frac{IRR^{NP}}{IRR^{FP} - IRR^{NP}} \tag{5.24}$$

Now, X^{REH} can be written as:

$$X^{REH} = \frac{IRR - IRR^{NP}}{IRR^{FP} - IRR^{NP}} \tag{5.25}$$

When IRR^{NP} and IRR^{FP} are known, a relationship between customers' participation and IRR can be obtained, which is discussed later in Subsection 5.3.2.

5.2.3 Incentive Design Model (IDM) for Flexibility Provisions from REHs

A new mathematical model is proposed to determine the optimal incentives to households and the corresponding optimal penetration of REHs.

Objective Function: Minimize the investment and operating cost of the LDC, given by:

$$Min \ [C^{OP} + C^{Flex}] \tag{5.26}$$

Where C^{OP} denotes the operation cost of the LDC that includes the payment towards purchasing power from the grid, peak demand charge incurred, net of the revenue from selling power to customers who did not transform to REH, given by:

$$C^{OP} = [\sum_{k=1}^{24} \rho_k P_{ss,k}^{SS}] n_d + C^{PK} P^{PK} - \sum_i [\sum_k C_k^{TOU} P d_{i,k} (1 - X_r^{REH})] n_d \tag{5.27}$$

In (5.26), C^{Flex} is the flexibility cost of the LDC that includes rebate paid to the households for transforming houses to REHs, and incentives to households for providing power

flexibility, net of the revenue from selling power to REHs.

$$C^{Flex} = \sum_r \omega_r X_r^{REH} C^{REH} nh_r + \sum_r \rho_r^{Inc} \sum_k P_{r,k}^{+S} - \sum_r [\sum_k C_k^{TOU} P_{r,k}^{-S}] n_d \quad (5.28)$$

The following constraints apply:

Power Flow Equations: These constraints ensure that the power injected at the substation bus, net of the load, and power flexibility in unloaded and loaded states are governed by power flow equations.

$$P_{ss,k}^{SS} - Pd_{i,k}(1 - X_r^{REH}) - P_{r,k}^{-S} + P_{r,k}^{+S} = f(V_{i,k}, \delta_{i,k}) \qquad \forall (i,r) \in N, \forall k \quad (5.29)$$

$$Q_{ss,k}^{SS} - Qd_{i,k} = g(V_{i,k}, \delta_{i,k}) \qquad i\forall N, \forall k \quad (5.30)$$

Power Flexibility in Unloaded and Loaded States of REHs: This constraint ensures that the power flexibility in unloaded and loaded states should be within the demand supply balance of the REH.

$$(X_r^{REH} P_{r,k}^{PV} nh_r) + P_{r,k}^{-ABESS} + P_{r,k}^{-ADR} + P_{r,k}^{-S} = (X_r^{REH} Pd_{r,k}) + P_{r,k}^{+ABESS} + P_{r,k}^{+ADR} + P_{r,k}^{+S} \quad (5.31)$$

Where aggregated DR should not exceed the maximum available power considering the percentage of deferrable load and penetration of REHs, as follows:

$$P_{r,k}^{+ADR} \leq \gamma X_r^{REH} Pd_{r,k} \qquad \forall r \in N, \forall k \quad (5.32)$$

$$P_{r,k}^{-ADR} \leq \gamma X_r^{REH} Pd_{r,k} \qquad \forall r \in N, \forall k \quad (5.33)$$

Likewise, aggregated power charging and discharging of the BESS should be within the power limit of the BESS and the penetration limit of the REHs, given by:

$$P_{r,k}^{+ABESS} \leq X_r^{REH} Psize^{BESS} nh_r \qquad \forall r \in N, \forall k \quad (5.34)$$

$$P_{r,k}^{-ABESS} \leq X_r^{REH} Psize^{BESS} nh_r \qquad \forall r \in N, \forall k \tag{5.35}$$

Power Conversion Limits: The converted power from the aggregated PV generation and BESSs should be within the inverter limits.

$$P_{r,k}^{PV} \leq X_r^{REH} nh_r P^{Inverter^{PV}} \qquad \forall r \ \forall k \tag{5.36}$$

$$P_{r,k}^{-BESS} \leq X_r^{REH} nh_r P^{Inverter^{BESS}} \qquad \forall r \ \forall k \tag{5.37}$$

$$P_{r,k}^{+ABESS} \leq X_r^{REH} nh_r P^{Inverter^{BESS}} \qquad \forall r \ \forall k \tag{5.38}$$

Coordination Constraints of Aggregated REHs Resources: The following constraints ensure that charging/discharging aggregated BESS, inducing upward/downward aggregated DR, and power flexibility in loaded and unloaded states of REHs do not occur simultaneously, as follows:

$$P_{k,y}^{+ABESS} P_{k,y}^{-ABESS} = 0 \qquad \forall r \ \forall K \tag{5.39}$$

$$P_{k,y}^{+ADR} P_{k,y}^{-ADR} = 0 \qquad \forall r \ \forall K \tag{5.40}$$

$$P_{k,y}^{+S} P_{k,y}^{-S} = 0 \qquad \forall r \ \forall K \tag{5.41}$$

State of Charge of the BESS of the Aggregated REHs:

$$SOC_{r,k+1} = SOC_{r,k} + (P_{r,k}^{+ABESS} \eta^{in} - P_{r,k}^{-ABESS} / \eta^{out}) \Delta t \qquad \forall r, \forall k \tag{5.42}$$

$$X_r^{REH} C^E nh_r) \leq SOC_{r,k} \leq X_r^{REH} C^E nh_r) \qquad \forall r, \forall k \tag{5.43}$$

Participation of Residential Customers: This is based on their economic benefits, measured by the IRR, which depends on the incentives offered by the LDC:

$$X_r^{REH} = \frac{IRR_r - IRR^{NP}}{IRR^{FP} - IRR^{NP}} \tag{5.44}$$

$$IRR_r = A\rho_r^{Inc} + B\omega_r + C \tag{5.45}$$

The coefficients A and B, and constant C will be determined using the proposed CPM along with MCS, which will be discussed and presented in Subsection 5.3.2.

Maximum Rebate Limit: The rebate given to the customer for transforming a house to REH can be limited as follows:

$$\omega_r \leq \overline{\omega} \tag{5.46}$$

Constraints of Peak Load: These constraints, in conjunction with (5.27), ensure that the peak load is minimized.

$$P^{SS}_{ss,k} \leqslant P^{PK} \qquad \forall ss, \ \forall k \tag{5.47}$$

Maximum Reverse Power Flow Limits: This constraint ensures that the allowable power flexibility in a supportive state of aggregated REHs, which causes the maximum reverse power flow for the minimum load condition, is limited as follows:

$$\sum_{r\in N} P^{+S}_{r,k} \leqslant \sum_{i\in N} Pd^{Min}_{i,k} + 0.6 S^{SScap}_{ss} \tag{5.48}$$

Feeder Capacity Limits: The power flow through any distribution feeder should comply with the feeder capacity limit.

$$f(V_{i,k}, \delta_{i,k}) \leqslant S^{Fcap}_{(i,j)} cos\theta^{F}_{(i,j),k} \qquad \forall (i,j) \in N : \exists (i,j), \forall k \tag{5.49}$$

$$g(V_{i,k}, \delta_{i,k}) \leqslant S^{Fcap}_{(i,j)} sin\theta^{F}_{(i,j),k} \qquad \forall (i,j) \in N : \exists (i,j), \forall k \tag{5.50}$$

Substation Capacity Limits: The total power delivered by the substation transformer should be within the capacity limit of the substation.

$$(P^{SS}_{ss,k})^2 + (Q^{SS}_{ss,k})^2 \leqslant S^{SScap^2}_{ss} \qquad \forall k \tag{5.51}$$

Voltage Limits: The bus voltage constraints are defined as follows:

$$V^{Min} \leqslant V_{i,k} \leqslant V^{Max} \qquad i\forall N, \forall k \tag{5.52}$$

The proposed IDM is a nonlinear programing model and solved using the MINOS solver in GAMS.

5.3 Results and Discussions

5.3.1 Test System and Input Data

The 33 bus radial distribution system presented in [76], shown in Figure 3.4, is considered in this study. The total system peak demand is 4.4 MW, and base voltage is 12.66 kV. The substation connected at bus 1 has two transformers of 1.5 MVA each, and one of 2 MVA. The shape of the load profile is taken from the IEEE Reliability Test System base load. All loads are assumed to be residential loads, the house peak load is assumed to be 2.08 kW, and hence the number of houses at each bus can be calculated.

The house, when transformed to an REH, is equipped with a 10 kW rooftop PV, a 3 kW/ 6 kWh BESS; the PV and BESS inverters are rated 12 kW and 6 kW, respectively. The charging and discharging efficiencies of the BESS are 95%. The cost of transforming the house to an REH is $33,944 [93], and the annualized installation cost of the REH considering a life of ten years, and 10% discount rate is obtained to be $5,524. The percentage of deferrable loads is assumed to be 15%. Three years of HOEP data from May 2012 to May 2015 is used to generate the average price profile. Ontario TOU electricity price is considered for residential customers.

The empirical model described in [81] is used to estimate the PV output for a typical day, considering three years of historical hourly temperature and insolation data from from Solar Radiation Research Laboratory. The fixed O&M cost of PV units is 19 $/kW-year. The fixed and variable O&M costs of the BESS are 26.8 $/kW-year and 0.0011 $/kWh, respectively 89.

5.3.2 House Transformation to REH

Using MCS of the proposed CPM, a large data set of ω, ρ^{Inc}, and IRR is obtained by varying ω from [0 - 0.4] and IRR from [0.05 - 1]; subsequently the CPM determines the optimal ρ^{Inc} for any set of ω and IRR, and hence 1000 samples of data is generated and used as inputs to a multiple linear regression model to determine a mathematical relationship as follows, and presented in Figure 5.3.

$$IRR_r = 0.591\rho_r^{Inc} + 0.716\omega_r - 0.212 \tag{5.53}$$

For k-fold cross-validation, the value of k is taken to be 5, and each of the five subsets have 200 samples of data. The error in each iteration is calculated, and the cross-validation error, the average of these errors, is found to be 0.050, which implies a superior level of model prediction performance.

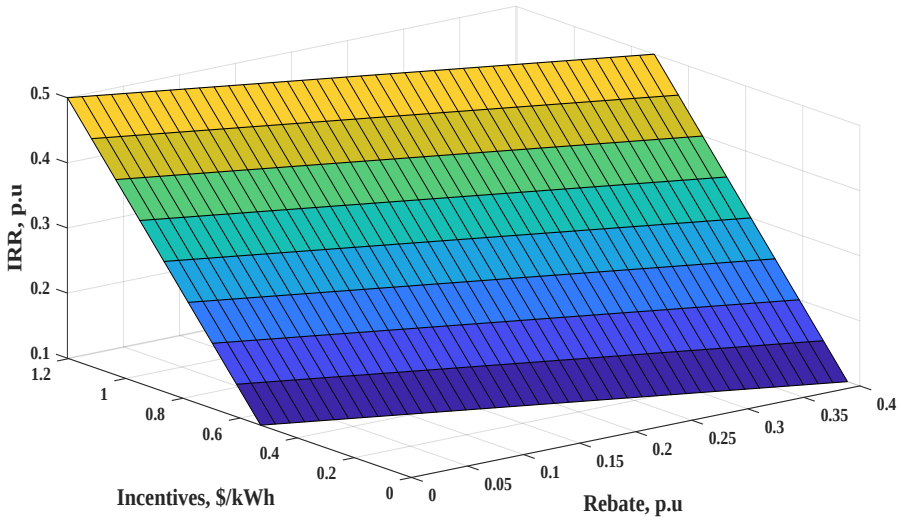

Figure 5.3: IRR with respect to rebate and incentives.

For correlating the customers participation with IRR on investment to transform the house to REH, MARR is assumed to be 14%, and hence IRR^{NP} can be any value between [0

- 13%], however, the upper value, 13% is selected for IRR^{NP} as it guarantees $X^{REH} = 0$. As the decision makers cannot know with certainty, the value of IRR^{FP} at which all households will participate in transforming their houses to REHs, pessimistic and optimistic scenarios are considered, and hence two values of IRR^{FP} are assumed as follows:

- *Pessimistic Scenario:* all households will transform their houses to REHs when $IRR^{FP} = 40\%$.
- *Optimistic Scenario:* all households will transform their houses to REHs when $IRR^{FP} = 20\%$.

In the pessimistic scenario, the relationship between customer participation with the IRR is obtained as:

$$X_r^{REH} = 3.704 IRR_r - 0.481 \tag{5.54}$$

By substituting (5.54) into (5.53), X_r^{REH} is obtained as:

$$X_r^{REH} = 2.189 \rho_r^{Inc} + 2.652 \omega_r - 1.266 \tag{5.55}$$

while in the optimistic scenario, the relationship is as follows:

$$X_r^{REH} = 14.286 IRR_r - 1.857 \tag{5.56}$$

Likewise, substituting (5.56) into (5.53), X_r^{REH} is obtained as:

$$X_r^{REH} = 8.443 \rho_r^{Inc} + 10.228 \omega_r - 4.885 \tag{5.57}$$

5.3.3 Penetration of REHs, Incentives, and Flexibility Provisions

The optimal penetration of REHs and associated incentives, and the associated flexibility provisions from REHs are determined using the proposed IDM. Figure 5.4 illustrates the

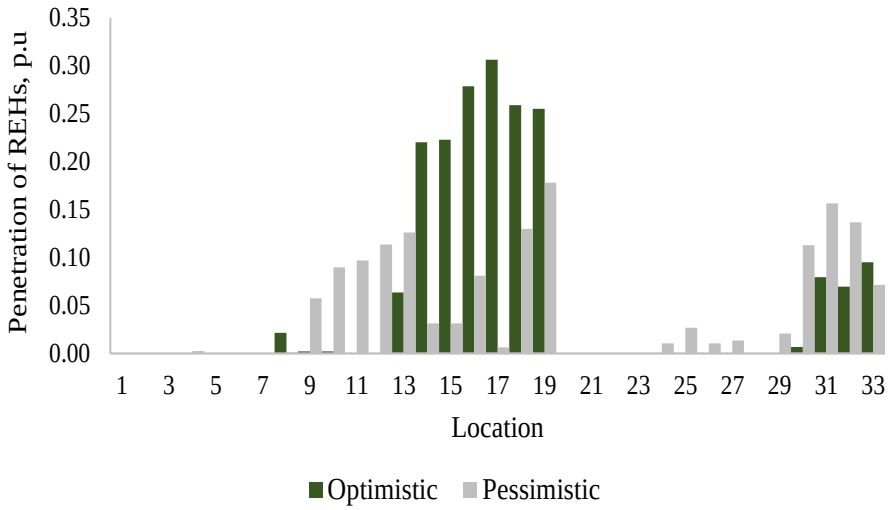

Figure 5.4: Optimal penetration of REHs for different scenarios.

optimal penetration of REHs in the distribution system, for different scenarios. It is economical for the LDC to distribute the penetration of REHs over some locations rather than having high penetration of REHs at few locations in the system. Hence, the penetration of REHs is low but distributed over locations in pessimistic scenario due to the higher IRR sought by residential customers, compared to the optimistic scenario.

Optimal economic benefits of the LDC from penetrating REHs in the system is provided in Table 5.1. The rebate in both scenarios is found to be $1657, which is 30% of the

Table 5.1: Optimal Economic Benefits of the LDC

Scenarios	Rebate ($)	Economic Benefits of LDC ($)
Optimistic	1657	1,712,140
Pessimistic	1657	1,677,417

annualized cost of transforming the house to an REH. It is observed that there is no significant difference in economic benefits between the optimistic and pessimistic scenarios due to the fact that the penetration of REHs is lower but more distributed over locations

in the pessimistic scenario.

Figure 5.5 presents the optimal incentives paid by the LDC for residential customers, so as to transform houses to REHs to provide power flexibility in the system. It is noted that the incentives are higher in the pessimistic scenario as compared to the optimistic scenario since $IRR^{FP}$is chosen to be high in the pessimistic scenario.

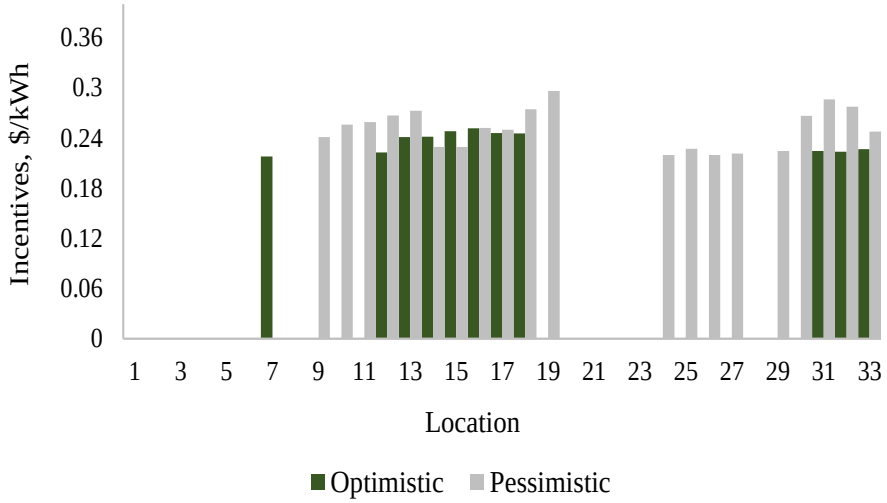

Figure 5.5: Optimal incentives paid by the LDC

The plot of IRRs on investment of houses for transformation to REHs, for different scenarios, is presented in Figure 5.6. Note that, the IRRs result from the incentives paid by the LDC, which is higher in the pessimistic scenario. These incentives paid by the LDC to residential customers are as low as possible, so as to minimize the cost of LDC, and hence results in IRRs close to the MARR (14%).

For a fair comparison, in terms of flexibility provisions between the two scenarios, the number of transformed houses to REHs should be the same in both scenarios. Hence, location-18 in the optimistic scenario and location-31 in the pessimistic scenario are selected, where fifteen houses are transformed to REHs in both scenarios. Load profiles of these fifteen houses, before and after transformation to REHs, in the different scenarios, are

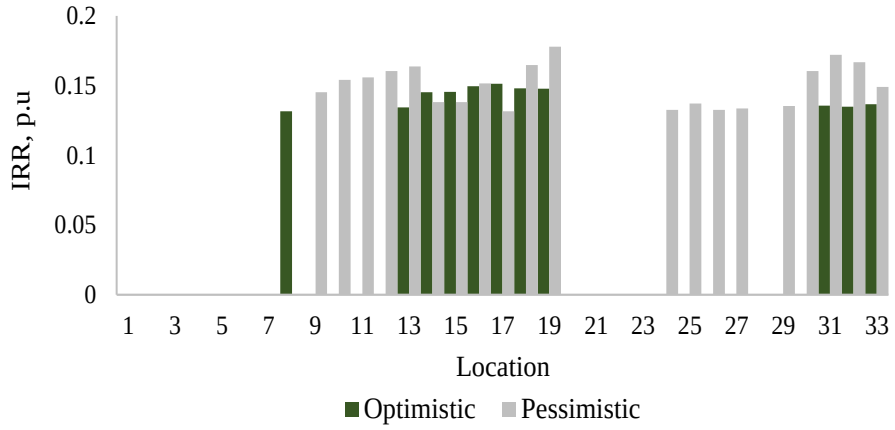

Figure 5.6: IRR on investment of houses for transformation to REHs.

presented in Figure 5.7. The modified consumption/ capacity provisions of fifteen REHs are not the same as they occur at different locations in the system. Such transformation helps to shift the demand from on-peak hour, *i.e* hour-20 to off-peak hours, *i.e* hours-4 and -22 in the optimistic scenario while hours-7 and -22 in the pessimistic scenario.

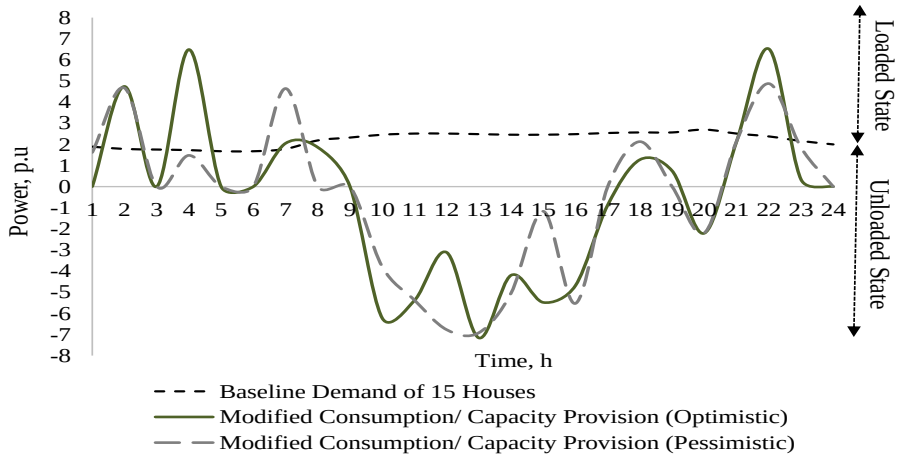

Figure 5.7: Load profiles of 15 houses before and after transformation to REHs.

Figure 5.8 shows the effect of transforming fifteen houses to REHs on the total load at location-18 in the optimistic scenario while at location-31 in the pessimistic scenario. The

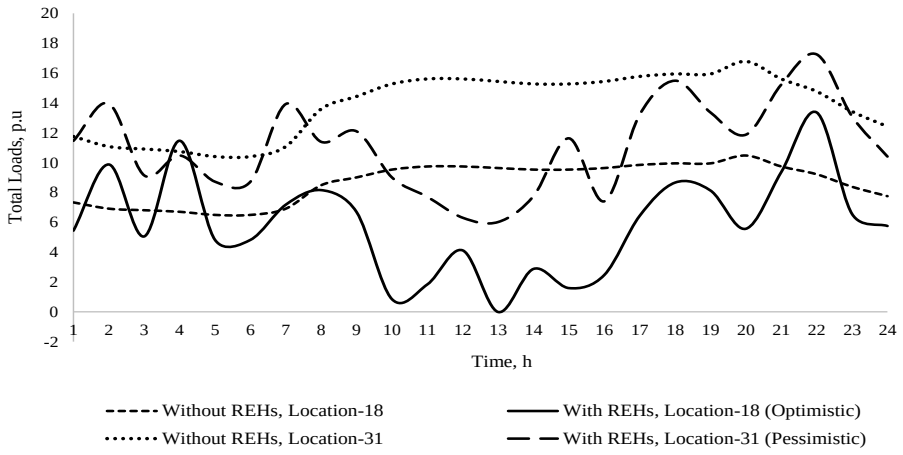

Figure 5.8: Total load profiles without and with REHs.

shape of the load profiles at the two locations are changed and reduced, and that illustrates the effectiveness of penetrating REHs into the distribution system. More reduction in the total load is observed during the times from hour-10 to -16 because of availability of PV generation at these hours. Such reduction in system load at the two locations come also from the aggregated BESSs and DRs, as presented in Figures 5.9 and 5.10. That is, both discharging the BESS and downward DR take place at peak hour, *i.e* hour-20 while charging the BESS and upward DR occur during off-peak times, such as hours-2 and 7.

5.4 Summary

The chapter presented a novel framework for design of optimal incentives for flexibility provisions from penetrating REHs in smart grids, considering the perspectives of the LDC and residential customers. The relationship of residential customers' participation with the incentives offered by the LDC was modelled. A new concept of unloaded and loaded states of REH was thereafter introduced to quantify the flexible power availability of REHs, which was necessary for quantifying flexibility provisions from REHs. Finally, the proposed IDM simultaneously determined the optimal penetration of REHs in the distribution grid and

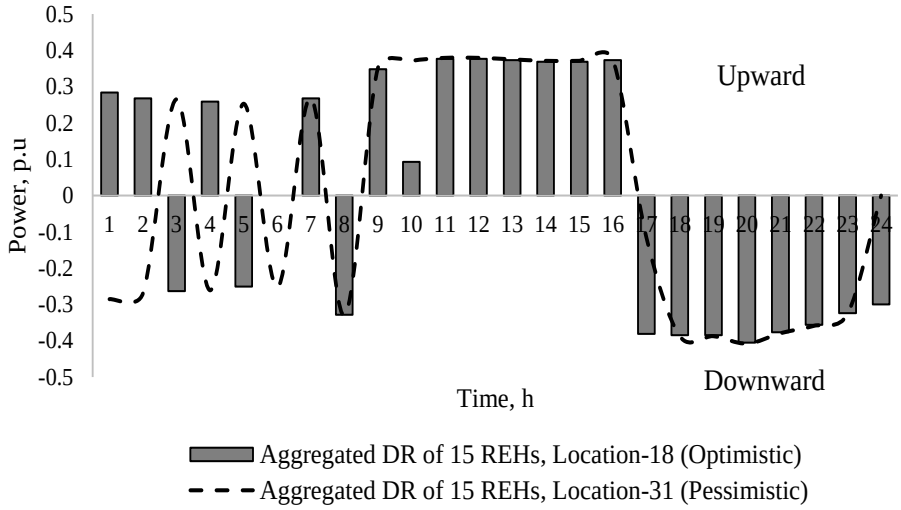

Figure 5.9: Aggregated BESSs of 15 REHs in different scenarios.

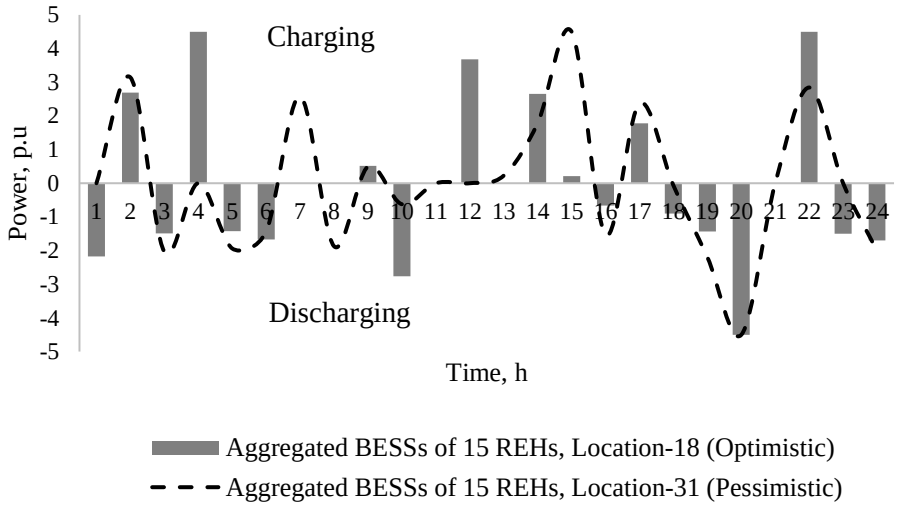

Figure 5.10: Aggregated DR of 15 REHs in different scenarios.

the optimal incentives paid by the LDC to residential customers for flexibility provisions. Case studies and numerical results were presented to demonstrate the performance of the proposed framework. The LDC can use the proposed framework to assess and quantify the required flexibility from the optimal penetration of REHs, and make a decision on the appropriate incentives to be paid to residential customers for the provision of flexibility in smart grid. Uncertainties in rooftop PV generation, system load, and market price will be considered in a future work.

Chapter 6

Conclusions, Contributions and Future Work

6.1 Summary

The goal of the research presented in the thesis was to develop models to address some of the pertinent issues relating to flexibility provisions from energy hubs. The motivations for this research, and review of associated literature, that laid out the main research objectives, were presented in Chapter 1.

In Chapter 2, the relevant topics related to the research were presented. A background to power system flexibility was discussed, followed by DERs including rooftop PV generation and BESS. The chapter also included discussion on DR, and PEV types and charging levels. Thereafter, a background on queuing theory and optimal power flow was presented.

Chapter 3 presented a novel framework for designing an EVCF as a smart energy hub from the perspectives of both an investor and LDC. The proposed framework includes a VDT, a QM, a distribution margin assessment model, a DG penetration assessment model, an EAM, and a distribution operations model. Three design options for EVCFs commis-

sioned in distribution systems were examined; BESS, renewables based DG, and an energy hub that incorporated both BESS and renewables-based DG with the option of exchanging power with the main grid. Detailed results considering a 33 bus distribution system and realistic vehicle statistics extracted from the 2009 (US) NHTS data were presented and discussed. The effects of different PEV battery types and specific geographies, *i.e.*, rural and urban, on the probability of PEV arrivals at an EVCF and the design decisions of the EVCF were investigated.

In Chapter 4, two different ownership structures were introduced to examine the effectiveness of using an EVCF with DERs for wind integrated grids, from the perspectives of WGF and EVCF owners. A new mathematical model to design an EVCF with DERs to provide flexibility services in wind integrated power grids was proposed. The DER options considered for EVCF design are PV units and BESS. An energy management system was included in the proposed model to determine the optimal power supplied by DERs, and the power exchanged with the WGF or with the grid. The effects of wind power uncertainty on power system operations are mitigated through the designed EVCF with DERs via the upward and downward flexibility provisions. MCS was used to simulate the uncertainties in PV and wind generation, and market price. Studies considering an 18 MW WGF and the NHTS 2009 data were presented to illustrate the effectiveness of the flexibility provisions from the design of EVCF with DERs.

In Chapter 5, houses were transformed to REHs to develop an inherent flexibility in their portfolios, and hence offer a wide range of benefits to power grids, such as peak reduction, congestion relief and capacity deferral. A novel framework was proposed to simultaneously determine the optimal penetration of REHs in distribution systems and optimal incentives remunerated by the LDC to residential customers for flexibility provisions, considering economic benefits of both parties. The proposed framework modeled the relationship between the participation of residential customers in transforming their houses to REHs and the incentives to be offered by the LDC. A new concept of unloaded and loaded states of REHs was also introduced for quantifying the power availability of REHs, from which power flexibility could be provided considering the penetration of REHs in the system.

Detailed findings considering a 33-bus distribution system were reported and discussed. The LDC can use the proposed framework to assess and quantify the required flexibility from the optimal penetration of REHs, and make a decision on the appropriate incentives to be paid to residential customers for the provision of flexibility in smart grid.

The following conclusions can be drawn from the thesis:

- The studies revealed that PEV charging behavior in rural and urban areas do not differ significantly, but the probability of PEVs needing fast charging is higher, early in the day, in rural areas. The opposite is true for urban areas, where PEVs are more likely to need fast charging during the night than the day. The results of this comparison are reasonable and valid and are supported by the fact that more real-world activities and movements occur at night in urban than in rural areas. When it comes to the design of the EVCF with DERs considering a specific geography, the results revealed that more PV units would be required for EVCF design in a rural area, while more BESS units would be recommended for an urban area, adjustments that would help match the times PEVs need fast charging during the evening.

- Among the three provided design options, the design of an EVCF as a smart energy hub is the most desirable option in terms of profitability of the investor and deferment of the system upgrades from the perspective of the LDC.

- With the participation of WGF in electricity market, and unique ownership of WGF and EVCF, when wind wind imbalance penalties are high, it is economical to invest in the design of an EVCF with DERs and avoid such penalties. On the other hand, in different ownership of WGF and EVCF, and WGF contracts with grid, it requires high flexibility service prices to encourage an EVCF owner to design its facility with DERs to provide flexibility service to the gird to mitigate wind power imbalances.

- The design of an EVCF with DERs is a superior solution for wind integrated smart grid as it can exploit the compatibility of PV units and PEV charging loads with WGF, and thus not only relying on the BESS for mitigating wind power imbalances.

The installation cost of energy resources is expected to reduce in the future, and this will enhance the return on investments in EVCFs with DERs.

- The LDC should offer residential customers with proper incentives to transform their houses to REHs, and an effective interaction between REHs and LDCs should be established to increase the system flexibility and accrue benefits through deferment of system reinforcements and capacity investments, that can benefit both parties.

6.2 Research Contributions

The main contributions of the research presented in this thesis are as follows:

- The PEV charging load at an EVCF was modeled using a novel concept of a VDT coupled with a QM, considering medium and high PEV penetration levels in the long-term. Realistic vehicle statistics were used in the proposed VDT to predict the times PEVs needed fast charging in rural and urban areas, and the PEV charging load profile for multiple PEVs served at an EVCF was estimated using the developed QM.

- An inherent flexibility was introduced in EVCF portfolio by equipping it with DERs to mitigate the impact of fast charging loads on the power grid while facilitating wind power integration in power systems.

- A generic and novel framework was proposed for the optimal design and sizing of an EVCF as a smart energy hub that optimally controls the energy flow between the PV unit, the BESS, the external grid, and local consumption. The proposed framework was based on a 'bottom-up approach' to the design and planning of an EVCF, incorporating a detailed representation of vehicle mobility statistics in order to estimate the charging load profile, and then integrating all dimensions of planning, such as technical feasibility assessment, economics, and distribution system operations impact assessment.

- Two different ownership structures were studied for the first time to examine the feasibility of an EVCF designed with DERs for wind integrated grids, from the perspectives of the WGF and EVCF owners, respectively.

- A generic framework and an associated mathematical optimization model was proposed to design the EVCF with DERs, that provides the upward and downward flexibility provisions for hedging wind power forecast uncertainty, in each ownership structure. MCS was adopted in the proposed framework to investigate the impact of variability and uncertainty of wind and PV generation, and market price, on the optimum design in both ownership structures.

- A novel concept of unloaded and loaded states of REHs was presented to mathematically quantify the flexibility provisions from an REH.

- A Customer Profitability Model (CPM) along with an MCS based approach was proposed to determine the mathematical relationship between customer profitability of adoption of REHs and the incentives offered by the LDC.

- A generic and novel mathematical model was proposed to simultaneously determine the optimal incentives to be paid by the LDC and the optimal penetration of REHs for flexibility provisions in distribution grids, considering system operations and economic benefits of both the LDC and REHs.

6.3 Future work

Based on the work presented in this thesis, further research can be conducted to explore the following issues.

- EVCFs are planned and operated as a smart energy hub to mitigate the effects of PEV loads and enhance distribution grid capability. The option of upgrading the distribution system was not considered. A comprehensive planning study need be

carried out to determine which option is economically the best for the LDC, whether to upgrade the distribution system or provide incentives to the EVCF owner to reinforce their flexibility provisions.

- PEV charging occurring at the home was not considered in flexibility provisions from REHs; this could be a possible avenue for future work.
- Provisions of ancillary services such as frequency regulation from REHs and/or a reinforced EVCF with DERs were not considered in this work. It might be useful to examine such services which would affect the benefits accrued to the LDC and hence the incentives, penetration of REHs and the design of EVCF with DERs.
- Reliability aspects of the distribution system, when houses and EVCFs are transformed to residential and commercial energy hubs, respectively, need be investigated, and to what extent such transformation can enhance the system reliability.

References

[1] S. Labatt and R. R. White, *Carbon finance: the financial implications of climate change*, vol. 362. John Wiley & Sons, 2011.

[2] A. E. Outlook *et al.*, "Us energy information administration," *US Department of Energy, United States Government Printing Office: Washington, DC*, 2013.

[3] http://www.mto.gov.on.ca/english/dandv/vehicle/electric/electric-vehicles.shtml

[4] "Ontario power authority: Long term energy plan 2013. [online]" http://www.powerauthority.on.ca/power-planning/long-term-energy-plan-2013

[5] http://www.energy.gov.on.ca/

[6] J. Garcia-Gonzalez, R. M. R. de la Muela, L. M. Santos, and A. M. Gonzalez, "Stochastic joint optimization of wind generation and pumped-storage units in an electricity market," *IEEE Transactions on Power Systems*, vol. 23, no. 2, pp. 460–468, 2008.

[7] M. Ghofrani, A. Arabali, M. Etezadi-Amoli, and M. S. Fadali, "Smart scheduling and cost-benefit analysis of grid-enabled electric vehicles for wind power integration," *IEEE Transactions on Smart Grid*, vol. 5, no. 5, pp. 2306–2313, 2014.

[8] M. C. Bozchalui, S. A. Hashmi, H. Hassen, C. A. Cañizares, and K. Bhattacharya, "Optimal operation of residential energy hubs in smart grids," *IEEE Transactions on Smart Grid*, vol. 3, no. 4, pp. 1755–1766, 2012.

[9] J. Ma, V. Silva, R. Belhomme, D. S. Kirschen, and L. F. Ochoa, "Evaluating and planning flexibility in sustainable power systems," *IEEE Transactions on Sustainable Energy*, vol. 4, pp. 200–209, 2013.

[10] J. Zhao, T. Zheng, and E. Litvinov, "A unified framework for defining and measuring flexibility in power system," *IEEE Transactions on Power Systems*, vol. 31, pp. 339–347, 2016.

[11] E. Lannoye, D. Flynn, and M. O'Malley, "Evaluation of power system flexibility," *IEEE Transactions on Power Systems*, vol. 27, pp. 922–931, May 2012.

[12] E. Lannoye, D. Flynn, and M. O'Malley, "Power system flexibility assessment—state of the art," in *Power and Energy Society General Meeting, 2012 IEEE*, pp. 1–6, IEEE, 2012.

[13] A. M. L. L. da Silva, W. S. Sales, L. A. da Fonseca Manso, and R. Billinton, "Long-term probabilistic evaluation of operating reserve requirements with renewable sources," *IEEE Transactions on Power Systems*, vol. 25, no. 1, pp. 106–116, 2010.

[14] N. Navid, G. Rosenwald, and D. Chatterjee, "Ramp capability for load following in the miso markets," *Midwest Independent System Operator*, vol. 20, 2011.

[15] L. Xu and D. Tretheway, "Flexible ramping products," *CAISO Proposal*, 2012.

[16] S. Gottwalt, J. Gärttner, H. Schmeck, and C. Weinhardt, "Modeling and valuation of residential demand flexibility for renewable energy integration," *IEEE Transactions on Smart Grid*, vol. 8, no. 6, pp. 2565–2574, 2017.

[17] S. Huang and Q. Wu, "Real-time congestion management in distribution networks by flexible demand swap," *IEEE Transactions on Smart Grid*, pp. 1–1, 2017.

[18] S. Hanif, T. Massier, H. B. Gooi, T. Hamacher, and T. Reindl, "Cost optimal integration of flexible buildings in congested distribution grids," *IEEE Transactions on Power Systems*, vol. 32, pp. 2254–2266, May 2017.

[19] H. Hao, D. Wu, J. Lian, and T. Yang, "Optimal coordination of building loads and energy storage for power grid and end user services," *IEEE Transactions on Smart Grid*, vol. PP, pp. 1–1, 2017.

[20] M. Nistor and C. H. Antunes, "Integrated management of energy resources in residential buildings:a markovian approach," *IEEE Transactions on Smart Grid*, vol. 9, pp. 240–251, Jan 2018.

[21] K. Oikonomou and M. Parvania, "Optimal coordination of water distribution energy flexibility with power systems operation," *IEEE Transactions on Smart Grid*, pp. 1–1, 2018.

[22] E. Yao, P. Samadi, V. W. S. Wong, and R. Schober, "Residential demand side management under high penetration of rooftop photovoltaic units," *IEEE Transactions on Smart Grid*, vol. 7, pp. 1597–1608, May 2016.

[23] M. Geidl and G. Andersson, "Optimal power flow of multiple energy carriers," *IEEE Transactions on Power Systems*, vol. 22, no. 1, pp. 145–155, 2007.

[24] M. Geidl, G. Koeppel, P. Favre-Perrod, B. Klockl, G. Andersson, and K. Frohlich, "Energy hubs for the future," *IEEE power and energy magazine*, vol. 5, no. 1, pp. 24–30, 2007.

[25] M. Schulze, L. Friedrich, and M. Gautschi, "Modeling and optimization of renewables: applying the energy hub approach," pp. 83–88, 2008.

[26] Energy Hub Management System. http://www.energyhub.uwaterloo.ca/

[27] M. C. Bozchalui, C. A. Cañizares, and K. Bhattacharya, "Optimal energy management of greenhouses in smart grids.," *IEEE Transactions Smart Grid*, vol. 6, no. 2, pp. 827–835, 2015.

[28] S. Paudyal, C. A. Cañizares, and K. Bhattacharya, "Optimal operation of industrial energy hubs in smart grids," *IEEE Transactions on Smart Grid*, vol. 6, no. 2, pp. 684–694, 2015.

[29] M. Rastegar, M. Fotuhi-Firuzabad, H. Zareipour, and M. Moeini-Aghtaieh, "A probabilistic energy management scheme for renewable-based residential energy hubs," *IEEE Transactions on Smart Grid*, vol. 8, no. 5, pp. 2217–2227, 2017.

[30] C. Canizares, J. Nathwani, K. Bhattacharya, M. Fowler, M. Kazerani, R. Fraser, I. Rowlands, and H. Gabbar, "Towards an ontario action plan for plug-in-electric vehicles (pevs)," *Waterloo Institute for Sustainable Energy, University of Waterloo*, 2010.

[31] D. Wu, D. C. Aliprantis, and K. Gkritza, "Electric energy and power consumption by light-duty plug-in electric vehicles," *IEEE transactions on power systems*, vol. 26, no. 2, pp. 738–746, 2011.

[32] "U.S. Department of Transportation. National Household Travel Survey 2009." http://nhts.ornl.gov.

[33] M. F. Shaaban, Y. M. Atwa, and E. F. El-Saadany, "Pevs modeling and impacts mitigation in distribution networks," *IEEE Transactions on Power Systems*, vol. 28, no. 2, pp. 1122–1131, 2013.

[34] S. Bae and A. Kwasinski, "Spatial and temporal model of electric vehicle charging demand," *IEEE Transactions on Smart Grid*, vol. 3, no. 1, pp. 394–403, 2012.

[35] G. Li and X.-P. Zhang, "Modeling of plug-in hybrid electric vehicle charging demand in probabilistic power flow calculations," *IEEE Transactions on Smart Grid*, vol. 3, no. 1, pp. 492–499, 2012.

[36] Z. Liu, F. Wen, and G. Ledwich, "Optimal planning of electric-vehicle charging stations in distribution systems," *IEEE Transactions on Power Delivery*, vol. 28, no. 1, pp. 102–110, 2013.

[37] Y. Zheng, Z. Y. Dong, Y. Xu, K. Meng, J. H. Zhao, and J. Qiu, "Electric vehicle battery charging/swap stations in distribution systems: comparison study and optimal planning," *IEEE Transactions on Power Systems*, vol. 29, no. 1, pp. 221–229, 2014.

[38] W. Yao, J. Zhao, F. Wen, Z. Dong, Y. Xue, Y. Xu, and K. Meng, "A multi-objective collaborative planning strategy for integrated power distribution and electric vehicle charging systems," *IEEE Transactions on Power Systems*, vol. 29, no. 4, pp. 1811–1821, 2014.

[39] M. Brenna, A. Dolara, F. Foiadelli, S. Leva, and M. Longo, "Urban scale photovoltaic charging stations for electric vehicles," *IEEE Transactions on Sustainable Energy*, vol. 5, no. 4, pp. 1234–1241, 2014.

[40] N. Machiels, N. Leemput, F. Geth, J. Van Roy, J. Büscher, and J. Driesen, "Design criteria for electric vehicle fast charge infrastructure based on flemish mobility behavior," *IEEE Transactions on Smart Grid*, vol. 5, no. 1, pp. 320–327, 2014.

[41] J. Van Roy, N. Leemput, F. Geth, J. Büscher, R. Salenbien, and J. Driesen, "Electric vehicle charging in an office building microgrid with distributed energy resources," *IEEE Transactions on Sustainable Energy*, vol. 5, no. 4, pp. 1389–1396, 2014.

[42] U. C. Chukwu and S. M. Mahajan, "V2g parking lot with pv rooftop for capacity enhancement of a distribution system," *IEEE Transactions on Sustainable Energy*, vol. 5, no. 1, pp. 119–127, 2014.

[43] F. Marra, G. Y. Yang, C. Træholt, E. Larsen, J. Østergaard, B. Blažič, and W. Deprez, "Ev charging facilities and their application in lv feeders with photovoltaics," *IEEE Transactions on Smart Grid*, vol. 4, no. 3, pp. 1533–1540, 2013.

[44] Y. Liu, Y. Tang, J. Shi, X. Shi, J. Deng, and K. Gong, "Application of small-sized smes in an ev charging station with dc bus and pv system," *IEEE Transactions on Applied Superconductivity*, vol. 25, no. 3, pp. 1–6, 2015.

[45] S. Kamalinia, M. Shahidehpour, and A. Khodaei, "Security-constrained expansion planning of fast-response units for wind integration," *Electric Power System Research*, pp. 107–116, 2011.

[46] T.-Y. Lee, "Optimal spinning reserve for a wind-thermal power system using eipso," *IEEE Transactions on Power Systems*, pp. 1612–1621, 2007.

[47] Y. Sang, M. Sahraei-Ardakani, and M. Parvania, "Stochastic transmission impedance control for enhanced wind energy integration," *IEEE Transactions on Sustainable Energy*, vol. PP, no. 99, pp. 1–1, 2017.

[48] H. Bludszuweit and J. A. Domínguez-Navarro, "A probabilistic method for energy storage sizing based on wind power forecast uncertainty," *IEEE Transactions on Power Systems*, pp. 1651–1658, 2011.

[49] Y. V. Makarov, P. Du, M. C. W. Kintner-Meyer, C. Jin, and H. F. Illian, "Sizing energy storage to accommodate high penetration of variable energy resources," *IEEE Transactions on Sustainable Energy*, vol. 3, pp. 34–40, Jan 2012.

[50] J. Tan and Y. Zhang, "Coordinated control strategy of a battery energy storage system to support a wind power plant providing multi-timescale frequency ancillary services," *IEEE Transactions on Sustainable Energy*, vol. 8, pp. 1140–1153, July 2017.

[51] H. Bitaraf and S. Rahman, "Reducing curtailed wind energy through energy storage and demand response," *IEEE Transactions on Sustainable Energy*, vol. 9, pp. 228–236, Jan 2018.

[52] Q. Huang, Q. S. Jia, and X. Guan, "Robust scheduling of EV charging load with uncertain wind power integration," *IEEE Transactions on Smart Grid*, vol. PP, no. 99, pp. 1–1, 2017.

[53] A. Tavakoli, M. Negnevitsky, D. T. Nguyen, and K. M. Muttaqi, "Energy exchange between electric vehicle load and wind generating utilities," *IEEE Transactions on Power Systems*, pp. 1248–1258, 2016.

[54] Q. Huang, Q. S. Jia, and X. Guan, "A multi-timescale and bilevel coordination approach for matching uncertain wind supply with ev charging demand," *IEEE Transactions on Automation Science and Engineering*, vol. 14, pp. 694–704, April 2017.

[55] Y. Sun, J. Zhong, Z. Li, W. Tian, and M. Shahidehpour, "Stochastic scheduling of battery-based energy storage transportation system with the penetration of wind power," *IEEE Transactions on Sustainable Energy*, vol. 8, no. 1, pp. 135–144, 2017.

[56] B. F. Hobbs, J. C. Honious, and J. Bluestein, "What's flexibility worth? the enticing case of natural gas cofiring," *The Electricity Journal*, vol. 5, no. 2, pp. 37–47, 1992.

[57] Elnozahy, Mohamed,"Accommodating a High Penetration of PHEVs and PV Electricity in Residential Distribution Systems", PhD thesis, University of Waterloo,2015.

[58] I. Hadjipaschalis, A. Poullikkas, and V. Efthimiou, "Overview of current and future energy storage technologies for electric power applications," *Renewable and sustainable energy reviews*, vol. 13, no. 6-7, pp. 1513–1522, 2009.

[59] T. Sels, C. Dragu, T. Van Craenenbroeck, and R. Belmans, "Overview of new energy storage systems for an improved power quality and load managing on distribution level," in *Electricity Distribution, 2001. Part 1: Contributions. CIRED. 16th International Conference and Exhibition on (IEE Conf. Publ No. 482)*, vol. 4, pp. 5–pp, IET, 2001.

[60] S. S. Choi, K. Tseng, D. Vilathgamuwa, and T. Nguyen, "Energy storage systems in distributed generation schemes," in *Power and Energy Society General Meeting-Conversion and Delivery of Electrical Energy in the 21st Century, 2008 IEEE*, pp. 1–8, IEEE, 2008.

[61] D. E. Olivares, C. A. Cañizares, and M. Kazerani, "A centralized energy management system for isolated microgrids.," *IEEE Transactions on Smart Grid*, vol. 5, no. 4, pp. 1864–1875, 2014.

[62] C. W. Gellings, "The concept of demand-side management for electric utilities," *Proceedings of the IEEE*, vol. 73, no. 10, pp. 1468–1470, 1985.

[63] D. Kathan, C. Daly, E. Eversole, M. Farinella, J. Gadani, R. Irwin, C. Lankford, A. Pan, C. Switzer, and D. Wright, "National action plan on demand response," *The Federal Energy Regulatory Commission Staff, Federal Energy Regulatory Commission, Washington, DC, Tech. Rep. AD09-10*, 2010.

[64] K. Bhattacharya, M. H. Bollen, and J. E. Daalder, "Real time optimal interruptible tariff mechanism incorporating utility-customer interactions," *IEEE Transactions on Power Systems*, vol. 15, no. 2, pp. 700–706, 2000.

[65] http://www.peaksaver.com

[66] H. Aalami, G. Yousefi, and M. P. Moghadam, "Demand response model considering edrp and tou programs," in *Transmission and Distribution Conference and Exposition, 2008. T&D. IEEE/PES*, pp. 1–6, IEEE, 2008.

[67] J. L. Mathieu, P. N. Price, S. Kiliccote, and M. A. Piette, "Quantifying changes in building electricity use, with application to demand response," *IEEE Transactions on Smart Grid*, vol. 2, no. 3, pp. 507–518, 2011.

[68] "IEEE-USA, board of directors, position statement: Plug-in electric hybrid vehicles, 15 june 2007,."

[69] D. P. Tuttle and R. Baldick, "The evolution of plug-in electric vehicle-grid interactions," *IEEE Transactions on Smart Grid*, vol. 3, no. 1, pp. 500–505, 2012.

[70] V. G. Kulkarni, *Modeling, Analysis, Design, and Control of Stochastic Systems*, vol. 362. 1st ed. New York: Springer, 1999.

[71] D. G. Kendall, "Stochastic processes occurring in the theory of queues and their analysis by the method of the imbedded markov chain," *The Annals of Mathematical Statistics*, pp. 338–354, 1953.

[72] H. W. Dommel and W. F. Tinney, "Optimal power flow solutions," *IEEE Transactions on Power Apparatus and Systems*, no. 10, pp. 1866–1876, 1968.

[73] P. S. R. Council, "Traffic choices study–summary report," *Prepared for the Value Pricing Pilot Program, Federal Highway Administration, Washington, DC*, 2008.

[74] "Hydro one. technical DG interconnection requirements of hydroone. [online]." Available: http://www.hydroone.com.

[75] G. D. Corporation, "General algebraic modeling system (GAMS), software." https://www.gams.com/optimization-solvers/

[76] M. E. Baran and F. F. Wu, "Network reconfiguration in distribution systems for loss reduction and load balancing," *IEEE Transactions on Power Delivery*, vol. 4, no. 2, pp. 1401–1407, 1989.

[77] J. Pinheiro, C. Dornellas, M. T. Schilling, A. Melo, and J. Mello, "Probing the new IEEE reliability test system (RTS-96): Hl-II assessment," *IEEE Transactions on Power Systems*, vol. 13, no. 1, pp. 171–176, 1998.

[78] IESO,Hourly Ontario Energy Price (HOEP), Toronto, Ontario, Canada. Available:http://www.ieso.ca.

[79] N. EPRI, "Environmental assessment of plug-in hybrid electric vehicles. volume I: Nationwide greenhouse gas emissions," *Electric Power Research Institute (EPRI), Final Report*, 2007.

[80] Y. Zeng, K. C. Land, Z. Wang, and D. Gu, "US family household momentum and dynamics: an extension and application of the profamy method," *Population Research and Policy Review*, vol. 25, no. 1, p. 1, 2006.

[81] J. V. Paatero and P. D. Lund, "Effects of large-scale photovoltaic power integration on electricity distribution networks," *Renewable Energy*, pp. 216–234, 2007.

[82] Fit and Microt Program, Ontario Power Authority."http:/t.powerauthority.on.ca

[83] A. A. Akhil, G. Huff, A. B. Currier, B. C. Kaun, D. M. Rastler, S. B. Chen, A. L. Cotter, D. T. Bradshaw, and W. D. Gauntlett, *DOE/EPRI 2013 electricity storage handbook in collaboration with NRECA*. Sandia National Laboratories Albuquerque, NM, 2013.

[84] http://www.nrel.gov/docs/fy14osti/62558.pdf

[85] W. Alharbi and K. Bhattacharya, "Electric vehicle charging facility as a smart energy microhub," *IEEE Transactions on Sustainable Energy*, vol. 8, no. 2, pp. 616–628, April 2017.

[86] M. C. Mabel, R. E. Raj, and E. Fernandez, "Adequacy evaluation of wind power generation systems," *Energy*, pp. 5217–5222, 2010.

[87] "NREL." https://midcdmz.nrel.gov/apps/go2url.pl?site=BMS

[88] "https://www.iso-ne.com/isoexpress/web/reports/pricing//tree/lmps-rt-hourly-nal

[89] G. He, Q. Chen, C. Kang, P. Pinson, and Q. Xia, "Optimal bidding strategy of battery storage in power markets considering performance-based regulation and battery cycle life," *IEEE Transactions on Smart Grid*, vol. 7, no. 5, pp. 2359–2367, 2016.

[90] M. Musallam and C. M. Johnson, "An efficient implementation of the rainflow counting algorithm for life consumption estimation," *IEEE Transactions on Reliability*, vol. 61, no. 4, pp. 978–986, 2012.

[91] *N. R. Draper and H. Smith, Applied Regression Analysis, 3rd ed. New York: Wiley, 1998.*

[92] R. Kohavi *et al.*, "A study of cross-validation and bootstrap for accuracy estimation and model selection," in *Ijcai*, vol. 14, pp. 1137–1145, Montreal, Canada, 1995.

[93] K. Ardani, E. O'Shaughnessy, R. Fu, C. McClurg, J. Huneycutt, and R. Margolis, "Installed cost benchmarks and deployment barriers for residential solar photovoltaics with energy storage: Q1 2016," tech. rep., National Renewable Energy Laboratory (NREL), Golden, CO (United States), 2016.

APPENDICES

Appendix A

33-Bus Distribution System Data

Table A.1: Load Data for 33-Bus System

Bus i	P (kW)	Q (kVAR)
2	100	60
3	90	40
4	120	80
5	60	30
6	60	20
7	200	100
8	200	100
9	60	20
10	60	20
11	45	30
12	60	35
13	60	35
14	120	80
15	60	10
16	60	20
17	60	20
18	90	40
19	90	40
20	90	40
21	90	40
22	90	40
23	90	50
24	420	200
25	420	200
26	60	25
27	60	25
28	60	20
29	120	70
30	200	600
31	150	70
32	210	100
33	60	40

Table A.2: Feeder Data for 33-Bus System

Line i-j	R (ohms)	X (ohms)
1-2	0.0922	0.0477
2-3	0.493	0.2511
3-4	0.366	0.1864
4-5	0.3811	0.1941
5-6	0.819	0.707
6-7	0.1872	0.6188
7-8	0.7114	0.2351
8-9	1.03	0.74
9-1	1.044	0.74
10-11	0.1966	0.065
11-12	0.3744	0.1238
12-13	1.468	1.155
13-14	0.5416	0.7129
14-15	0.591	0.526
15-16	0.7463	0.545
16-17	1.289	1.721
17-18	0.732	0.574
2-19	0.164	0.1565
19-2	1.5042	1.3554
20-21	0.4095	0.4784
21-22	0.7089	0.9373
3-23	0.4512	0.3083
23-24	0.898	0.7091
24-25	0.896	0.7011
6-26	0.203	0.1034
26-27	0.2842	0.1447
27-28	1.059	0.9337
28-29	0.8042	0.7006
29-3	0.5075	0.2585
30-31	0.9744	0.963
31-32	0.3105	0.3619
32-33	0.341	0.5302